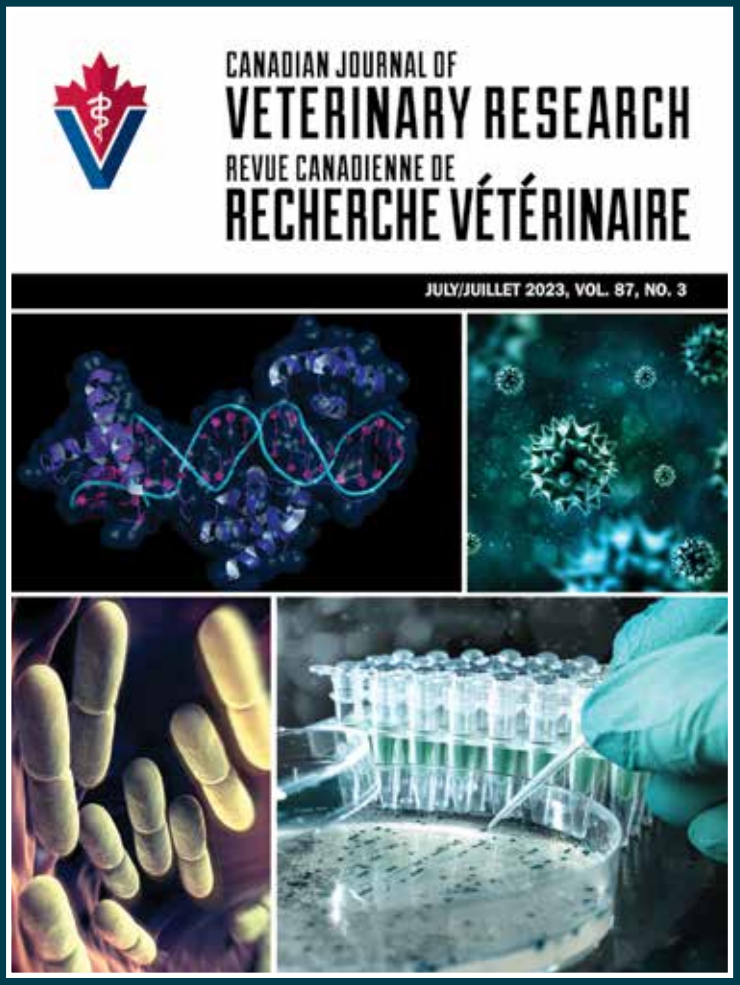
Provided for non-commercial research and education use.
Not for reproduction, distribution or commercial use.

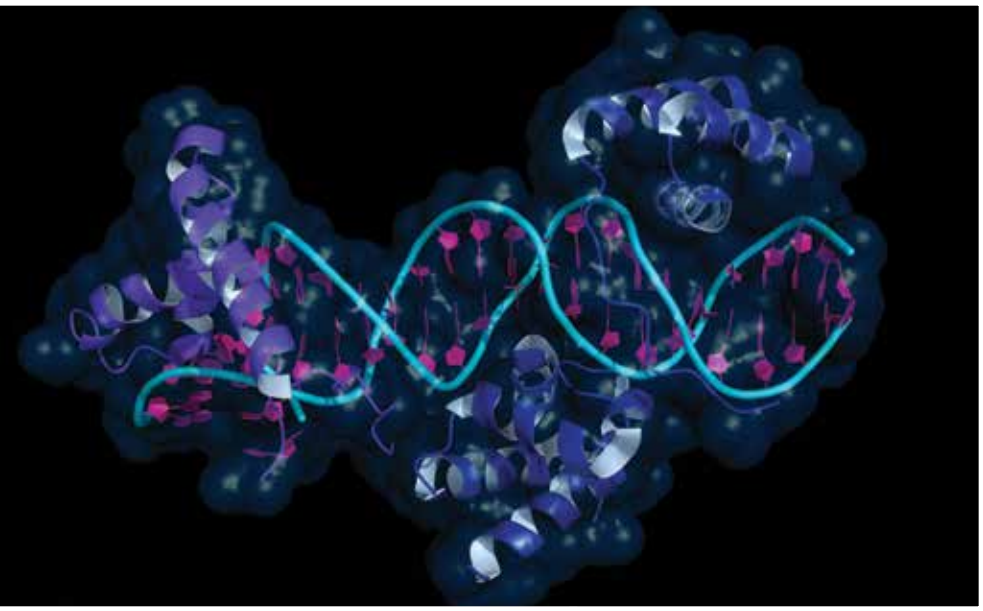


The Canadian Journal of Veterinary Research is published by Canadian Veterinary Medical Association. The attached copy is furnished to readers for personal, non-commercial research and education use. Other uses, including reproduction and distribution, or selling or licensing copies, or posting to personal, institutional or third party Web sites are prohibited. Those who require further information regarding reprints or archiving and manuscript policies are encouraged to contact hbroughton@cvma-acmv.org.

FOR PERSONAL USE ONLY

CANADIAN JOURNAL OF
VETERINARY RESEARCH
REVUE CANADIENNE DE
RECHERCHE VÉTÉRINAIRE

JULY/JUILLET 2023, VOL. 87, NO. 3









FOR PERSONAL USE ONLY

Established in 1937 ISSN 0830-9000

Canadian Journal of Veterinary Research

Formerly CANADIAN JOURNAL OF COMPARATIVE MEDICINE

The journal publishes the results of original research in veterinary and comparative medicine. Manuscripts must be as concise as possible, and the research described must represent a significant contribution to knowledge in veterinary medicine. Full-length papers, short communications, and review papers are welcome. All manuscripts will be reviewed for scientific content and editorial accuracy.

Manuscripts must conform to the Instructions for Authors found on the CVMA website. Consultation of a recent issue of the journal to ensure that the manuscript conforms to current style is also recommended. Please use the website (www.canadianveterinarians.net) to submit articles. **A publication fee will be charged according to the article category. Authors will be charged $1000.00 for non-members or $800.00 for CVMA members for Short Communications, $1500.00 for non-members or $1200.00 for CVMA members for Review Articles and Scientific Articles.** Payment information is due at the acceptance stage.

Revue canadienne de recherche vétérinaire

Remplace la REVUE CANADIENNE DE MÉDECINE COMPARÉE

La revue publie les résultats de recherches originales en médecine vétérinaire et comparative. Les manuscrits doivent être aussi brefs que possible et la recherche décrite doit apporter une contribution importante à la médecine vétérinaire. Les exposés complets, les communications brèves et les comptes rendus sont bienvenus. Nous vérifierons le fonds scientifique et la forme de tous les manuscrits.

Les manuscrits doivent être conformes aux directives aux auteurs qui se trouvent sur le site Web de l'ACMV. La consultation d'un récent numéro de la revue est aussi profitable, afin de s'assurer qu'un manuscrit se conforme au style courant. Veuillez utiliser le site Web (www.veterinairesaucanada.net) pour soumettre les articles. **Les frais exigés varient selon le type d'article. Ils sont de 1000 $ pour les communications brèves (800 $ pour les membres de l'ACMV), et de 1500 $ pour les comptes rendus et les articles scientifiques (1200 $ pour les membres de l'ACMV).** Les renseignements pour le paiement doivent être fournis à l'étape de l'acceptation du manuscrit.

Canadian Journal of Veterinary Research
Revue canadienne de recherche vétérinaire
Editor — Rédactrice
Patricia Shewen, Guelph, Ontario
Associate Editors — Rédacteurs adjoints
Marcio C. Costa, Montreal, Québec
Collins Kamunde, Charlottetown, Prince Edward Island
Assistant Editors — Assistants à la rédaction
Serge Messier, Saint-Hyacinthe, Québec
Juan Hernandez-Medrano, Calgary, Alberta
Managing Editor — Directrice de la publication
Heather Broughton, Ottawa, Ontario
Assistant Managing Editor — Directrice adjointe de la publication
Stella Wheatley, Ottawa, Ontario
Editorial Coordinator — Coordonnatrice de la publication
Kelly Gray-Sabourin, Ottawa, Ontario
Advertising and Sponsorship Consultant — Consultante, publicité et commandites
Laima Laffitte, Prescott, Ontario

Abstracted and/or indexed in:/Résumé et/ou catalogué dans :

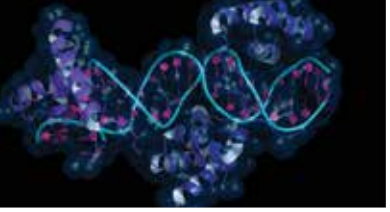
Biological Abstracts	Index Veterinarius
Chemical Abstracts	Nutrition Abstracts
Current Contents (Agric. Section)	Science Citation Index
EMBASE/Excerpta Medica	Veterinary Bulletin
Index Medicus	Derwent Veterinary Drug File

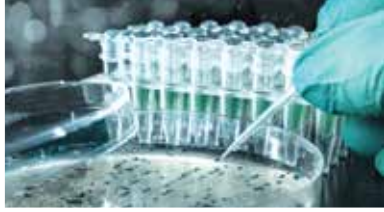
Subscription/Abonnement	**2023**
Personal Subscription/ Abonnement personnel (Canada)	$220 $ (+ GST/HST as applicable; TPS/TVH en vigueur)
Personal Subscription/ Abonnement personnel (Foreign/Étranger)	$240 $ US/É.-U.
Institutional Subscription/ Abonnement institutionnel	$290 $ (+ In Canada, GST/HST as applicable; Au Canada, TPS/TVH selon le cas)
Institutional Subscription/ Abonnement institutionnel (Foreign/Étranger)	$290 $ US/É.-U.

Address all correspondence to/Adresser toute correspondance à :
Canadian Journal of Veterinary Research
Revue canadienne de recherche vétérinaire
339, rue Booth Street, Ottawa, Ontario K1R 7K1
Tel./Tél. : (613) 236-1162 — Fax/Télécopieur : (613) 236-9681
email/Courriel : hbroughton@cvma-acmv.org
© Canadian Veterinary Medical Association 2023
L'Association canadienne des médecins vétérinaires 2023

Typesetting/Typographie
AN Design Communications
www.an-design.ca

Published quarterly by the Canadian Veterinary Medical Association
Publication trimestrielle de l'Association canadienne des médecins vétérinaires



FOR PERSONAL USE ONLY

JULY/JUILLET 2023, VOL. 87, NO. 3

Greetings **166**

Editorial **167**

ARTICLES

Microbiology

Prevalence of equine parvovirus-hepatitis in healthy broodmares in Ontario, Canada
Maria A. Papapetrou, Luis G. Arroyo, Toni L. Meister, John D. Baird, Eike Steinmann, Brandon N. Lillie **169**

Development of an indirect ELISA method based on the VP1 protein for detection of IgG antibodies against porcine sapelovirus
Jiajia Liu, Benqiang Li, Jie Tao, Jinghua Cheng, Ying Shi, Changtao Qiao, Xiaohui Shen, Huili Liu **176**

Clinical Studies

Neourethra creation using autologous vascularized intestinal graft in cats
Barbra G.O. de Faria, Vanessa M. da Silva, Jéssica A. Silva, Sheila C.A. Santos, Ana M. Quessada, Caterina Muramoto, João M. da Costa Neto **184**

Relationship between the degree of stifle flexion and the proximal patellofemoral angle in the sagittal plane: A radiographic study
Juan José Camarasa, Rosario Vallefuoco, Felipe De Vicente **191**

Iliopsoas strain demographics, concurrent injuries, and grade determined by musculoskeletal ultrasound in 72 agility dogs
Danny Sack, Debra Canapp, Sherman Canapp, Stephanie Majeski, Jeff Curry, Angela Sutton, Robert Cullen **196**

Long-term outcomes after arthroscopic treatment of dogs affected by osteochondrosis dissecans of the humeral trochlea, with or without medial coronoid disease: 23 cases (2012–2020)
Joachim Lahiani, Antoine Dunié-Mérigot, Alexandre Caron, Kevin Le Boedec, Guillaume Ragetly **202**

Comparison of rostral spread of lumbosacral epidural volume calculated by body weight or length of the vertebral column in small-sized anesthetized dogs
Flavio A.V. Freitag, Alexander Valverde, Monica Jensen, Andrea Sanchez, Diego E. Gomez, Craig Bailey **208**

Rostral spread of lumbosacral epidural volumes of dye and contrast medium calculated using body weight or length of the vertebral column in dog cadavers
Flavio A.V. Freitag, Alexander Valverde, Monica Jensen, Andrea Sanchez, Diego E. Gomez, Craig Bailey **217**

Comparison of two ratios of xylazine:ketamine for the anesthesia of free-ranging North American beavers *(Castor canadensis)* in a remote setting
Stéphane Lair, Gregory Bourguelat, Gaétan Fournier **224**

SHORT COMMUNICATIONS/COMMUNICATIONS BRÈVES

mRNA expression of immune factors by milk somatic cells from healthy Holstein lactating cows
Kenji Murakami, Tomochika Fukuhara, Shunsuke Kure, Takaaki Shimosakai, Ayano Sato, Ryo Murata, Keigo Kosenda, Hiromichi Ohtsuka **231**

Effect of supplementation with *Saccharomyces boulardii* CNCM I-1079 on vaccine response to an inactivated bacterial vaccine in young Japanese Black calves: A field trial
Kazusa Mori, Asato Uchiumi, Kai Yamamoto, Yuki Shimizu, Risa Ueda, Keigo Kosenda, Tomochika Fukuhara, Syunsuke Kure, Hiroyuki Fukazawa, Hiromichi Ohtsuka. **237**

FOR PERSONAL USE ONLY

Greetings from the new *CJVR* Editor

The opportunity to serve the veterinary research community as Editor of the *Canadian Journal of Veterinary Research (CJVR)* is a privilege that I am honoured to undertake. My first research paper was published in this journal, then the Canadian Journal of Comparative Medicine, in 1980. As a graduate student, that experience taught me to appreciate the peer review process and value the critical insights of fellow researchers. Later, as a mentor, I typically directed my students to the *CJVR* for their publications, where I trusted that their efforts would be met with fair appraisal and sound advice. I will endeavour as Editor to continue to uphold those ethics in our publication. I am fortunate to follow the exceptional example of retiring Editor, Éva Nagy, who served the journal with skill and integrity for more than two decades. I know that the entire CVMA Editorial Committee is grateful for her highly competent management and collegiality.

With pleasure, I confirm that Marcio Costa and Serge Messier, both from the Université de Montréal at St. Hyacinthe, will continue as Associate and Assistant *CJVR* Editors, respectively. I am also delighted to announce the appointment of Collins Kamunde, University of Prince Edward Island, as a new Associate Editor, and Juan Hernandez-Medrano, University of Calgary, as a new Assistant Editor for the *CJVR*. With the anticipated future appointment of a third Assistant Editor from Saskatoon, we will have 'boots on the ground' at all five Canadian veterinary colleges. They join the *CVJ* editorial team and the CVMA management team who continue to serve the Canadian veterinary community by ensuring the high quality of our publications.

We appreciate your support of this journal and invite you and your colleagues to continue publishing meaningful research in the *CJVR*.

FOR PERSONAL USE ONLY

Editorial Éditorial

Changing of the guard: Exits from and entrances to the Canadian Veterinary Medical Association Editorial Committee

Changement de la garde au sein du Comité de la rédaction de l'Association canadienne des médecins vétérinaires



Dr./Dr John Kastelic



Dr./Dr Tim Ogilvie

The Canadian Veterinary Medical Association (CVMA) Editorial Committee oversees publication of the CVMA's two national, peer-reviewed scientific journals: *The Canadian Veterinary Journal (The CVJ)* and the *Canadian Journal of Veterinary Research (CJVR)*. Historically, most members of the Editorial Committee have graciously served lengthy terms. This continues, but coincidentally, there are several recent changes.

First, we had mixed emotions when **Dr. Ron Lewis** announced that he is stepping down as Chair of the CVMA Editorial Committee. We are truly saddened to see him go, as we have deeply appreciated and benefitted from his thoughtful leadership and wise counsel over the last 14 years.

Next, we are also reticent to bid farewell to **Dr. Éva Nagy** in her role as Editor of the *CJVR*. Remarkably, Éva has held this job for the past 25 years, providing a "voice" for researchers, domestic and foreign, in many disciplines. She was always very professional and extremely patient and supportive.

Another departure is **Heather Broughton,** who has served as Manager, Journals for 21 years. She oversaw many of the business aspects and had direct involvement in production, drawing on many years of experience as a writer and editor.

We also acknowledge the departure of 3 other persons. **Stella Wheatley,** Assistant Managing Editor, Journals who did scientific editing for both journals, recently withdrew from *The CVJ* (after 17 years) but continues to do editing for the *CJVR*. Finally, both **Dr. Aylin Atilla,** a small animal surgeon at the University of Calgary, and **Dr. Emily John,** a large animal internist at the University of PEI, recently indicated they are relinquishing positions as Assistant Editors of *The CVJ*. We will deeply miss all three and thank them for their contributions.

Clearly, all these departures have created numerous vacancies. However, we are thrilled that those gaps are being filled.

We are delighted to welcome **Dr. Craig Stephen** as the new Chair of the Editorial Committee. Craig has had a long and distinguished career as a veterinary epidemiologist, with a very

Le Comité de la rédaction de l'Association canadienne des médecins vétérinaires (ACMV) dirige la publication des deux revues scientifiques nationales aux articles évalués par des pairs de l'ACMV : *La Revue vétérinaire canadienne* (*La RVC*) et la *Revue canadienne de recherche vétérinaire* (*RCRV*). Jusqu'à maintenant, la plupart des membres du Comité de la rédaction ont effectué de longs mandats. La tradition se poursuit, mais il y a eu plusieurs changements récemment.

Le **Dr Ron Lewis** a annoncé qu'il quittait son poste de président du Comité de la rédaction de l'ACMV. Son départ nous attriste, car nous avons immensément bénéficié de son leadership réfléchi et de ses conseils avisés au cours des 14 dernières années.

C'est aussi avec regret que nous devons dire au revoir à la **Dre Éva Nagy**, rédactrice de la *RCRV*. Fait remarquable, elle occupait ce poste et s'affairait à faire entendre la « voix » des chercheurs canadiens et étrangers de diverses disciplines depuis 25 ans! Elle a toujours été très professionnelle, extrêmement patiente et d'un grand soutien.

Un autre départ important est celui de **Heather Broughton**, directrice des publications depuis 21 ans. Elle a supervisé de nombreux aspects administratifs et a participé directement à la production des revues, en s'appuyant sur ses nombreuses années d'expérience en tant que rédactrice et réviseure.

Trois autres membres de l'équipe de la rédaction ont également quitté leurs fonctions. **Stella Wheatley**, directrice adjointe des publications et responsable de la révision scientifique pour les deux revues, s'est récemment retirée de *La RVC* (après 17 ans), mais elle poursuit son travail avec la *RCRV*. De plus, la **Dre Aylin Atilla**, spécialiste en chirurgie des animaux de compagnie à l'Université de Calgary, et la **Dre Emily John**, spécialiste en médecine interne des grands animaux à l'Université de l'Île-du-Prince-Édouard, ont récemment indiqué qu'elles renonçaient à leurs postes de rédactrices adjointes de *La RVC*. Toutes les trois nous manqueront beaucoup et nous les remercions pour leurs contributions.

Use of this article is limited to a single copy for personal study. Anyone interested in obtaining reprints should contact the CVMA office (hbroughton@cvma-acmv.org) for additional copies or permission to use this material elsewhere.

L'usage du présent article se limite à un seul exemplaire pour étude personnelle. Les personnes intéressées à se procurer des réimpressions devraient communiquer avec le bureau de l'ACMV (hbroughton@cvma-acmv.org) pour obtenir des exemplaires additionnels ou la permission d'utiliser cet article ailleurs.

FOR PERSONAL USE ONLY

strong focus on One Health. Based on Vancouver Island, Craig has held various academic positions, conducting research both domestically and internationally.

Dr. Patricia (Pat) Shewen, who has served as Associate Editor, *CJVR,* has graciously agreed to assume the duties of Editor of the *CJVR.* Pat is a Professor Emerita and has had a long and productive career with a focus on respiratory disease in cattle. Joining **Dr. Marcio Costa,** University of Montreal, as an Associate Editor of the *CJVR* is **Dr. Collins Kamunde,** a scholar in biomedical sciences at the Atlantic Veterinary College with interests in metals toxicology in aquatic species and systems.

Kelly Gray-Sabourin has agreed to become Manager, Journals, drawing on her experiences as Editorial Coordinator for both journals for more than a decade. In addition, **Dr. Heather Kinkaid,** who has a background in animal science, has been hired to fill the role of Assistant Managing Editor for *The CVJ* that was vacated by Stella Wheatley.

A position as Associate Editor of *The CVJ* created by the retirement of **Dr. Wayne McDonell** has been filled by **Dr. Carolyn Kerr,** an anesthesiologist at the Ontario Veterinary College. The 2 Assistant Editor vacancies at *The CVJ* are not yet filled.

The CVMA Editorial Committee has undergone substantial changes. However, all replacements have much enthusiasm and experience, and in the cases of Pat and Kelly, a recent history of working with one or both journals. Therefore, the journals remain in very good hands and we have much optimism for the future. Stay tuned and please let us know if you have an interest in learning more about any potential positions. ■

Tim Ogilvie (ogilvie@upei.ca)
John Kastelic (jpkastel@ucalgary.ca)
Éva Nagy
Pat Shewen

Évidemment, tous ces départs ont créé de nombreux postes vacants, qui ont heureusement pour la plupart été comblés.

Nous sommes ravis d'accueillir le **D^r^ Craig Stephen** à titre de nouveau président du Comité de la rédaction. Il a eu une longue et brillante carrière en épidémiologie vétérinaire axée sur le concept « Une seule santé ». Résidant sur l'île de Vancouver, il a occupé divers postes universitaires et a travaillé sur des projets de recherche tant à l'échelle nationale qu'internationale.

La **D^re^ Patricia (Pat) Shewen**, qui était rédactrice adjointe à la *RCRV*, a accepté de prendre le relais à titre de rédactrice de la *RCRV*. Professeure émérite, elle a eu une carrière fructueuse pendant laquelle elle s'est particulièrement intéressée aux maladies respiratoires chez les bovins. Le **D^r^ Collins Kamunde**, chercheur en sciences biomédicales à l'Atlantic Veterinary College, s'intéresse à la toxicologie des métaux pour les espèces et les systèmes aquatiques. Il se joint au **D^r^ Marcio Costa**, de l'Université de Montréal, en tant que rédacteur adjoint de la *RCRV*.

Kelly Gray-Sabourin a accepté le poste de directrice des publications, après avoir été coordonnatrice des publications pour les deux revues pendant plus d'une décennie. De plus, la **D^re^ Heather Kinkaid**, qui a œuvré dans le domaine des sciences animales, a été embauchée pour occuper le poste laissé vacant par Stella Wheatley et assurer la révision de *La RVC*.

Le poste de rédacteur en chef adjoint de *La RVC* qu'occupait le **D^r^ Wayne McDonell** avant son départ à la retraite a été repris par la **D^re^ Carolyn Kerr**, anesthésiologiste à l'Ontario Veterinary College. Les deux postes vacants de rédacteurs adjoints de *La RVC* n'ont pas encore été pourvus.

Le Comité de la rédaction de l'ACMV a subi d'importants changements, mais les nouveaux venus sont très enthousiastes et compétents, et Pat et Kelly travaillaient déjà pour l'une des publications ou les deux. Par conséquent, les revues de l'ACMV restent en bonnes mains et nous sommes très optimistes pour l'avenir. N'hésitez pas à communiquer avec nous si vous souhaitez en savoir plus sur les possibilités de collaboration et les postes vacants. ■

Tim Ogilvie (ogilvie@upei.ca)
John Kastelic (jpkastel@ucalgary.ca)
Éva Nagy
Pat Shewen

FOR PERSONAL USE ONLY

Prevalence of equine parvovirus-hepatitis in healthy broodmares in Ontario, Canada

Maria A. Papapetrou, Luis G. Arroyo, Toni L. Meister, John D. Baird, Eike Steinmann, Brandon N. Lillie

Abstract

Equine parvovirus-hepatitis (EqPV-H) was first reported from the serum and liver tissue of a horse diagnosed with Theiler's disease in the United States in 2018. Theiler's disease, also known as equine serum hepatitis, is a severe hepatitis with fulminant hepatic necrosis. The disease has most frequently been reported following the administration of equine-origin biological products; however, it has also been reported in in-contact horses with no prior biologic administration. EqPV-H has been detected in clinically healthy horses in North America (USA, Canada), Europe (Germany, Austria, Slovenia), Asia (China, South Korea), and South America (Brazil). Previous prevalence studies conducted worldwide have shown the presence of EqPV-H DNA in serum or plasma ranging from 3.2 to 19.8%. This study investigated the prevalence of EqPV-H DNA in 170 healthy broodmares of various breeds located on 37 farms in southern Ontario, Canada. The occurrence of EqPV-H infection was determined by quantitative PCR for EqPV-H DNA in serum samples. The effects of age, breed, season, pregnancy status, and equine herpesvirus-1 (EHV-1) vaccination history on EqPV-H status were also investigated. There was a prevalence of 15.9% (27/170) with viral loads of EqPV-H ranging from detectable to 2900 copies/mL. Statistical analysis showed that increasing age was a significant factor in the detection of EqPV-H DNA. Neither breed, season, pregnancy status, nor EHV-1 vaccination history was significant in predicting EqPV-H infection status.

Résumé

L'hépatite à parvovirus équin (EqPV-H) a été signalée pour la première fois à partir du sérum et du tissu hépatique d'un cheval diagnostiqué avec la maladie de Theiler aux États-Unis en 2018. La maladie de Theiler, également connue sous le nom d'hépatite sérique équine, est une hépatite sévère avec nécrose hépatique fulminante. La maladie a été le plus souvent rapportée à la suite de l'administration de produits biologiques d'origine équine; cependant, il a également été signalé chez des chevaux en contact sans administration préalable de produit biologique. EqPV-H a été détecté chez des chevaux cliniquement sains en Amérique du Nord (États-Unis, Canada), en Europe (Allemagne, Autriche, Slovénie), en Asie (Chine, Corée du Sud) et en Amérique du Sud (Brésil). Des études de prévalence antérieures menées dans le monde entier ont montré la présence d'ADN EqPV-H dans le sérum ou le plasma allant de 3,2 à 19,8 %. Cette étude a examiné la prévalence de l'ADN EqPV-H chez 170 poulinières en bonne santé de différentes races situées dans 37 fermes du sud de l'Ontario, au Canada. La survenue d'une infection par EqPV-H a été déterminée par PCR quantitative pour l'ADN d'EqPV-H dans des échantillons de sérum. Les effets de l'âge, de la race, de la saison, de l'état de grossesse et des antécédents de vaccination contre l'herpèsvirus équin-1 (EHV-1) sur le statut EqPV-H ont également été étudiés. Il y avait une prévalence de 15,9 % (27/170) avec des charges virales d'EqPV-H allant de détectable à 2900 copies/mL. L'analyse statistique a montré que l'augmentation de l'âge était un facteur significatif dans la détection de l'ADN EqPV-H. Ni la race, ni la saison, ni l'état de grossesse, ni les antécédents de vaccination contre l'EHV-1 n'étaient significatifs pour prédire l'état de l'infection par l'EqPV-H.

(Traduit par Docteur Serge Messier)

Introduction

Theiler's disease (TD), also known as equine serum hepatitis, idiopathic acute hepatic disease, and post-vaccinal hepatitis, is an acute to subacute hepatitis that is one of the most commonly recognized causes of acute hepatic failure in adult horses (1–12). Theiler's disease was first reported in South Africa in 1918 by Sir Arnold Theiler while attempting to prevent African horse sickness following the simultaneous administration of live virus and convalescent equine antiserum to healthy horses. The disease was characterized by acute liver atrophy and diffuse hepatic necrosis, especially of the centrilobular region (13). In 2018, equine parvovirus-hepatitis (EqPV-H) was detected in the serum and liver tissue of a horse that died of TD in Nebraska, USA 65 d after treatment with equine origin

Department of Pathobiology (Papapetrou, Lillie) and Department of Clinical Studies (Arroyo, Baird) Ontario Veterinary College, University of Guelph, Ontario, Canada; Department of Molecular and Medical Virology, Faculty of Medicine, Ruhr-University Bochum, 44801 Bochum, Germany (Meister, Steinmann).

Address all correspondence to Dr. Luis G. Arroyo; Telephone: +1-226-924-5827; email: larroyo@uoguelph.ca

This research was funded by Equine Guelph.

Received November 3, 2022. Accepted January 19, 2023.

FOR PERSONAL USE ONLY

tetanus antitoxin (TAT). The virus was detected by unbiased next-generation sequencing from liver tissue of the fatal case (10). The association of EqPV-H with TD has been made despite the lack of a pure, clonal EqPV-H inoculum to confirm disease causation (14). The administration of EqPV-H contaminated biologic products of equine origin such as plasma, tetanus and botulism antitoxins, antiserum against *Streptococcus equi* subsp. *equi*, and allogenic stem cells transplants had been strongly associated with the development of the disease (2,6,7,10,12,13,15–17). Cases of TD have also been reported in horses that did not receive any equine biologic products, as well as in-contact horses with EqPV-H-associated cases suggesting horizontal transmission of EqPV-H (3,13,18). EqPV-H has been shown to be hepatotropic and has been associated with clinical and subclinical cases of TD (10–12,15,16), and the virus has been shown to infect and replicate in hepatocytes (15,16).

EqPV-H is a non-enveloped, icosahedral, single-stranded DNA virus with a genome size of 4 to 6 kb. This virus belongs to the species *Ungulate copiparvovirus 6*, genus *Copiparvovirus*, and family *Parvoviridae* (10,19,20), and is present worldwide (14,19,21–28). In a study of 18 commercial equine serum samples, 11 had detectable EqPV-H DNA with a viral load up to 10^5 copies/mL. The countries of origin with detectable viral genomes included the USA, Canada, New Zealand, Italy, and Germany, suggesting a worldwide distribution of EqPV-H (22,23). Studies on clinically healthy horses in the USA, China, Germany, Austria, Brazil, South Korea, France, and Australia, have shown the prevalence of EqPV-H DNA in the serum and blood to range from 3.2 to 19.8% (10,14,23,24,26–31). Most horses that become infected with EqPV-H do not exhibit any clinical signs or laboratory evidence of infection (10,21,27). When EqPV-H causes disease, it is mostly subclinical or mild hepatitis, with fulminant hepatic necrosis (Theiler's disease) being a rare outcome (21). Oral, nasal, and fecal shedding of viral DNA has been demonstrated and successful oral transmission in 1 horse has been reported; however, the primary routes of EqPV-H transmission are not yet known (15,21).

Several factors including increasing age, breed, and sampling season are known to affect the prevalence of EqPV-H in clinically healthy horse population; however, the epidemiology of this virus is largely unknown (14,17). Research on EqPV-H transmission, epidemiology, risk factors, pathogenesis, and clinical presentation continues to be conducted. Most cases of TD have been reported during the summer and fall (3,5,11,18). Recent studies suggest a possible oral transmission; however, the seasonal presentation of TD suggests a potential role for mechanical insect transmission through horse flies, although this has not yet been demonstrated (15).

Although EqPV-H-associated hepatic disease had been reported in several countries, the worldwide prevalence remains largely unknown. It has been suggested that further prevalence studies of EqPV-H from various continents would be required to obtain a more detailed epidemiology of EqPV-H (22). Prevalence studies of EqPV-H in healthy horses have not been conducted in Canada. The aim of this study was to determine the prevalence of viral EqPV-H DNA in serum among healthy broodmares of various breeds located on farms in Ontario, Canada using serum samples collected between 2016 and 2017 from a previous study on EHV-1. The relationship of age, farm location, season, and breed with molecular prevalence of EqPV-H was also investigated. Pregnancy and EqPV-H has not been studied in the current literature, and thus this study also aimed to investigate whether pregnancy influenced the EqPV-H molecular prevalence. In addition, the EHV-1 vaccination information was available and included in the analysis for a possible relationship to EqPV-H.

Materials and methods

Study design and population

For this study, a subset of serum samples (n = 170) collected from 388 healthy broodmares (aged 2 to 27 y; mean: 10.7 y) between December 2016 to October 2017 were selected. The horses were from 37 farms in southern Ontario. Mares were determined healthy by physical examination at the time of sample collection. The number of serum samples required was calculated using the Ontario horse population and the average EqPV-H prevalence (9.72%) reported from other countries. According to the Canadian Census of Agriculture, there were 64 536 horses located on 9294 farms in Ontario (32). With an expected prevalence in Ontario of 9.72%, and a confidence interval (CI) of 95%, the required sample size was 135 (33). Of the 388 broodmares available, 170 broodmares were selected based on age, breed, and geographical location of the farm, with only 1 sample per mare included in the study (Table I). The number of farms within the study was based on the number of farms from a previous study on EHV-1. This study aimed to have the largest geographical variety and greatest breed variety within the 170 broodmares chosen in this study. The location of the farms where the horses were sampled is shown in Figure 1. The ages of the horses were separated into groups based on increments of 8 y and ranged from 2 to 27 y (mean age = 10.7 y): ages 2 to 8 y (n = 67), ages 9 to 17 y (n = 75), ages 18 to 27 (n = 25); with 3 horses not having an age recorded. Breeds were reduced to 5 categories for analysis: Thoroughbreds (n = 48), Warmbloods (Dutch and Hanoverian) (n = 43), Standardbreds (n = 40), Drafts (Belgian, Clydesdale, Friesian, Percheron, and Canadian) (n = 26), and other breeds (Rocky Mountain, Quarter horse, and pony breeds) (n = 12); the breed of 1 horse was not recorded. The pregnancy status of the broodmares at the time of sampling was pregnant (n = 103) or not pregnant (n = 67). Mares were confirmed pregnant by the farm veterinarian and either live foaling or abortions were recorded. Therefore, all the mares chosen for this study were known to deliver a live foal before the samples were selected for testing. EHV-1 vaccination status was also investigated and grouped as vaccinated (n = 138) or unvaccinated (n = 32). The study aimed to account for a possible seasonal distribution, by sampling across 4 seasons defined as winter (December, n = 34), spring (June, n = 41), summer (August, n = 38), and fall (October, n = 47).

Serum samples and EqPV-H DNA detection

Serum samples previously collected for another study stored at −80°C were used. DNA was isolated from 200 μL of serum using the QIAamp Minelute virus kit as per the manufacturer's instructions (Cat. No. 57704, Qiagen, Hilden, Germany). DNA was eluted into 50 μL volumes and stored at −20°C. DNA was then aliquoted into 15 μL quantities, frozen at −20°C for storage and shipped on dry ice from Canada to Germany for a probe-based quantitative polymerase

FOR PERSONAL USE ONLY

Table I. Age, breed, month of sampling, pregnancy status, and EHV 1 vaccination status of 170 healthy broodmares sampled in Ontario.

Age of broodmares *(n)*	Breed	*(n)*	Sampling date	*(n)*	Pregnancy status	*(n)*	EHV-1 vaccination status	*(n)*
2 to 8 y								
67	Thoroughbred	48	December 2016	34	Pregnant	103	Vaccinated	138
9 to 17 y								
75	Warmblood	43	June 2017	41	Not pregnant	67	Unvaccinated	32
18 to 27 y								
25	Standardbred	40	August 2017	48				
Unknown								
3	Draft	26	October 2017	47				
	Other	12						
	Unknown	1						

EHV — Equine herpes virus.

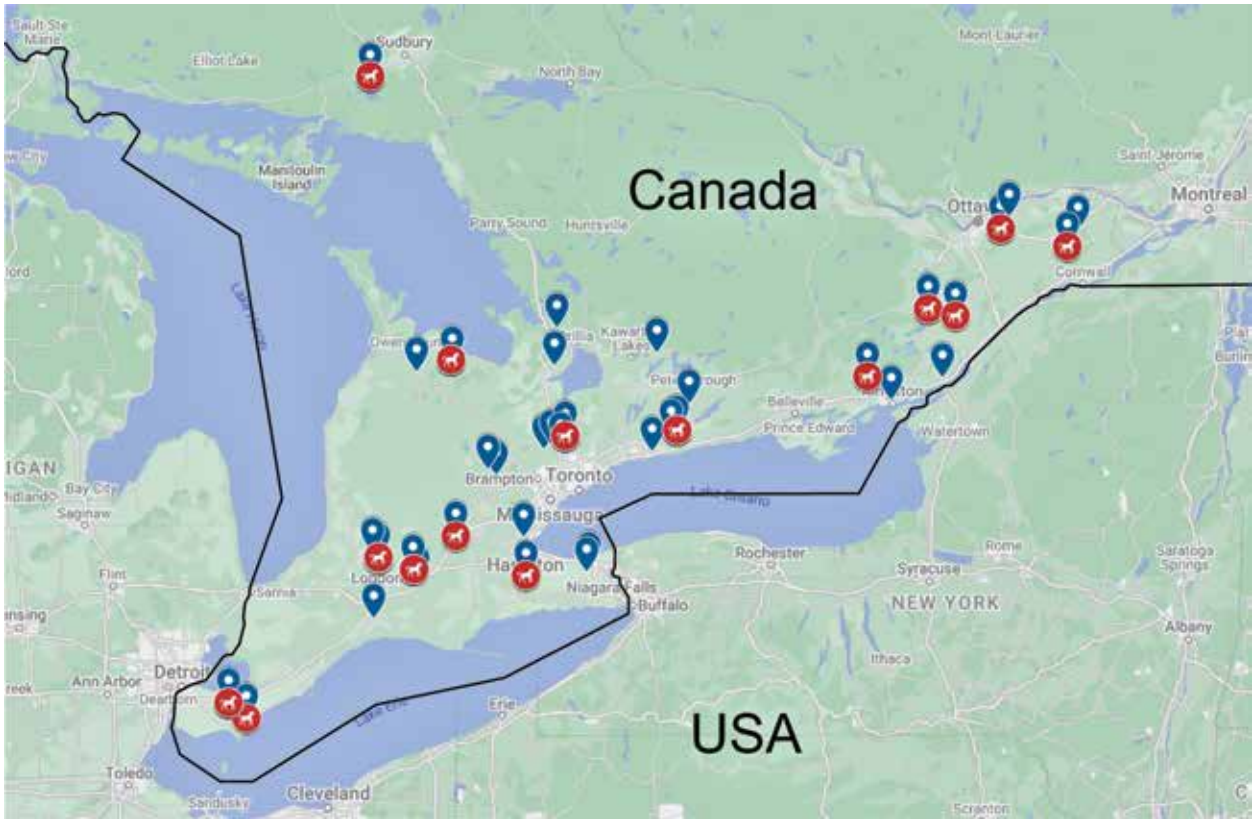


Figure 1. Location in Ontario of 37 breeding farms with at least one EqPV-H DNA serum positive horse (red circles with white horse) (*n* = 15) and farms with no EqPV-H serum positive horses (blue inverted drops) (*n* = 22).

chain reaction (qPCR). The qPCR for EqPV-H DNA was performed using primers and probes previously described by Divers *et al* (10), with the qRT-PCR was completed under the parameters as described in Meister *et al* (22,23). In brief, a serial dilution of a plasmid containing the EqPV-H structural protein (VP1)-encoding sequence was to provide a standard curve for the quantification of EqPV-H viral loads. qPCR measurements were performed using the LightCycler 480 real-time PCR system (Roche, Mannheim, Germany). The limit of detection (LOD) was 10 DNA copies/reaction.

Data and statistical analysis

All statistical analyses compared the EqPV-H DNA positive (DNA+) group against the EqPV-H DNA negative group (DNA−). Relationship of EqPV-H infection status using DNA prevalence, was evaluated between age, season, and/or breed using binary logistic regression models in IBM SPSS Statistics version 28 (IBM Corp, 2021). Chi-square tests were used to analyze the difference in frequency of distribution for some parameters studied (pregnancy status,

FOR PERSONAL USE ONLY

Table II. Farms sampled with at least 1 positive broodmare, broodmares sampled *per* farm, number of EqPV-H DNA positive mares, and mean age of EqPV-H DNA positive mares.

Farm ID	Number sampled	Number DNA+	Mean age (y)
1	3	3	11.7
2	2	1	19.5
3	2	1	13.5
4	2	1	9
5	7	3	12.6
6	9	3	9.5
7	6	2	10.6
8	3	1	9.7
9	7	2	5.7
10	8	2	14.9
11	5	1	11.8
12	5	1	10.8
13	11	2	9.5
14	13	2	11.9
15	17	2	9.5

EqPV-H — Equine parvovirus-hepatitis.

vaccination status, age, season, and breed). Pairwise comparisons with estimated marginal means between the DNA+ against the DNA− group for the different age groups and breeds. Any horses with unknown ages ($n = 3$) were excluded in the age-related statistical analyses. The null hypothesis was rejected when $P < 0.05$. The number of other horses on farm, and data on their demographics was not available. Therefore, accurate information on total number of horses per farm, or the breeds on farm, use of the horse, *etc.*, could not be included in the statistical analysis. As some farms had only one animal sampled, the absence of within-farm variation on some farms could bias the model significance so farm effect was not included in the data analysis.

Results

EqPV-H detection

In this study, EqPV-H DNA was detected in serum samples of 27 of 170 broodmares resulting in a prevalence of 15.9%. The EqPV-H DNA positive horses were located on 15 of the 37 farms sampled in southern Ontario, Canada, and the location of the EqPV-H positive horses according to the farm of origin is depicted in Figure 1. Farms with EqPV-H DNA positive horses were discovered throughout the sampling area in southern Ontario (Windsor to Cornwall, see Figure 1). Detection rates across farms varied between 0 and 100.0% (Table II). On 22 farms none of the horses tested positive for EqPV-H DNA.

Characteristics of EqPV-H DNA positive horses and statistical analysis

In this study, the highest percentage of EqPV-H DNA positive horses were the 18 to 27-year-old group of horses with 36.0%, whereas the lowest number of EqPV-H DNA positive horses was in the youngest group with 11.9% (Figure 2, Table III). Accordingly,

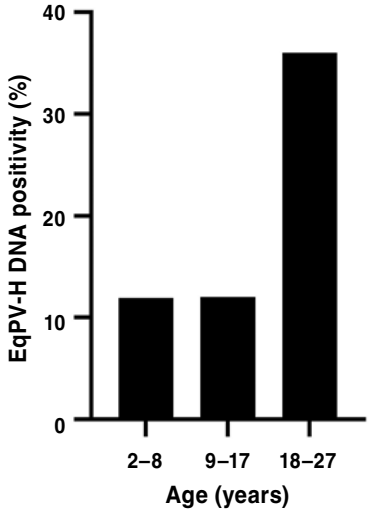


Figure 2. Presence of EqPV-H DNA in serum as percent positivity by age group.

the mean age of horses that were EqPV-H DNA positive was 13.6 y; this depicted a 2.9-year increase from the average age of 10.7 y in the sampled population. The Chi-square test comparing the difference in age groups with and without infection was statistically significant [χ^2 ($n = 2$) = 9.337, $P = 0.009$]. Furthermore, pairwise comparisons with marginal means estimated from a generalized linear model between different age groups with all pairwise comparisons corrected using least significant difference indicated significant comparisons between age groups 2 to 8 y *versus* 18 to 27 y ($P = 0.021$) and 9 to 17 y *versus* 18 to 27 y ($P = 0.020$).

EqPV-H DNA positivity based on breed was 12/40 for Standardbreds (30%), 9/43 for Warmbloods (20.9%), 4/48 for Thoroughbreds (8.3%), 1/12 for Other (8.3%) and 1/26 for Drafts (3.8%) (Table III). Statistical comparisons between breeds, Drafts *versus* Standardbreds ($P = 0.001$), Thoroughbreds *versus* Standardbreds ($P = 0.009$), Warmbloods *versus* Drafts ($P = 0.019$), and Other breeds *versus* Standardbreds ($P = 0.031$) were performed. The binomial logistic regression on the different breeds showed that breed had a statistically significant effect on EqPV-H status ($P = 0.034$), but individual breeds did not have a significant effect. Conversely, the Chi-square test comparing the difference in breed groups with and without infection was statistically significant [χ^2 ($n = 4$) = 12.307, $P = 0.015$].

When comparing the seasonal distribution, the same Chi-square test as well as pairwise comparisons were not statistically significant in predicting EqPV-H status [χ^2 ($n = 3$) = 6.996, $P = 0.072$; and $P = 0.09$], although different positivity rates between sample months were observed. The highest EqPV-H DNA prevalence in serum (25.5%) was detected in October followed by June (19.5%). The lowest number of EqPV-H DNA positive horses was identified in August (8.3%) and December (8.8%) (Table III).

EqPV-H DNA positivity based on pregnancy status was 16.5% (17/103) for pregnant broodmares 14.9% (10/67) for non-pregnant mares (Table III) showing no significant difference according to Chi-square tests ($\chi^2 = 0.076$, $P = 0.783$). Similarly, the EHV-1 vaccination status did not correlate with EqPV-H DNA positivity

FOR PERSONAL USE ONLY

Table III. Number and percentage of EqPV-H DNA positive mares according to age, breed, month of sampling, pregnancy status and EHV 1 vaccination status of 170 healthy broodmares sampled in Ontario.

	Number tested	EqPV-H DNA+	Positive %
Age			
2 to 8 y	67	8	11.9
9 to 17 y	75	9	12.0
18 to 27 y	25	9	36.0
Unknown	3	1	33.3
Breed			
Standardbred	40	12	30.0
Warmblood	43	9	20.9
Thoroughbred	48	4	8.3
Other breeds	12	1	8.3
Drafts	26	1	3.8
Unknown	1	0	0
Sample month			
June	41	8	19.5
August	48	4	8.3
October	47	12	25.5
December	34	3	8.8
Pregnancy status			
Pregnant	103	17	16.5
Not pregnant	67	10	14.9
Vaccination status			
Vaccinated	138	23	16.7
Unvaccinated	32	4	12.5

($\chi^2 = 0.338$, $P = 0.561$). EqPV-H DNA positivity based on vaccination status was 16.7% (23/138) for vaccinated mares, and 12.5% (4/32) for unvaccinated mares (Table III).

In conclusion, these data suggest a correlation between age and EqPV-H DNA positivity as well as breed and EqPV-H DNA positivity. All the other factors reported in this study did not affect EqPV-H DNA prevalence.

Discussion

A prevalence of 15.9% for EqPV-H DNA was determined in a population of clinically healthy broodmares of various breeds and ages in Ontario. This prevalence is consistent with previous studies of clinically healthy horses in other countries worldwide (10,23,24,26,28–30). Similar percentages have been reported in the USA, China, Brazil, and South Korea, whereas lower prevalences were reported in Germany, Austria, France, or Australia (Table IV). However, multiple studies performed in Germany, USA, and South Korea have shown varying detection rates of EqPV-H DNA. Similar variations were observed across farms sampled in this study in the area from Windsor to Ottawa (Table II) as well as 5 farms in the Guandong province in China (24), and on farms in Brazil (26). These data suggest environmental factors and other characteristics such as age, seasonality, breed, and the route of transmission potentially affect the geographical distribution of EqPV-H.

Table IV. Prevalence of EqPV-H DNA in serum and blood reported in clinically healthy horse populations throughout the world.

Country	Number of horses tested	EqPV-H DNA detected in	EqPV-H PCR positive	Reference
USA	100	Serum	13%	(10)
China	143	Serum	11.9%	(24)
USA	41	Plasma	17%	(34)
Germany	392	Serum	7.1%	(23)
China	60	Serum	8.3%	(29)
Brazil	96	Serum	12.5%	(26)
South Korea	321	Serum	4.4%	(25)
France	259	Serum	4.6%	(27)
Australia	188	Serum	3.2%	(27)
USA	87	Blood	5.7%	(35)
Germany	80 81	Serum	5.0% 19.8%	(28)
South Korea	160	Serum	10.6%	(31)
Austria	259	Serum	8.9%	(14)
Canada	170	Serum	15.9%	This study

EqPV-H — Equine parvovirus-hepatitis.

For instance, active infection with EqPV-H has been seen more commonly in older horses (23). In a study of Austrian horses, a significantly higher probability of active EqPV-H infection was identified in 16- to 31-year-old horses, compared with 1- to 8-year-old horses and 9- to 15-year-old horses (14). In a study from South Korea, however, the breeding horse population with the oldest average age (12.1 y) had the highest serum prevalence rate of EqPV-H DNA (12/32, 37.5%) (30). In general, the risk of active EqPV-H infection was 1.1 times higher with every year increase in age (14). Similar to previous reports we determined that EqPV-H DNA was significantly more likely to occur in aged horses. Age was the main factor affecting the EqPV-H serum DNA status of the mares, as the risk of exposure to EqPV-H increases over time. Whether older horses become more susceptible to infection remains to be determined.

This study discovered a higher prevalence in June and October, although this difference was not statistically significant. Other studies on TD have reported cases occurring mainly in summer and fall; however, the specific month(s) of occurrence was not reported (3,5,11,16,18). Given the similar seasonality in our results, this suggests further investigation is warranted. In addition, the effect of breed on farm prevalence of EqPV-H is largely unknown. In Thoroughbred racehorses, a similar EqPV-H molecular

FOR PERSONAL USE ONLY

prevalence (11.9% and 8.33%) was reported in China, whereas in Germany, 7% of broodmares and stallions examined tested positive (23,24,29). In China, EqPV-H infection was highly prevalent in imported Thoroughbred horses (9/17, 52.9%) (24), whereas in South Korea the highest prevalence of EqPV-H DNA in serum was reported in breeding horses from the USA with 11 of 23 (47.8%) being positive (30). In contrast, 54 serum samples from Jeju horses, an indigenous Korean breed, were all EqPV-H DNA negative (30). This study reported that the overall impact of breed on predicting EqPV-H status was significant based on binominal logistic regression. However, the binomial logistic regression on the individual breed groups did not have a significant effect on predicting EqPV-H status. Thus, it is difficult to state which breed group is most at risk for EqPV-H infection.

Previous research has provided evidence that many routes of transmission of EqPV-H are possible, including through plasma-derived products of equine origin that test positive for EqPV-H (10,15). Whether EqPV-H was introduced by equine-origin biological products in this study is unknown. Although administration of contaminated biologics of equine origin remains the most likely route of transmission, horse-to-horse transmission is suspected to occur where no equine-origin biologic products have been administered (11,13,18). Studies on farms that have had recent confirmed clinical cases of TD have shown a high prevalence of EqPV-H viremia in the in-contact horses (54 to 61.8%), which suggests direct contact as a potential route of transmission (11,19,36). However, another study investigating vertical and mechanical arthropod vectors using horse flies could not demonstrate transmission of EqPV-H (15). Further studies are needed to investigate and confirm infection through other routes of transmission. Experimental studies have demonstrated shedding of EqPV-H *via* multiple routes including nasal/oral secretions and *via* feces (15). Low levels of fecal shedding of EqPV-H have been reported around the time of EqPV-H viremia (14,21).

In Germany, persistent infections with EqPV-H have been identified in horses that did not show biochemical or pathological signs of liver disease. EqPV-H viremia was detected in the serum of 45 horses over a 5-year period. Prolonged EqPV-H viremia without clinical disease emphasizes the diagnostic difficulty with ascribing hepatitis to parvoviral infection when the viral load is low (28). Of note, low levels of genetic diversity have been demonstrated in the EqPV-H sequences reported throughout the world suggesting there is a high degree of conservation and genomic stability (10,11,14,23–26,29,30), and broad relevance of results in this study to other regions.

In conclusion, EqPV-H DNA was detected in the serum of 15.9% (27/170) healthy broodmares of various breeds located on 15/37 farms in Ontario, Canada. The EqPV-H DNA viral loads in the 27 positive horses ranged from detectable to 2900 copies/mL. Increasing age was a significant predictor (P = 0.009) of testing EqPV-H DNA positive. The season when sampled or pregnancy status was not a significant factor in predicting EqPV-H infection status in this study. Further studies are needed to fully explore the effect that breed may have on EqPV-H infection status.

Acknowledgment

We are grateful to Jutta Hammermueller for her technical assistance.

References

1. Hjerpe CA. Serum hepatitis in the horse. J Am Vet Med Assoc 1964;144:734–740.
2. Panciera RJ. Serum hepatitis in the horse. J Am Vet Med Assoc 1969;155:408–410.
3. Thomsett LR. Acute hepatic failure in the horse. Equine Vet J 1971;3:15–19.
4. Tennant B, Baldwin B, Evans CD, Kaneko JJ. Diseases of the equine liver. Proceedings of the 21st Annual Convention of American Association of Equine Practitioners, December 1–3, 1975, Boston, Massachusetts, 1975;21:410–426.
5. Tennant B. Acute hepatitis in horses: Problems of differentiating toxic and infectious causes in the adult. Proceedings of the 24th Annual Convention of American Association of Equine Practitioners, December 2–6, 1978, St. Louis, Missouri, 1978; 24:465–471.
6. Messer NT, Johnson PJ. Serum hepatitis in two brood mares. J Am Vet Med Assoc 1994;204:1790–1792.
7. Messer NT, Johnson PJ. Idiopathic acute hepatic disease in horses: 12 cases (1982–1992). J Am Vet Med Assoc 1994;204:1934–1937.
8. Guglick MA, MacAllister CG, Ely RW, Edwards WC. Hepatic disease associated with administration of tetanus antitoxin in eight horses. J Am Vet Med Assoc 1995;206:1737–1740.
9. Aleman M, Nieto JE, Carr EA, Carlson GP. Serum hepatitis associated with commercial plasma transfusion in horses. J Vet Intern Med 2005;19:120–122.
10. Divers TJ, Tennant BC, Kumar A, *et al.* A new parvovirus associated with serum hepatitis in horses after inoculation of common biological product. Emerg Infect Dis 2018;24:303–310.
11. Baird J, Tegtmeyer B, Arroyo L, *et al.* The association of Equine Parvovirus-Hepatitis (EqPV-H) with cases of non-biologic-associated Theiler's disease on a farm in Ontario, Canada. Vet Microbiol 2020;242:108575.
12. Divers TJ, Tomlinson JE, Tennant BC. The history of Theiler's disease and the search for its aetiology. Vet J 2022;287:105878.
13. Theiler A. Acute liver-atrophy and parenchymatous hepatitis in horses, The Fifth and Sixth Reports of the Director of Veterinary Research, Department of Agriculture, Union of South Africa. Pretoria, South Africa: Government Printing and Stationery Office, 1918:7–164.
14. Badenhorst M, de Heus P, Auer A, *et al.* Active equine parvovirus-hepatitis infection is most frequently detected in Austrian horses of advanced age. Equine Vet J 2022;54: 379–389.
15. Tomlinson JE, Jager M, Struzyna A, *et al.* Tropism, pathology, and transmission of equine parvovirus-hepatitis. Emerg Microbes Infect 2020;9:651–663.
16. Vengust M, Jager MC, Zalig V, *et al.* First report of equine parvovirus-hepatitis-associated Theiler's disease in Europe. Equine Vet J 2020;52:841–847.
17. Tomlinson JE, Kapoor A, Kumar A, *et al.* Viral testing of 18 consecutive cases of equine serum hepatitis: A prospective study (2014–2018). J Vet Intern Med 2019;33:251–257.
18. Tomlinson JE, Tennant BC, Struzyna A, *et al.* Viral testing of 10 cases of Theiler's disease and 37 in-contact horses in the

FOR PERSONAL USE ONLY

absence of equine biologic product administration: A prospective study (2014–2018). J Vet Intern Med 2019;33:258–265.
19. Ramsauer AS, Badenhorst M, Cavalleri JMV. Equine parvovirus-hepatitis. Equine Vet J 2021;53:886–894.
20. Pénzes JJ, Söderlund-Venermo M, Canuti M, *et al.* Reorganizing the family *Parvoviridae*: A revised taxonomy independent of the canonical approach based on host association. Arch Virol 2020;165:2133–2146.
21. Jager MC, Tomlinson JE, Lopez-Astacio RA, Parrish CR, Van de Walle GR. Small but mighty: Old and new parvoviruses of veterinary significance. Virol J 2021;18:210.
22. Meister TL, Tegtmeyer B, Postel A, *et al.* Equine parvovirus-hepatitis frequently detectable in commercial equine serum pools. Viruses 2019;11:461.
23. Meister TL, Tegtmeyer B, Brüggemann Y, *et al.* Characterization of equine parvovirus in thoroughbred breeding horses from Germany. Viruses 2019;11:965.
24. Lu G, Sun L, Ou J, Xu H, Wu L, Li S. Identification and genetic characterization of a novel parvovirus associated with serum hepatitis in horses in China. Emerg Microbes Infect 2018;7:170.
25. Lee SK, Park D, Lee I. Molecular prevalence of equine parvovirus-hepatitis in the sera of clinically healthy horses in South Korea. Vet Sci 2021;8:282.
26. de Moraes MV dos S, Salgado CRS, Godoi TLOS, *et al.* Equine parvovirus-hepatitis is detected in South America, Brazil. Transbound Emerg Dis 2022;69:3022–3027.
27. Fortier C, El-Hage C, Hue E, *et al.* Hepatitis viruses: Prevalence of equine parvovirus-hepatitis virus and equine hepacivirus in France and Australia. Equine Vet J 2021;53:68.
28. Reinecke B, Klöhn M, Brüggemann Y, *et al.* Clinical course of infection and cross-species detection of equine parvovirus-hepatitis. Viruses 2021;13:1454.
29. Lu G, Wu L, Ou J, Li S. Equine parvovirus-hepatitis in China: Characterization of its genetic diversity and evidence for natural recombination events between the Chinese and American strains. Front Vet Sci 2020;7:121.
30. Yoon J, Park T, Kim A, *et al.* First report of equine parvovirus-hepatitis and equine hepacivirus coinfection in horses in Korea. Transbound Emerg Dis 2021;10:1111.
31. Yoon J, Park T, Kim A, *et al.* First clinical case of equine parvovirus-hepatitis-related Theiler's disease in Asia. Viruses 2021;13:1917.
32. Statistics Canada. Table 32-10-0373-01 Other livestock inventories on farms, Census of Agriculture, 2021. DOI: https://doi.org/10.25318/3210037301-eng
33. Sergeant ESG. Epitools Epidemiological Calculators. Ausvet. Available from: http://epitools.ausvet.com.au Last accessed April 14, 2023.
34. Altan E, Li Y, Sabino-Santos G, Jr, *et al.* Viruses in horses with neurologic and respiratory diseases. Viruses 2019;11:942.
35. Pusterla N, James K, Barnum S, Delwart E. Investigation of three newly identified equine parvoviruses in blood and nasal fluid samples of clinically healthy horses and horses with acute onset of respiratory disease. Animals (Basel) 2021;11:3006.
36. Meister TL, Arroyo LG, Shanahan R, *et al.* Infection of young foals with equine parvovirus-hepatitis following a fatal non-biologic case of Theiler's disease. Vet Microbiol 2022;274:109557.

FOR PERSONAL USE ONLY

Development of an indirect ELISA method based on the VP1 protein for detection of IgG antibodies against porcine sapelovirus

Jiajia Liu, Benqiang Li, Jie Tao, Jinghua Cheng, Ying Shi, Changtao Qiao, Xiaohui Shen, Huili Liu

Abstract

Porcine sapelovirus (PSV) is a newly emerging enterovirus that is widely prevalent in China. Since there is no clinical serological testing for PSV, the objective of this study was to develop an indirect enzyme-linked immunosorbent assay (i-ELISA) for detection of PSV immunoglobulin G (IgG) antibody in pigs. A PSV strain, named SHPD202148, was first isolated from the fecal samples of piglets. Its structural protein, VP1, was prokaryotic-expressed in the pET expression system, followed by purification. Using the recombinant protein with reactogenicity as coating antigen, an i-ELISA, characterized by high sensitivity and specificity, had a detection limit at 1:12 800 dilution with a determined cutoff value of 0.352. Finally, field sera collected from different pig herds were tested in parallel by the serum neutralization (SN) test. The result showed that 126 samples were positive and 36 were negative, with an agreement of 97.0% in both cases. This i-ELISA can be used as an alternative serological test for detecting antibodies against PSV in blood serum.

Résumé

Le sapelovirus porcin (PSV) est un entérovirus nouvellement émergent largement répandu en Chine. Puisqu'il n'y a pas de test sérologique clinique pour le PSV, l'objectif de cette étude était de développer un test immuno-enzymatique indirect (i-ELISA) pour la détection d'immunoglobuline G (IgG) anti-PSV chez les porcs. Une souche de PSV, nommée SHPD202148, a d'abord été isolée à partir d'échantillons fécaux de porcelets. Sa protéine structurale, VP1, a été exprimée par un procaryote dans le système d'expression pET, suivie d'une purification. Utilisant la protéine recombinante à réactogénicité comme antigène de revêtement, un i-ELISA, caractérisé par une sensibilité et une spécificité élevées, avait une limite de détection à une dilution de 1:12 800 avec une valeur seuil déterminée de 0,352. Enfin, des sérums de terrain collectés dans différents troupeaux de porcs ont été testés en parallèle par le test de neutralisation sérique (SN). Le résultat a montré que 126 échantillons étaient positifs et 36 étaient négatifs, avec un accord de 97,0 % dans les deux cas. Cet i-ELISA peut être utilisé comme test sérologique alternatif pour détecter les anticorps anti-PSV dans le sérum sanguin.

(Traduit par Docteur Serge Messier)

Introduction

Porcine sapelovirus (PSV), also known as porcine enterovirus 8 (PEV8), is a member of the *Picornaviridae* family (1). It is a newly emerging infectious disease in pigs transmitted by the fecal-oral route that can cause multiple system syndromes, such as porcine cerebral poliomyelitis, diarrhea, pneumonia, respiratory distress, and reproductive disorder (2,3). In pregnant sows, PSV can cause stillbirth, mummified fetuses, and fetal malformation.

Porcine sapelovirus mainly replicates in the intestinal epithelial cells of pigs. Infected pigs will continue to shed virus after recovery, thereby becoming an important source of infection. This may explain the high infection rate of PSV. It is worth noting that PSV has often co-infected with porcine epidemic diarrhea virus (PEDV), classical swine fever virus (CSFV), porcine reproductive and respiratory syndrome virus (PRRSV), porcine parvovirus virus (PPV), and other viruses, which may aggravate the disease through synergistic pathogenicity (4,5).

Porcine sapelovirus (PSV) was first reported in the United Kingdom in 1958 (6). Today, it is prevalent worldwide, including in China, Japan, Australia, Spain, and Brazil, with a positive rate of 6.4 to 75.5% (7–9). In China, PSV was first isolated in 2009 (10). It has been reported that the positivity rates of PSV in East China, South China, Sichuan, Hunan, and Ningxia were 17.2%, 18.21%, 20.4%, 42.21%, and 61.25%, respectively (11). Data on the prevalence and genetic evolution of PSV are still limited.

Porcine sapelovirus also exists in healthy pigs, similar to porcine astrovirus (PAstV) and porcine bocavirus (PBoV). Li *et al* (12)

Institute of Animal Husbandry and Veterinary Sciences, Shanghai Academy of Agricultural Sciences, Shanghai, 201106, PR China (J. Liu, Li, Tao, Cheng, Shi, Qiao, Shen, H. Liu); National Demonstration Center for Experimental Fisheries Science Education, Shanghai Ocean University, Shanghai, 201306, PR China (J. Liu).

Address all correspondence to Dr. Xiaohui Shen and Dr. Huili Liu; telephone: 86-021-62202473 (O); email: huilil@163.com; shenxiaohui@saas.sh.cn

Benqiang Li contributed an equal amount to this work as its first author.

Availability of data and materials

The datasets used and/or analyzed during this study are available from the corresponding author upon reasonable request.

Received October 31, 2022. Accepted March 14, 2023.

FOR PERSONAL USE ONLY

reported that both the single infection rates and the co-infected rates of PSV were higher than those in asymptomatic pigs. This could mean that the presence of PSV promotes the infection and pathogenesis of PEDV and other diarrhea pathogens. It is therefore urgent that clinical technology be developed for detection of PSV.

VP1 is a structural protein with an antigen epitope, which is an ideal object for establishing an effective clinical detection technology (13,14). Although antibody surveillance is a key step in controlling and preventing disease, there are limited methods for monitoring PSV antibodies in pig herds.

In this study, a newly isolated PSV strain was identified, followed by expression and purification of VP1 protein. An indirect enzyme-linked immunosorbent assay (i-ELISA) was then established to detect anti-PSV-specific serum immunoglobulin (IgG) antibody by coating the ELISA plate with purified protein as antigen. This will be an effective technology for monitoring clinical antibodies, as results showed that it had high sensitivity and specificity.

Materials and methods

All animal experiments were conducted in accordance with approved guidelines (approved permit number SAASPZ0522054).

Plasmid and serum samples

Plasmid pET-30a(+), positive serum and negative serum against PSV, were prepared and preserved in our laboratory. PSV-positive serum was produced by piglets infected with the SHPD202148 strain. Positive serum against other pathogens, including classical swine fever virus (CSFV), porcine epidemic diarrhea virus (PEDV), porcine pseudorabies virus (PRV), porcine reproductive and respiratory syndrome virus (PRRSV), foot-and-mouth disease virus (FMDV), and bovine viral diarrhea virus (BVDV), were purchased from the China Institute of Veterinary Drug Control. All sera were stored at −80°C.

Clinical samples and virus isolation

Piglet fecal samples were collected from a pig herd in Jiangsu, China. Resuspended and oscillated, the samples were centrifuged at 3500 × *g* for 10 min. The supernatant was treated with 1000 units/mL and 1000 μg/mL of Penicillin-Streptomycin Solution (Item No. 1S140122; ThermoFisher Scientific, Waltham, Massachusetts, USA) overnight at 4°C. Filtered using 0.22-μM Millex filters (MilliporeSigma, Burlington, Massachusetts, USA), the liquid was inoculated into porcine kidney (PK15) cells, adding 0.5 μg/mL TPCK-treated Trypsin (Sigma-Aldrich, St. Louis, Missouri, USA).

Cell cultures were collected 72 h later, after 3 freeze-thaw cycles. The sixth-passaged virus (SHPD202148) was identified by both real-time polymerase chain reaction (RT-PCR) and indirect immunofluorescence assay (IFA). Finally, the complete genome of the SHPD202148 strain was sequenced.

Indirect immunofluorescence assay (IFA)

The PK-15 cells were inoculated into 96-well plates for 24 h to 70% fusion. Cells were infected with PSV virus [multiplicity of infection (MOI) = 1] for 48 h. The plates were washed 3 times with phosphate-buffered saline with Tween20 (PBST), fixed with 4% paraformaldehyde for 15 min at room temperature, and washed again 3 times with PBST. Plates were then coated with 5% bovine serum albumin (BSA) diluted in phosphate-buffered saline (PBS) and placed in an incubator at 37°C for 2 h.

The plates were washed 3 times with PBST, then negative and positive piglet sera, diluted 1:200 in PBST were added and plates were incubated at 37°C for 2 h. After 3 washes with PBST, goat anti-pig fluorescein isothiocyanate conjugated (FITC)-labeled secondary antibody diluted 1:1000 (6911; Abcam, Shanghai, China) was added and plates were incubated at 37°C for 60 min. Plates were then washed with PBS and 4′6′-diamidino-2-phenylindole (DAPI) fluorescent stain (Beyotime, Shanghai, China) was added and plates were examined by fluorescence microscopy (Carl Zeiss, Oberkochen, Baden-Württemberg, Germany).

Expression and purification of recombinant VP1 protein

The viral VP1 gene sequence was amplified and ligated into BL21 (DE3) competent cells for subsequent expression. The primers for amplification of VP1 protein were: 5′-CATATGATGGGAGAT GTAAAGGAAGTDGTRAG-3′; 5′-AAGCTTAGHYTGGGTTGCAG GTARTA-3′.

Polymerase chain reaction (PCR) amplification conditions were 94°C, 5 s; 94°C, 30 s; 52°C, 30 s; 72°C, 35 s; 72°C, 8 min; 4°C cycle. The genome sequence has not been submitted to GenBank or other international databases. A positive colony of *Escherichia coli* BL21(DE3) was selected and incubated overnight at 37°C in a triangular flask of Luria-Bertani (LB) liquid medium containing 50 μg/mL of kanamycin, then centrifuged at 200 × *g*. Overnight cultures were inoculated into 1 L of LB medium at a ratio of 1:100 and incubated at 37°C. When OD_{600nm} values reached 0.6 to 0.8, isopropyl β-d-thiogalactopyranoside (IPTG) (Yuanye, R21348) was added at a final concentration of 0.5 mM and is induced at 200 × *g* at 37°C for 4 h.

Cells were collected by centrifugation at 5000 × *g* for 20 min and the supernatant was discarded. Collected bacterial cells were rinsed 3 times with PBS, resuspended in fragmentation buffer, and sonicated in an ice bath for fragmentation. The lysate was centrifuged at 4°C at 12 000 × *g* for 20 min and the supernatant and precipitate were collected for analysis by sodium dodecyl sulfate-polyacrylamide gel electrophoresis (SDS-PAGE). The recombinant VP1 protein was purified by His-Tag using Ni2+-NTA agarose gel affinity chromatography.

Western blot analysis

The specificity of the purified anti-PSV VP1 protein antiserum was tested by western blotting and immunofluorescence assay (IFA). A polyacrylamide gel was prepared and the PSV-VP1 protein was electrophoresed through this gel and then electrotransferred to the negative concordance (NC) membrane. The blocked membrane was washed 3 times with TBST for 10 min each time and placed in a 1:200 dilution of PSV-positive serum and incubated for 2 h at room temperature.

The membrane was again washed 3 times with TBST and HRP-labeled goat anti-pig IgG (H+L) conjugate (6915; Abcam), diluted 1:5000, was added and the membrane was incubated for 1 h at room temperature. The membrane was again washed 3 times with TBST and visualized with an appropriate amount of chemiluminescent reagent.

FOR PERSONAL USE ONLY

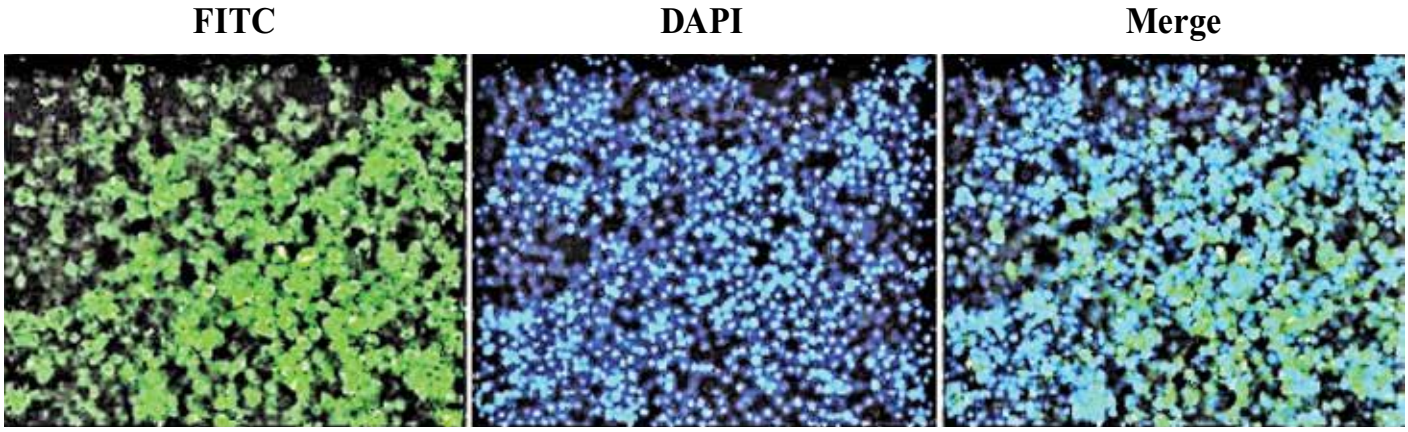


Figure 1. Immunofluorescence analysis by laser confocal microscopy of PSV-infected PK-15 cells. Immunofluorescence detection confirmed that strain SHPD202148 is recognized by anti-PSV polyclonal antibodies.

DAPI: Blue fluorescent stain; Abcam, 6911: Green fluorescence. ×200

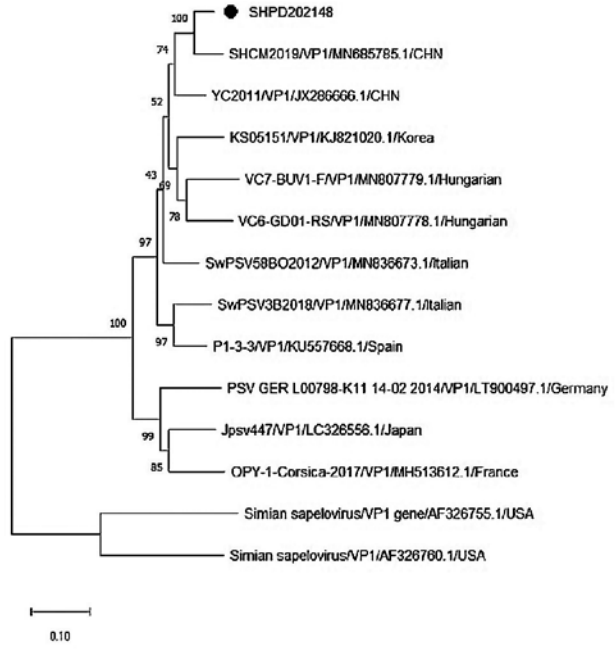


Figure 2. Phylogenetic analysis of PSV based on the VP1 gene. The phylogenetic trees were generated using MEGA-X with the neighbor-joining method with the Kimura 2-parameter with 1000 bootstrap replication. The black circle indicates that PSV was isolated in this study. The scale bars represent the number of substitutions per site.

Establishment of an indirect ELISA method

A volume of 50 μL of the diluted antigen was added to each well of a 96-well ELISA plate (ThermoFisher Scientific) and incubated at 37°C for 1 h. The purified VP1 protein was diluted (1:200, 1:400, 1:800, 1:1200, 1:1600) with 50-mM carbonate buffer (pH 9.6) (Coolaber, Beijing, China). The microplate was washed with PBS containing 0.05% Tween 20 (PBST). PBST containing 5% BSA was used as the blocking buffer and plates were blocked at 4°C for 12 h. Serum samples, diluted with PBST containing 5% BSA, were inoculated in triplicate and plates were incubated at 37°C for 1 h.

HRP-labeled goat anti-pig IgG conjugate (6915; Abcam) diluted (1:5000, 1:10 000, 1:15 000, 1:20 000) with PBST was added and plates were incubated at 37°C for 30 min. After each operation, the microplate was washed 3 times with 100 μL of PBST. The peroxidase reaction was visualized with 3,30,5,50-tetramethylbenzidine (TMB) solution as the substrate at 37°C for 8 min. The reaction was terminated by adding 100 μL of 2M sulfuric acid to each well.

All samples were tested in 3 replicates and optical density (OD) values were measured using a Microplate Spectrophotometer (Model 680; Bio-Rad, Shanghai, China) at a wavelength of 450 nm (OD_{450}). Conditions that produced the largest positive/negative (P/N) ratio of OD_{450} (OD_{450} of positive serum/OD_{450} of negative serum) were deemed the best reaction conditions.

In this experiment, *E. coli*-lacking VP1 protein insertion was used as a 'mock antigen preparation' and induction and purification were carried out according to the same protocol.

Determination of cutoff value

The OD_{450} values of 38 PSV-negative sera were determined by ELISA and the experiment was repeated 3 times. The mean and standard deviation of the OD values were calculated. The ELISA method used the mean OD value plus 3 times the standard deviation as the cutoff value for determining positive sera and the mean OD value plus 2 times the standard deviation as the cutoff value for determining negative sera, with the intermediate value being the suspect sample.

Specificity analysis

The OD_{450} values of CSFV, PEDV, PRV, PRRSV, FMDV, and BVDV-positive pig-derived sera were simultaneously tested using the ELISA method previously described to verify whether the recombinant VP1 protein cross-reacted with positive sera for other pathogens.

Repeatability analysis

For the intra-batch repeat test, the same batch of the viral solution was encapsulated in ELISA plates and 6 groups of samples with different antibody levels were taken. Each group was divided into

FOR PERSONAL USE ONLY

3 samples and the ELISA was carried out at 3 different time points. The assay results were counted and the standard deviation, mean, and coefficient of variation were calculated.

For the batch-to-batch repeat test, 3 different batches of viral solution were encapsulated in ELISA plates and 6 groups of samples with different antibody levels were subjected to ELISA. The results were counted and the coefficient of variation was calculated.

Sensitivity analysis

Three positive samples of serum were taken for multiplicative dilution, starting at 1:100 and diluted 2-fold, and their OD_{450nm} values were measured using the established ELISA method to evaluate their sensitivity.

Comparison of ELISA and SN tests

A total of 167 pig serum samples were collected from 5 pig herds in Shanghai and Jiangsu, China. All serum samples were detected by both the i-ELISA method and the serum neutralization (SN) test. The positive concordance (PC) and negative concordance (NC) rates of the 2 methods were calculated using the following formula:

PC (%) = (TP/total number of positives in SN test) × 100

where TP is the number of positives in both tests, NC (%) = (TN/total number of negatives in SN test) × 100 (where TN is the number of negatives in both tests). The total concordance rate (TC) = (TP + TN)/total number of serum samples tested × 100.

This established i-ELISA method was simultaneously applied to 435 porcine clinical sera. The clinical sera were collected in 2022 and provided by 11 farms in Shanghai and surrounding areas. The selection of farms was completely random.

Results

Identification and genomic characteristics of a newly isolated PSV strain

The fecal samples were treated and inoculated in PK-15 cells for continuous passage culture. Results of RT-PCR indicated that a positive band of 624 bp was amplified from the sixth-passaged cellular culture. Indirect immunofluorescence assay (IFA) confirmed that the polyclonal antibody against PSV VP1 protein could recognize the virus with specific green fluorescence (Figure 1).

The isolated PSV was named SHPD202148 and sequencing results showed that its full-length genome was 7425 bp. It was indicated that there were 73.1 to 92.0% (nucleotide) and 80.5 to 98.3% (amino acid) homology identities among SHPD202148 and other PSV reference strains of VP1 gene, respectively.

The phylogenetic tree based on the gene encoding VP1 protein showed that the SHPD202148 strain was most closely related to the SHCM2019 strain, which was isolated in Shanghai in 2019. All the Chinese strains were grouped in the same evolutionary cluster (Figure 2). The sequence similarity of the VP1 protein coding region between SHPD202148 isolate and representative strains from other countries was 72.3 to 98.6% (Figure 3).

Prokaryotic expression and identification of VP1 protein

The recombinant expression plasmid pET-30a(+)-VP1 gene was transferred into *E. coli* strain BL21(DE3) competent cells for prokaryotic expression. Results of SDS-PAGE showed that the recombinant protein VP1 was successfully expressed in the form of inclusion bodies with a band of 32.5 kDa (Figure 4 A). Further western blot testing confirmed that the VP1 recombinant protein could be recognized by PSV-positive serum (Figure 4 B).

Establishment and optimization of i-ELISA method

According to the checkerboard titration method, the antigen working concentration was selected as 2, 1, 0.5, and 0.25 μg/mL. The serum dilution was 1:200, 1:400, 1:800, 1:1200, and 1:1600 and the P/N ratio was determined. Results of checkerboard titration showed that, when the working concentration of antigen was 1 μg/mL and the serum dilution was 1:800, the P ratio was the closest to 1 and the P/N ratio was the largest at 7.037617. Therefore, the optimal concentration of VP1 protein was 1 μg/mL and the serum dilution was 1:800.

After incubating at 37°C for 1 h, the coated wells were washed 5 times with PBST, followed by blocking overnight at 4°C using 5% BSA. Serum samples were added at a dilution of 1:800 and the ELISA plate was incubated at 37°C for 1 h. After washing again, the HRP-goat anti-pig IgG at a dilution of 1:15 000 was added and the samples were incubated at 37°C for 45 min. When the "mock antigen preparation" was used as the antigen in the experiment, the clinical pig serum did not react in ELISA.

Determination of cutoff value for the i-ELISA method

The IgG antibody of 38 pig-negative sera samples was detected by the i-ELISA method developed in this study. Results showed that the mean OD_{450} value was 0.193, with a standard deviation (SD) of 0.053. According to the critical value judgment criterion of the mean OD value of negative sera ± 3 SD, the critical value of this i-ELISA method was determined to be 0.352. The OD_{450} values of ≥ 0.352 were judged as positive sera, whereas OD_{450} values of < 0.299 were judged as negative sera, with suspected positive sera between those 2 levels (Figure 5 A). The samples between negative and positive are suspected positive samples.

Specificity analysis

Specificity analysis confirmed that the i-ELISA method has great specificity, detecting only antibodies against PSV and showing no cross-reactivity with the positive sera against other diarrhea pathogens (Figure 5 B).

Repeatability analysis

The intra-assay coefficient of variation for VP1 protein ranged from 1.59 to 5.77% and the inter-assay coefficient of variation ranged from 0.18 to 5.82%, both less than 10%, which indicated that the established i-ELISA method is reproducible (Figure 5 C).

FOR PERSONAL USE ONLY

Percent identity

	1	2	3	4	5	6	7	8	9	10	11	12	13	14		
1		72.3	98.6	96.4	94.1	94.1	95.8	94.3	92.8	79.6	81.5	81.1	47.5	47.3	1	SHPD202148
2	34.6		72.5	70.8	92.5	91.4	72.9	72.1	69.1	59.9	60.7	60.7	33.3	33.6	2	MN685785.1
3	1.5	34.3		96.0	94.1	94.1	96.2	93.2	92.7	79.4	81.6	80.5	47.4	47.6	3	JX286666.1
4	3.6	37.0	4.1		96.8	94.1	96.2	93.2	93.5	79.6	81.5	81.1	46.8	47.7	4	KJ821020.1
5	6.1	7.9	6.1	3.3		95.7	95.6	92.3	92.4	81.3	82.9	82.4	41.4	43.3	5	MN807779.1
6	6.1	9.1	6.1	6.1	4.4		95.6	91.8	90.8	80.2	82.9	81.3	39.8	41.7	6	MN807778.1
7	4.3	33.6	3.9	3.9	4.5	4.5		93.9	93.5	80.2	82.9	81.4	47.9	48.1	7	MN836673.1
8	5.9	34.9	7.2	7.2	8.1	8.7	6.4		97.7	79.5	80.6	80.6	48.3	49.2	8	MN807777.1
9	7.5	39.8	7.7	6.8	8.0	9.8	6.8	2.3		78.8	79.9	79.6	48.2	49.5	9	KU557668.1
10	23.8	56.7	24.1	23.8	21.6	23.0	23.0	24.0	25.0		91.4	91.1	47.7	46.8	10	LT900497.1
11	21.3	55.2	21.2	21.3	19.5	19.5	19.5	22.5	23.4	25.0		93.6	46.4	46.6	11	LC326556.1
12	21.8	55.2	22.6	21.8	20.2	21.6	21.5	22.5	23.9	9.5	6.7		46.0	47.7	12	MH513612.1
13	86.8	140.9	86.9	88.9	106.3	112.3	85.7	84.6	84.8	86.3	90.0	91.1		71.5	13	AF326755.1
14	87.3	139.6	86.4	86.3	99.7	105.2	85.1	81.9	81.3	88.9	89.4	86.3	35.9		14	AF326760.1
	1	2	3	4	5	6	7	8	9	10	11	12	13	14		

Divergence

Figure 3. Homology comparison of sequences in protein coding region. The homology comparison diagram was drawn by DNAstar. The highest sequence similarity of VP1 protein coding region between SHPD202148 isolate and representative strains from different countries was 98.6%.

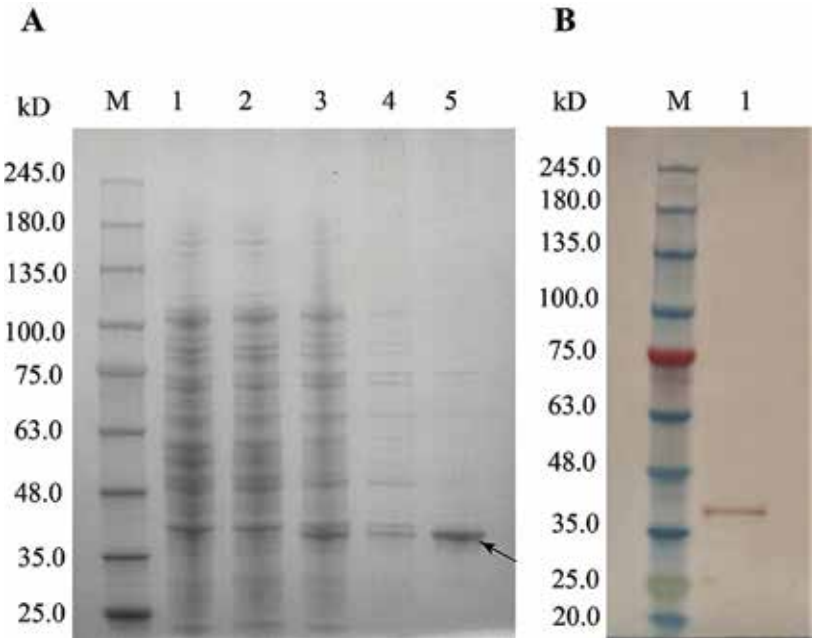


Figure 4. A — Identification of VP1 protein expressed by the pET-30a(+)-VP1 plasmid by SDS-PAGE. M — Molecular weight labeling; Lane 1 — pET-30a(+); Lane 2 — Uninduced pET-30a(+)-VP1; Lane 3 — Culture of pET-30a(+) after induction in *E. coli* BL21(DE3); Lane 4 — Supernatant of pET-30a(+)-VP1 after induction in *E. coli* BL21(DE3); and Lane 5 — Inclusion bodies of pET-30a(+)-VP1 after induction in *E. coli* BL21(DE3). B — Western blot analysis of the VP1 protein. M — Molecular weight marker; Lane 1 — *E. coli*-expressing pET-30a(+)-VP1.

Sensitivity analysis

Three porcine sapelovirus-positive sera were evaluated, starting at 1:100 dilution, and a 2-fold replacement was carried out using the conversion factor that would detect the maximum positive dilution as the sensitivity. The results showed positivity up to a dilution of 1:12 800, which indicated the high sensitivity of the method (Figure 5 D).

Agreement between i-ELISA method and SN test

A total of 167 field serum samples collected from different pig farms were examined in parallel using the i-ELISA method and the SN test. The SN test detected 39 negative sera and 128 positive sera, whereas i-ELISA reflected 38 negative sera and 129 positive sera (Table I).

FOR PERSONAL USE ONLY

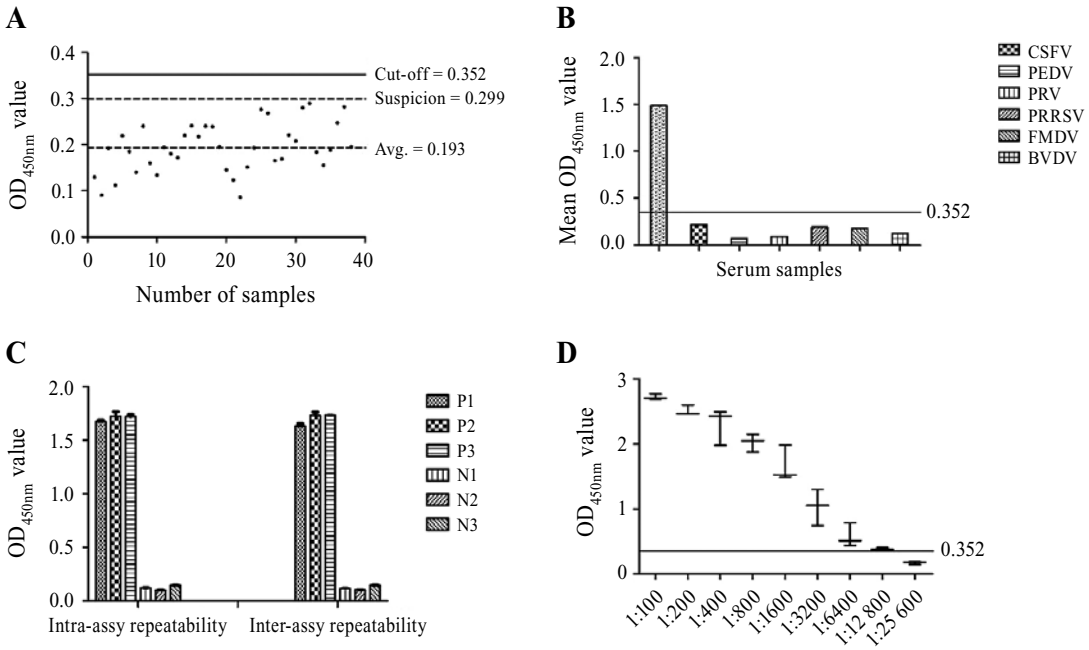


Figure 5. A — Determination of the cutoff value for the ELISA method. The average value plus 3 times the standard deviation was used as the cutoff value (0.352), *i.e.*, if the serum OD value of the test is ≥ 0.352, it is judged to be positive for PSV antibody, whereas OD values of < 0.299 are judged to be negative, with suspected positive sera between the 2 levels. B — Specificity analysis of the ELISA. The OD values of sera positive for common pathogens other than PSV were lower than the cutoff value of 0.352. C — PSV-VP1-ELISA method for reproducibility evaluation. Positive serum samples 1 to 3 (P1 to 3), negative serum samples 1 to 3 (N1 to 3). Reproducibility within and between assays was assessed using antigens from the same and different batches. Coefficients of variation were less than 10% for all samples. D — PSV-VP1-ELISA sensitivity analysis. PSV antiserum was serially diluted 2-fold (1:100 to 1:25 600) and tested using the established method. A maximum sensitivity of 1:12 800 was used as the cutoff value of 0.352.

Two samples were positive in the SN test, while being negative in the i-ELISA test and 3 samples were negative in the SN test, while being positive in the i-ELISA. In total, 126 samples were positive and 36 were negative in both cases, representing a consensus of 97.0% (162/167). The sensitivity of i-ELISA was therefore 98.4% (126/128) among PSV-seropositive samples and the specificity was 92.3% (36/39) among PSV-seronegative samples using the SN test as the standard evaluation method.

Meanwhile, the i-ELISA method was further applied to detect more clinical porcine serums. Altogether, 130 negative serums, 285 positive serums, and 20 suspected positive serums were used in a total of 435 serum samples (Figure 6).

Discussion

Porcine epidemic diarrhea virus (PEDV), porcine circovirus type 2 (PCV2), and porcine reproductive and respiratory syndrome virus (PRRSV) have long been considered important pathogens that cause multiple system syndromes in swine populations in China. Although researchers have focused on the pathogenesis of these viruses and the development of vaccines, there has been no improvement in the prevention and control of clinical epidemics, which have become increasingly complex. Perhaps this means that new angles and new breakthroughs should be explored in order to solve these clinical problems.

Clinical data have confirmed that the positive rates of PSV in domestic pig herds are rising continuously and the co-infection rate with PSV and other diarrheal pathogens is high. It has been speculated that there might be a synergistic pathogenic effect. We should therefore focus on the clinical monitoring of the viral variation of PSV.

In 2022, 4 strains of PSV were isolated in northern China. An epidemiological survey showed a positive infection rate of 79.3% for PSV, which indicates the widespread and high prevalence of this strain in the Chinese region (15). Recently, PSV strains have frequently been isolated in western China. Other studies have confirmed that PSV strains isolated in western China can cause diarrhea in piglets (16).

Genetic evolution analysis showed that the isolated PSVs had a close genetic relationship with other PSV strains isolated in China, which means that the PSV strains circulating in China have probably evolved from a common ancestor (15). The Korean SV-A strain can replicate in the intestinal tract of piglets and cause intestinal and parenteral lesions in piglets, but not in chicks (17). However, the PSV isolates in the UK cause ataxia and general paralysis in piglets and co-localize in spinal lesions in infected animals (18).

In the present study, a newly isolated PSV strain, SHPD202148, was identified and its genomic characteristics were further investigated. Phylogenetic analysis revealed that the VP1 gene of the SHPD202148 strain was more closely related to Chinese PSV strains

FOR PERSONAL USE ONLY

Table I. Agreement between the indirect ELISA method for detecting antibodies to PSV and the serum neutralization (SN) test.

	SN test		
	Positive	Negative	Total
i-ELISA			
Positive	126	3	129
Negative	2	36	38
Total	128	39	167
Data analysis			
Sensitivity	98.4%		
Specificity		92.3%	
Coincidence rate			97.0%

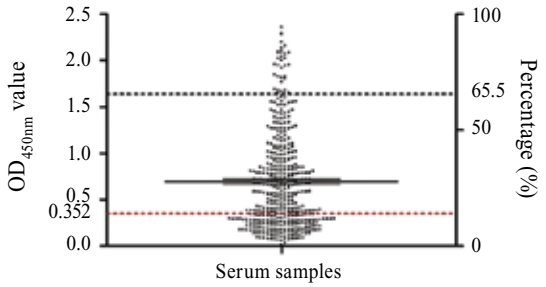


Figure 6. Application of i-ELISA method for detecting anti-PSV-protein antibodies in 435 piglet serum samples from pig farms in China.

than to those isolated from other countries. The Chinese PSV strains shared the closest genetic relationships and, therefore, may have evolved from a common ancestor with less variation. In addition, the VP1 protein sequence of this strain has a high homology of 72.3 to 98.6% compared with that of other countries. Therefore, the VP1 genes of the SHPD202148 strain were amplified and expressed in the pET system that was used for developing the detection test.

As there is no commercially available vaccine for PSV, early detection and monitoring for PSV antibodies is particularly important, especially antibody monitoring that can forecast pathogenic infection and the possibility of an epidemic. In the small ribonucleic acid virus Family, structural proteins are classified into VP4, VP2, VP3, and VP1. Structural proteins play an intermediary role in viral replication and pathogenicity and the VP1 protein is located at the outermost part of the viral particle in order to stabilize it (19). However, there are fewer studies on the PSV VP1 structural protein.

In this study, we explored the expression conditions of the PSV VP1 gene in *E. coli* strain BL21(DE3) and obtained polyclonal antibodies against VP1 protein. Western blot results showed that the PSV VP1 protein was specifically recognized by anti-PSV VP1-protein-positive sera and IFA results indicated that positive sera recognized the native PSV VP1 protein from PSV infection.

The test results showed that the PSV VP1 gene was expressed at a high level in *E. coli* and that the PSV VP1 protein had good immunogenicity. The recombinant protein did not cross-react with several common porcine-susceptible virus-positive sera and could specifically bind PSV-positive sera. Repeatability tests showed a coefficient of variation of less than 10%, which indicates that the method has good reproducibility.

In summary, the sensitivity, specificity, and reproducibility of the established PSV-VP1 protein can be used to identify PSV serum samples. The method was applied to clinical samples and the results showed a positive rate of 65.5%. This is higher than the previously reported prevalence of PSV in Shanghai (11). The positive serum in the ELISA test was randomly selected for VP1 protein sequencing. The sequencing results showed that the VP1 protein of individual strains of PSV was different from that of SHPD202148. Whole-genome sequencing will be carried out to explore whether it is a new epidemic strain of PSV.

Ibrahim *et al* (15) also used VP1 protein as the antigen to establish an i-ELISA method and no cross-reaction with known enterovirus antibodies was observed. The coincidence rate of i-ELISA was 95.7% among PSV samples using IFA as the standard evaluation method (15). In the present study, the serum neutralization (SN) test was used for parallel testing of serum and the results showed a 97.0% agreement between the 2 methods. The SN test used the SHPD202148 strain and the serum dilution was 1:4. Serum below 1:4 dilution was detected by IFA without fluorescence.

At the same time, the different PSV strains preserved in this study were detected using the same method and the SN test results were the same. The i-ELISA developed in this study may be a particularly valuable test for routinely diagnosing PSV infection on pig farms.

As the storage duration and temperature required for the preservation of the i-ELISA are uncertain at present, further studies should be carried out that focus on the stability of the assay.

In conclusion, in this study, a porcine sapelovirus strain, SHPD202148, was isolated and identified as PSV by RT-PCR. The ELISA method using this PSV's structural protein VP1 as antigen has good reproducibility and sensitivity and can be used as an alternative serological test for detecting antibodies against PSV in blood serum.

Acknowledgments

This research was funded by the Shanghai Agricultural Technology Development Program, China (Grant No. 2022-02-08-00-12-F01167) and the Shanghai Academy of Agricultural Sciences (SAAS) Program for Excellent Research Team (Grant No. [2022]012). The authors are grateful to all anonymous reviewers for their helpful discussion of the results.

References

1. Kaku Y, Sarai A, Murakami Y. Genetic reclassification of porcine enteroviruses. J Gen Virol 2001;82:417–424.
2. Bak GY, Kang MI, Son KY, *et al.* Occurrence and molecular characterization of Sapelovirus A in diarrhea and non-diarrhea feces of different age group pigs in one Korean pig farm. J Vet Med Sci 2017;78:1911–1914.
3. Buitrago D, Cano-Gómez C, Agüero M, *et al.* A survey of porcine picornaviruses and adenoviruses in fecal samples in Spain. J Vet Diagn Invest 2010;22:763–766.

FOR PERSONAL USE ONLY

4. Chen Q, Wang L, Zheng Y, *et al.* Metagenomic analysis of the RNA fraction of the fecal virome indicates high diversity in pigs infected by porcine endemic diarrhea virus in the United States. Virol J 2018;15:95.
5. Shan T, Li L, Simmonds P, Wang C, Moeser A, Delwart E. The fecal virome of pigs on a high-density farm. J Virol 2011;85:11697–11708.
6. Lamont PH, Betts AO. Enteroviruses in the pig. Nature 1958;182: 608–609.
7. Cano-Gómez C, García-Casado MA, Soriguer R, Palero F, Jiménez-Clavero MA. Teschoviruses and sapeloviruses in faecal samples from wild boar in Spain. Vet Microbiol 2013;165:115–122.
8. Hammerschmitt ME, de Almeida PR, de Cecco BS, *et al.* Swine polioencephalomyelitis in Brazil: Identification of Teschovirus A, Sapelovirus A, and Enterovirus G in a farm from Southern Brazil. Braz J Microbiol 2021;52:1617–1622.
9. Sunaga F, Masuda T, Ito M, *et al.* Complete genomic analysis and molecular characterization of Japanese porcine sapeloviruses. Virus Genes 2019;55:198–208.
10. Lan D, Ji W, Yang S, *et al.* Isolation and characterization of the first Chinese porcine sapelovirus strain. Arch Virol 2011;156: 1567–1574.
11. Li N, Tao J, Li B, *et al.* Molecular characterization of a porcine sapelovirus strain isolated in China. Arch Virol 2021;166: 2683–2692.
12. Li Y, Du L, Jin T, *et al.* Characterization and epidemiological survey of porcine sapelovirus in China. Vet Microbiol 2019;232: 13–21.
13. Fei D, Zhang H, Diao Q, *et al.* Codon optimization, expression in *Escherichia coli*, and immunogenicity of recombinant Chinese sacbrood virus (CSBV) structural proteins VP1, VP2, and VP3. PLoS One 2015;10:e0128486.
14. Cao YG, Hao Y, Wang L. A *Bacillus*-based Coxsackie virus A16 mucosal vaccine induces strong neutralizing antibody responses. Cent Eur J Immunol 2019;44:1–6.
15. Ibrahim YM, Zhang W, Werid GM, *et al.* Isolation, characterization, and molecular detection of porcine sapelovirus. Viruses 2022;14:349.
16. Chen J, Suo X, Cao L, *et al.* Virome analysis for identification of a novel porcine sapelovirus isolated in western China. Microbiol Spectr 2022;10:e0180122.
17. Kim DS, Kang MI, Son KY, *et al.* Pathogenesis of Korean Sapelovirus A in piglets and chicks. J Gen Virol 2016;97: 2566–2574.
18. Schock A, Gurrala R, Fuller H, *et al.* Investigation into an outbreak of encephalomyelitis caused by a neuroinvasive porcine sapelovirus in the United Kingdom. Vet Microbiol 2014;172: 381–389.
19. Fernández-Sainz IJ, Largo E, Gladue DP, *et al.* Effect of specific amino acid substitutions in the putative fusion peptide of structural glycoprotein E2 on classical swine fever virus replication. Virology 2014;456–457:121–130.

FOR PERSONAL USE ONLY

Article

Neourethra creation using autologous vascularized intestinal graft in cats

Barbra G.O. de Faria, Vanessa M. da Silva, Jéssica A. Silva, Sheila C.A. Santos, Ana M. Quessada, Caterina Muramoto, João M. da Costa Neto

Abstract

The objective of this study was to assess the application of a urethrostomy technique that utilizes an autologous vascularized intestinal graft as a "neourethra" and to analyze its short- and long-term feasibilities. Six cats with urethral rupture and 8 cats with urethral stricture and a history of urethrostomy were included. The inclusion criteria were the indication for urethroplasty and limited urethral length for perineal urethrostomy. A segment of intestine was prepared as a graft for urethral repair. The diameter of the aboral end was adjusted to facilitate anastomosis with the urethra or neck of the urinary bladder. An ostomy was created in the prepubic region using the oral end. The postoperative follow-up period was at least 1 y. Restoration of urinary flow was successful in all cases immediately after surgery. During postoperative follow-up, minimal complications were observed, with urinary incontinence being one of the most frequent, occurring in 28.5% (4/14) of the cases. Urine culture, carried out at different times during the follow-up period, was positive in 72.7% (8/11) of the cats. The autologous graft from the vascularized intestinal segment was an appropriate urethral substitute and this urethroplasty technique therefore proved to be feasible in cats. The postoperative complications observed were not exclusive to this technique and generally could either be corrected or tolerated. Periodic clinical follow-up examinations are recommended. This procedure allows the reestablishment of urinary flow and should be considered a favorable option, particularly when there is insufficient urethral tissue to allow repair using conventional techniques.

Résumé

L'objectif de cette étude était d'évaluer l'application d'une technique d'urétrostomie qui utilise une greffe intestinale vascularisée autologue comme « néo-urètre » et d'analyser ses faisabilités à court et à long terme. Six chats avec rupture urétrale et huit chats avec rétrécissement urétral et antécédents d'urétrostomie ont été inclus. Les critères d'inclusion étaient l'indication d'urétroplastie et la longueur urétrale limitée pour l'urétrostomie périnéale. Un segment d'intestin a été préparé comme greffon pour la réparation urétrale. Le diamètre de l'extrémité aborale était ajusté pour faciliter l'anastomose avec l'urètre ou le col de la vessie. Une stomie a été créée dans la région prépubienne en utilisant l'extrémité orale. La période de suivi postopératoire était d'au moins 1 an. La restauration du flux urinaire a réussi dans tous les cas immédiatement après la chirurgie. Au cours du suivi postopératoire, des complications minimes ont été observées, l'incontinence urinaire étant l'une des plus fréquentes, survenant dans 28,5 % (4/14) des cas. La culture urinaire, réalisée à différents moments de la période de suivi, était positive chez 72,7 % (8/11) des chats. La greffe autologue du segment intestinal vascularisé était un substitut urétral approprié et cette technique d'urétroplastie s'est donc avérée réalisable chez le chat. Les complications postopératoires observées n'étaient pas exclusives à cette technique et pouvaient généralement être soit corrigées soit tolérées. Des examens de suivi clinique périodiques sont recommandés. Cette procédure permet le rétablissement du flux urinaire et doit être considérée comme une option favorable, en particulier lorsque le tissu urétral est insuffisant pour permettre une réparation à l'aide de techniques conventionnelles.

(Traduit par Docteur Serge Messier)

Introduction

Urethral disorders secondary to trauma, stricture, congenital malformation, or neoplasia may require surgical reconstruction using compatible tissues (1). In humans, autologous intestinal segment grafts appear to be useful urethral substitutes with minimal complications (2). Such grafts possess their own blood supply (3) and have a mobile vascular pedicle, tubular shape, flexible walls, and adequate diameter for anastomosis to the urethra and mucosal lining (2).

In veterinary medicine, surgical techniques of urethrostomy for recurrent urethral obstruction have been described (4,5). In cases where the urethral length is insufficient for an ostomy without urethral tension or torsion (6), however, it is necessary to develop and improve grafting techniques and materials that maintain urethral functions with a low rate of complications.

School of Veterinary Medicine and Animal Science, Federal University of Bahia (UFBA), Salvador, Brazil (de Faria, da Silva, Silva, Santos, Muramoto, da Costa Neto); School of Veterinary Medicine, Paranaense University (UNIPAR), Umuarama, Brazil (Quessada).

Address all correspondence to Dr. Barbra Gabriela Oliveira de Faria; telephone: +55 71 3283-6728; email: barbra_faria@yahoo.com.br

Received March 7, 2022. Accepted September 8, 2022.

FOR PERSONAL USE ONLY

Based on the promising results achieved using the autologous vascularized intestinal segment for urethral replacement in dogs (7), humans (2,8,9), and 1 cat (10), we aimed to apply this urethroplasty technique in cats with limited urethral length that precludes the use of perineal urethrostomy and in which, for some reason, no other conventional urethrostomy technique can be used. We also aimed to analyze the short- and long-term feasibilities of this technique for functional urethral repair.

Due to the preliminary results our research group obtained after applying this technique to a cat (10), we hypothesized that this innovative technique is feasible in this species and is an appropriate option when additional tissue is required for urethral reconstruction and restoration of urinary flow. We also hypothesized that complications such as urethral tension and cicatricial stricture would be minimal with this technique.

Materials and methods

This study was approved by the Ethics Committee on the Use of Animals of the Federal University of Bahia (CEUA-UFBA 19/2018). Owners signed an informed consent form agreeing to their cats' participation in the study. Fourteen cats with urethral injury in which the location and/or extent of the lesion limited the options for reconstructive urethrostomy techniques were selected.

Anamnesis, physical examination, complementary blood tests (including serum urea and creatinine), and clinical stabilization were carried out on all animals preoperatively. Abdominal ultrasonography was done in cases of suspected urethral rupture, allowing the identification of abdominal free fluid. Due to technical and financial constraints, contrast radiography was unavailable during the study period. Clinical signs and history of previous urethral procedures conducted in other hospitals were also considered for the diagnosis. In some cats, the location and extent of the urethral lesion was only diagnosed during the intraoperative period.

Fifteen minutes before surgery, all animals received cephalothin (Kefalomax; BioChimico, Itatiaia, Brazil), 30 mg/kg body weight (BW), IV and metronidazole (Flagyl; Sanofi-Aventis, São Paulo, Brazil), 15 mg/kg BW. Subcutaneous meloxicam (Maxicam; Ourofino, Cravinhos, Brazil), 0.1 mg/kg BW, was also administered to non-azotemic animals.

Pre-anesthetic medication was administered based on the individual requirements and American Society of Anesthesiologists (ASA) classification of each animal. Intravenous propofol (Propovan; Cristália, São Paulo, Brazil), 4 mg/kg BW, was used to induce anesthesia, which was maintained using isoflurane (Isoforine; Cristália) diluted in 100% medicinal oxygen. All cats received an epidural block with 2% lidocaine hydrochloride without vasoconstrictor (Xylestesin; Cristália), 4 mg/kg BW, and morphine (Dimorf; Cristália), 0.1 mg/kg BW.

Cats were positioned in dorsal recumbency, and their abdominal and pelvic regions were prepared for aseptic surgery. A median celiotomy was carried out. The urethra was identified and carefully isolated, preserving the innervation and vascular supply whenever possible. The urethra was sectioned into the preprostatic segment in 12 cats. In 2 cats in which the original lesion was positioned more cranially, the urethra was sectioned close to the bladder neck.

Autologous vascularized intestinal segment grafts have been prepared for urological reconstruction in dogs and humans (7,8) and we adapted these techniques for cats. An enterectomy approximately 7 cm long was carried out, preserving the mesenteric vascularization (Figure 1 A). The enterectomy site was defined as the first segment of the small intestine, orally/cranially from the cecum, irrigated by vessels from the same branch (usually at ileum or jejunum-ileum transition).

A simple interrupted suture pattern (4-0 poliglecaprone; Bioline, Anápolis-GO, Brazil) was used for termino-terminal anastomosis of the intestine. The associated mesentery was sutured using 4-0 poliglecaprone in a simple continuous pattern (Figure 1 B). Sodium chloride (0.9%) isotonic solution (Fisiológico; Eurofarma, Ribeirão Preto, Brazil) was injected into the lumen near the anastomosis to check for leakage.

The vascularized intestinal graft was isolated and washed with a warm solution of 0.9% sodium chloride to completely remove the luminal content. To avoid torsion of the graft mesenteric pedicle due to anatomical positioning, the aboral end of the graft was anastomosed to the urethra and the oral end was positioned in the ostomy region.

Subsequently, incisions were made in the abdominal musculature, subcutaneous tissue, and skin of the prepubic region through which the oral end of the graft was passed from the inside to the outside of the abdominal cavity. A Foley catheter (Well Lead Medical, Guangzhou, China) (sizes 6, 8, or 10, depending on the urethral thickness) was passed through the lumens of the graft and remaining urethra (or bladder neck) until the urinary bladder was reached, where the cuff was inflated.

The diameter of the aboral end of the graft was reduced to match the diameter of the urethra. At the aboral end, a 0.5-cm wedge-shaped segment of the wall was removed from the circumference (Figure 1 C) and a simple interrupted 4-0 poliglecaprone suture was applied (Figure 1 D). To carry out the graft-urethra anastomosis, stay sutures were placed around the entire circumference of both walls (Figure 1 E) and the knots were then tightened in a simple interrupted suture pattern. In cats in which the section occurred in the neck of the urinary bladder, anastomosis was conducted directly, without previous reduction in diameter.

Subsequently, the intestinal anastomosis region was omentalized and the abdominal wall was closed in the usual manner using an interrupted cruciate pattern of suture (2-0 Nylon; Bioline) to the musculature, an intradermal suture (2-0 Catgut Chrome; Bioline), and a simple interrupted pattern (3-0 Nylon; Bioline) to the skin.

A 1-cm longitudinal incision was made on the antimesenteric side of the exteriorized graft end to create the ostomy (11). This incision facilitated eversion of the end around its entire circumference, forming a "rosebud"-like shape. It was then sutured to the edges of the skin orifice in the prepubic region using 4-0 poliglecaprone in a simple interrupted pattern, transfixing all layers of the graft wall. Finally, the Foley catheter was attached to the skin using simple interrupted 3-0 surgical nylon sutures (Figure 1 F). A video of the surgical procedure can be accessed at https://www.youtube.com/watch?v=uWdBXywQyKg

After 24 h of hospitalization, the animals were discharged with the following oral prescriptions: amoxicillin with potassium clavulanate

FOR PERSONAL USE ONLY

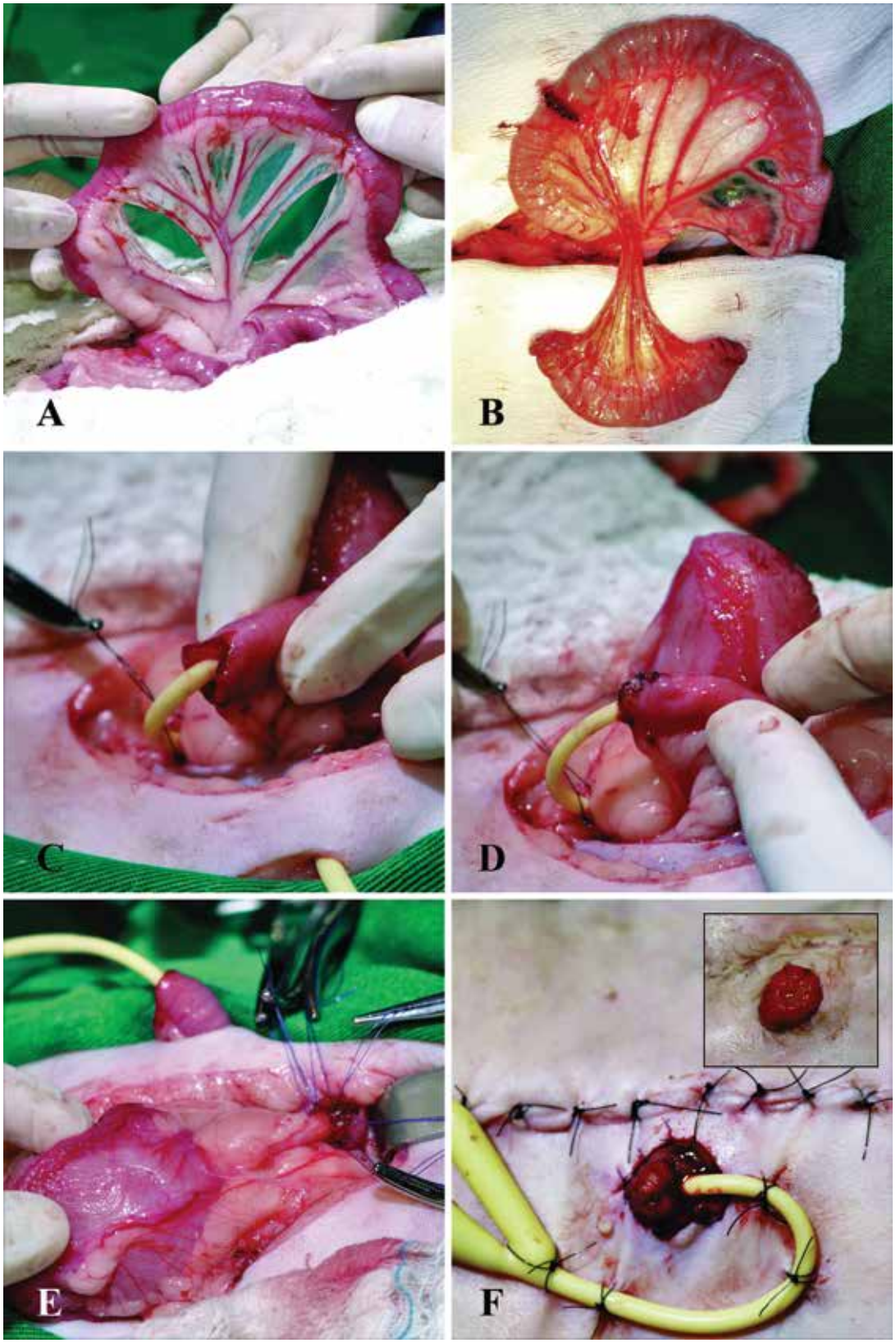


Figure 1. Photographs of urethroplasty using an autologous vascularized intestinal segment for urethral replacement preparation in cats. A — Identification of the intestinal segment with its vascular supply and mesenteric nerve for subsequent resection for grafting. B — Continuous suture of the mesentery and separation of the autologous vascularized intestinal segment graft. C — Removal of a wedge-shaped wall segment from the aboral end of the graft. D — Intestinal wall synthesis after removal of the wedge-shaped segment. E — Stay sutures passing through the walls of the urethra and graft. F — Immediate postoperative appearance of the ostomy and the Foley catheter fixed to the skin; the superimposed image shows the ostomy area on the 15th postoperative day after removing skin stitches and the Foley catheter.

FOR PERSONAL USE ONLY

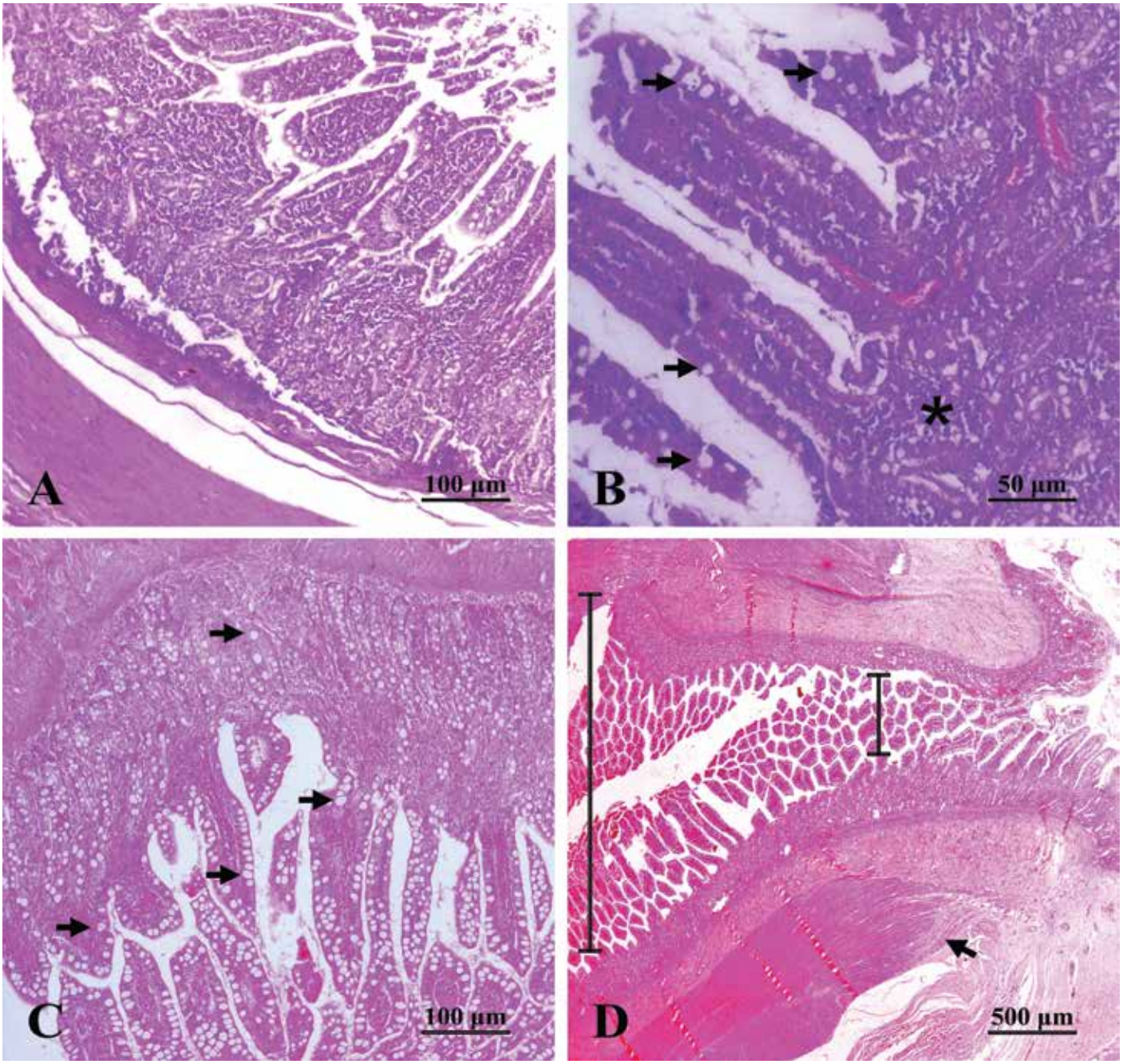


Figure 2. Histopathological images of the hematoxylin and eosin (H&E)-stained samples obtained from the normal ileum segment in a cat (A) and autologous grafts obtained from the ileum of cats (B, C, and D). A — The ileal fragment that was extracted from the intestinal tract and used as a control sample (H&E, 100×). B — Autologous ileal graft at 6 mo after surgery shows a slight increase in goblet cells (arrows) and submucosal lymphoplasmacytic inflammation (*) (H&E, 200×). C — Autologous ileal graft at 12 mo after surgery shows a marked increase in goblet cells (arrows) and no inflammation (H&E, 100×). D — Histological section of the stenotic ostomy region. A reduction in the size of the lumen (black bars) and bilateral symmetrical fibrosis in the ostomy area (arrows) are seen (H&E, 50×).

(Synulox; Zoetis, Campinas, Brazil), 15 mg/kg BW, q12h for 14 d; metronidazole (Flagyl; Sanofi-Aventis), 15 mg/kg BW q12h for 5 d; tramadol (Dorless; Agener-União, São Paulo, Brazil), 1 to 2 mg/kg BW q8h for 3 d; omeprazole (Gaviz V; Agener-União), 1 mg/kg BW q24h for 14 d; and meloxicam (for non-azotemic cats) (Flamavet; Agener-União), 0.05 mg/kg BW q24h for 2 d.

Other home care recommendations during surgical healing included the use of an Elizabethan collar, disposable diapers over the end of the Foley catheter, and cleaning the surgical wound with a chlorhexidine-based solution. After healing, 14 d following surgery, the Foley catheter and external sutures were removed (Figure 1 F).

Postoperative clinical examinations were carried out at 5, 14, 30, 60, 90, 180, and 360 d to assess the healing process and urination. Follow-up evaluations included anamnesis and conventional physical examination, along with inspection and cleaning of the incision

FOR PERSONAL USE ONLY

Table I. Clinical signs and location, type, and cause of urethral lesions in cats.

Preoperative/ intraoperative information	Description	Number (%)
Location of urethral lesion	Postprostatic pelvic urethra	9 (64.3)
	Preprostatic pelvic urethra	3 (21.4)
	Adjacent to the neck of the urinary bladder	2 (14.3)
Type and cause of urethral lesion	Urethral stricture following previous urethrostomy	8 (57.1)
	Extensive urethral rupture (iatrogenic/unknown cause) and unsuccessful urethral catheterization	4 (28.5)
	Extensive rupture due to blunt force trauma/being hit by a car and unsuccessful urethral catheterization	2 (14.3)
Clinical signs	Unable to urinate on their own	13 (92.9)
	Distended and firm urinary bladder	8 (57.1)
	Free fluid in the abdominal cavity	5 (35.7)
	Scrotal and preputial edema	4 (28.6)
	Unsuccessful urethral catheterization	2 (14.3)
	Vocalization	2 (14.3)
	Stranguria	1 (7.1)
	Penile hemorrhage	1 (7.1)
	Pyuria	1 (7.1)

Table II. Postoperative clinical signs and information obtained from anamnesis, physical examination, ultrasonography, and urine culture.

Postoperative clinical signs/information	Number (%)
Anamnesis and physical examination	
No clinical complications	6/14 (42.9)
Irritation of the skin adjacent to the ostomy	3/14 (21.4)
Frequent licking of the ostomy region	2/14 (14.3)
Graft lumen stricture at the ostomy site	2/14 (14.3)
Marked urinary incontinence	2/14 (14.3)
Skin and subcutaneous incisional dehiscence	1/14 (7.1)
Omental evisceration secondary to body wall dehiscence	1/14 (7.1)
Mild and intermittent urinary incontinence	1/14 (7.1)
Moderate urinary incontinence	1/14 (7.1)
Ultrasound examination	
Moderate amount of echogenic sediment suspended in urine	5/14 (35.7)
Small amount of echogenic sediment suspended in urine	4/14 (28.6)
Large amount of echogenic sediment suspended in urine	3/14 (21.4)
Thickening of the urinary bladder wall	3/14 (21.4)
Tiny calculi in the urinary bladder	1/14 (7.1)
Irregularity of the urinary bladder wall	1/14 (7.1)
Urine culture	
Not possible to collect urine	3/14 (21.4)
Escherichia coli	3/11 (27.3)
No bacterial growth	3/11 (27.3)
Staphylococcus sp.	2/11 (18.2)
Staphylococcus epidermidis	2/11 (18.2)

and ostomy, with attention to urine release, the ostium of the ostomy, and surrounding skin conditions.

Serum biochemical tests were done 5 to 30 d after surgery, according to the requirements of each cat and the availability of the cats' owners. Ultrasonography (Logiq-e; GE Medical Systems, Wuxi, China) of the urinary tract and urine collection through aseptic cystocentesis for urinalysis and culture were carried out at least once between 20 and 360 d after surgery.

Histopathological analysis of the graft was possible on 2 occasions: from a cat euthanized for tracheal obstructive neoplasia 180 d postoperatively (in this case, a tissue sample of healthy ileum from the digestive tract was also obtained as a control) and from a cat that underwent revision surgery for ostomy stricture 1 y after the primary surgery (Figure 2 A to D).

Results

Of the 14 selected cats, 8 had urethral strictures (in the ostium of previous urethrostomy or the path of the urethra) and 6 had urethral rupture. All cats were male, without a defined breed, from 3 mo to 14 y old (mean ± SD: 4.2 ± 3.9 y), and weighed 1.2 to 6 kg (mean ± SD: 3.8 ± 1.4 kg).

The location, type, and cause of the urethral lesion, as well as clinical signs, are presented in Table I. In most cases, a combination of clinical signs was observed. The 8 cats with urethral strictures had a history of 1 to 4 previous perineal and/or prepubic urethrostomies (Table I). Urethral ruptures were iatrogenic in 3 cats, due to blunt force trauma/being hit by a car in 2 cats and of unknown cause in 1 cat with signs of urethral obstruction for 3 d.

In 5 cats, the presence of abdominal free fluid, bladder repletion, inability to urinate, and unsuccessful urethral catheterization allowed the diagnosis to be suspected preoperatively. Concomitant traumatic injuries (hematomas in the pelvic region and fracture of the right femur) were observed in 2 cats. In all cases, urethral catheterization was unsuccessful, urethral lesions were extensive, and ruptures were confirmed intraoperatively (Table I). No complications occurred during any surgical or anesthetic procedures.

The proposed postoperative clinical follow-up was sufficient to assess the clinical condition of the cat, healing of the surgical wound, and integrity of the autologous graft, and allowed medical interventions when needed. In 7 cats (7/14; 50%), no complications were identifiable based on anamnesis and physical examination. In the other 7 cats, 1 or more complications occurred (total, 13) at different time periods and with different severities (Table II). Urinary

FOR PERSONAL USE ONLY

incontinence was the most frequent complication (4/14; 28.5%). Periodic assessments allowed early detection and correction of stricture in the ostomy region in 2 cats (2/14; 14.3%) 1 y after surgery in 1 cat and 6 mo after surgery in the other (Table II).

Although serum biochemical tests could not always be completed on the desired dates, at least 1 blood sample was obtained from all cats within the first 30 d after surgery. Seven cats were azotemic preoperatively. The mean values of preoperative urea and creatinine levels (130.2 ± 93.1 mg/dL and 3.8 ± 3.7 mg/dL, respectively) decreased considerably (55.4 ± 12 mg/dL and 1.3 ± 0.4 mg/dL, respectively) within 30 d after surgery. Urine culture could be carried out in 11 cats postoperatively [median (interquartile range): 150 (90 to 195) d after surgery]. Gram-negative and Gram-positive bacteria were seen in 3 and 5 samples, respectively (Table II).

Postoperative ultrasonography allowed evaluation of the graft, urinary bladder, adjacent tissues, and other abdominal organs. It was possible to follow the entire path of the graft from the anastomosis to the ostomy. Typical parietal stratification and peristalsis, with different degrees of intensity, were present in all cats. There were no signs of luminal dilation and no or minimal amount of urine in the lumen. The urinary bladder was not distended in any cats. No free fluid or increased echogenicity of the tissues adjacent to the graft that could suggest local inflammation was detected. No relevant alterations were observed in the gastrointestinal tract.

Histopathological analysis of the graft of the euthanized cat (tracheal neoplasia), carried out 6 mo after surgery, revealed a slight increase in goblet cells and submucosal lymphoplasmacytic inflammation (Figure 2 B). In the sample obtained 12 mo after surgery during the revision procedure for ostomy stricture, there was a marked increase in goblet cells and no signs of inflammation (Figure 2 C). These features were not observed in the control sample from the digestive tract (Figure 2 A).

Discussion

To the best of our knowledge, only 1 case report has described the use of urethroplasty with autologous intestinal graft in cats (10). This is the first study to describe and analyze the neourethra technique as a surgical treatment for cats in which urethral length restricted the use of other reconstructive techniques.

The preoperative clinical signs varied according to the cause, location, extent, severity, and duration of injury and were characteristic of compromised urinary flow. All cases presenting with abdominal free fluid were associated with urethral rupture (12). Penile hemorrhage and scrotal and preputial edema were perhaps secondary to the attempted urethral catheterization during previous care at another veterinary center (13).

The Foley catheter is important for adequate healing, reducing the risk of strictures, and preventing urine leakage in the suture line (14). A significant decline in serum urea and creatinine concentrations was expected in the postoperative period after the urinary flow was restored and azotemia was corrected (15).

We observed positive urine cultures in 72.7% (8/11) of the cats; 6 of them exhibited no clinical signs other than minor changes in complementary examinations, such as the presence of urinary sediment (6/6) and thickening (2/6) of the urinary bladder wall on ultrasonography. The other 2 cases with positive urine cultures were discovered in cats with incontinence. Periodic urinalysis by cystocentesis should be carried out for the early detection and treatment of urinary infections (4). The large diameter and different contraction pattern of the intestinal graft compared with a cat's urethra are factors that may facilitate urinary infections. Urinary infection due to bacteria of the intestinal flora of the graft was considered very unlikely since antibiotics were used prophylactically, in addition to washing the graft lumen.

We believe that the cases of postoperative urinary incontinence were not related to the surgical procedure itself but rather to the location of the lesion (close to the bladder neck) or the involvement of innervation due to the original trauma. Maintaining the maximum possible length of the urethra and innervation of the bladder and urethra are important for maintaining urinary continence (6). Although the surgical procedure was carefully carried out, in both cases in which the anastomosis was done at the bladder neck, there was marked incontinence due to the complete absence of the urethra.

Furthermore, excessive urethral distension in cases of obstruction can compromise innervation and cause incontinence (16). This probably explains the incontinence in the cat that presented with a ruptured urethra after signs of urinary obstruction. The urinary incontinence of the cat that had been run over was possibly related to traumatic injury to the urethral innervation.

The characteristics of an autologous intestinal segment are ideal for grafting as it has no antigenic properties, maintains innervation and vascular supply, and its length is adjustable, which contributes to its healing and integration (2,8). The vascular pedicle showed sufficient mobility to allow anastomosis with the urethra and ostomy site without tension (2). In addition, there were no complications or sequelae in the intestinal region from which the graft was obtained.

The ostomy strictures developed in 2 cats (2/14; 14%) could be correlated with excessive licking of the ostomy site. In both cases, the correction was possible by creating a new ostomy. A study related to conventional prepubic urethrostomy reported a higher rate of stricture of the urethrostomy site (4/16; 25%) at different postoperative periods and the correction was possible in only 1 case, with euthanasia indicated in the others (6). In the present study, the large diameter of the graft compared with the urethra of a normal cat may have contributed to the lower rate of ostomy stricture.

Leakage of urine is a common postoperative complication that is also observed with other urethrostomy techniques (16). Since there were only 4 cats with incontinence in our study, however, and the stricture in the ostomy region occurred precisely in the 2 cats that also showed excessive licking, licking was considered the most likely cause of the stricture and not contact with urine or the surgical technique itself.

Depending on the type and length of the intestinal segment used, long-term complications described in human medicine include metabolic imbalance, malabsorption of vitamins, cholelithiasis, and nephrolithiasis (17). These complications were not observed postoperatively in our patients, probably because graft extracted from the digestive tract was not long enough to cause impairment of the remaining intestinal function.

In our study, histopathological analysis revealed an increase in the number of goblet cells, which has also been observed in ileal grafts

FOR PERSONAL USE ONLY

in humans (18). The histological changes, observed in both studies, can be considered a tissue adaptation related to the new function of the intestinal graft, which remains in chronic contact with urine. The possibility of adaptation to prevent urine reabsorption was discussed in another study (19).

Long-term follow-up studies and histopathological evaluations can provide more information regarding other changes that may occur over time in the cats included in the present study. The sample size and follow-up time were not sufficient to establish precise correlations between postoperative findings and their causes. Owners of the cats should be aware that lifelong care will be required.

It is important to mention that other surgical techniques, such as transpelvic urethrostomy, would also be feasible for some of the cases included in this study. Due to the cat owner's limited financial resources and the surgeon's skill, however, the neourethra technique was the most viable alternative to euthanasia in these cases.

In conclusion, the applied urethroplasty technique proved to be feasible in cats. The ileal graft was a good urethral substitute, allowing the reestablishment of urinary flow. It is a favorable alternative for cases in which there is insufficient urethral tissue to allow repair using conventional techniques. In the present study, the rate of postoperative complications was low and not exclusive to the technique employed. In most cases, complications can be corrected or are well tolerated. Periodic clinical follow-up, including urinalysis and urine culture, are recommended at least every 6 mo.

Acknowledgments

The authors thank Coordination for the Improvement of Higher Education Personnel — Brazil (CAPES) for funding the doctoral scholarship (Funding Code 001). We also thank Suane N. Boaventura and Jaqueline A. Araújo for their help in caring for the cats.

References

1. Chen F, Yoo JJ, Atala A. Acellular collagen matrix as a possible "off the shelf" biomaterial for urethral repair. Urology 1999;54:407–410.
2. Aggarwal SK, Goel D, Gupta CR, Ghosh S, Ojha H. The use of pedicled appendix graft for substitution of urethra in recurrent urethral stricture. J Pediatr Surg 2002;37:246–250.
3. Brourman JD. Successful replacement of an obstructed ureter with an ileal graft in a cat. J Am Vet Med Assoc 2011;238:1173–1175.
4. Sousa-Filho RP, Nunes-Pinheiro DC, Sampaio KO, da Silva EC, Cavalcanti GA, Mori da Cunha MGM. Clinical outcomes of 28 cats 12–24 months after urethrostomy. J Feline Med Surg 2020;22:890–897.
5. Bernarde A, Viguier E. Transpelvic urethrostomy in 11 cats using an ischial ostectomy. Vet Surg 2004;33:246–252.
6. Baines SJ, Rennie S, White RS. Prepubic urethrostomy: A long-term study in 16 cats. Vet Surg 2001;30:107–113.
7. Yilmaz Y, Aydin M, Bakir B, Atilla MK, Odabaş O, Aydin S. Utilising an ileal segment in the posterior urethral replacement procedures using anal sphincter to provide continence in dogs. Tohoku J Exp Med 1998;185:263–270.
8. Bales GT, Kuznetsov DD, Kim HL, Gottlieb LJ. Urethral substitution using an intestinal free flap: A novel approach. J Urol 2002;168:182–184.
9. Lee YT, Cho TW, Jeong HS, Lee YK, Hong YK. Reconfigured sigmoid colon neourethra: Substitution of refractory posterior urethral stricture. Urology 2005;65:157–159.
10. de Faria BGO, da Silva VM, Silva JA, *et al.* Autogenous vascularized intestinal grafting for urethral reconstruction in feline. Acta Scientiae Veterinariae 2020;48:531.
11. Berek JS, Karam A, Cibula D. Surgical techniques. In: Berek JS, Hacker NF, eds. Berek and Hacker's Gynecologic Oncology. 6th ed. New York: Wolters Kluwer, 2015:779–823.
12. Boothe HW. Managing traumatic urethral injuries. Clin Tech Small Anim Pract 2000;15:35–39.
13. Addison ES, Halfacree Z, Moore AH, Demetriou J, Parsons K, Tivers M. A retrospective analysis of urethral rupture in 63 cats. J Feline Med Surg 2014;16:300–307.
14. Yippaditr W, Roongsitthichai A. An application of sublingual mucosa to establish a new urination passage in male cats with complications after urethrostomy. J Vet Med Sci 2019;18:771–775.
15. Canei DH, Pereira ME, de Freitas MN, *et al.* Biochemical, electrolytic, and cardiovascular evaluations in cats with urethral obstruction. Vet World 2021;14:2002–2008.
16. Seneviratne M, Stamenova P, Lee K. Comparison of surgical indications and short- and long-term complications in 56 cats undergoing perineal, transpelvic or prepubic urethrostomy. J Feline Med Surg 2021;23:477–486.
17. Martini A, Villari D, Nicita G. Long-term complications arising from bowel interposition in the urinary tract. Int J Surg 2017;44:278–280.
18. Thomas DJ, Goble NM, Gillatt DA, Hammonds JC, Smith PJ. Histological and environmental changes in longstanding ileal conduits. J R Soc Med 1990;83:557–558.
19. Hanke P, Hofmann M, Schneider M, Bickeböller R, Jonas D. Histological and scanning electron microscopic alterations in ileal conduit depending on the time factor. Urol Int 1990;45:84–87.

FOR PERSONAL USE ONLY

Relationship between the degree of stifle flexion and the proximal patellofemoral angle in the sagittal plane: A radiographic study

Juan José Camarasa, Rosario Vallefuoco, Felipe De Vicente

Abstract

The objective of this study was to evaluate the position of the patella in relation to the proximal femoral axis in the sagittal plane and to assess its reliability as a surgical landmark for femoral component placement in canine hip replacement. The relationship between the patella and the proximal femoral axis was assessed by defining the proximal patellofemoral angle in medio-lateral radiographic projections with 3 different stifle angles (full flexion, 90°, full extension) in medium to large breed skeletally mature dogs (N = 14). Proximal patellofemoral angle measurements were compared between the 3 different groups of stifle position using ANOVA for statistical analysis. The mean proximal patellofemoral angle measurements were −7.4° (± 1.3°) in the flexion group, −1.6° (± 1.5°) in the 90° group, and 2.1° (± 1.8°) in the extension group. Statistically significant differences were seen in the proximal patellofemoral angle between groups ($P \leq 0.001$). These results confirm that position of the patella related to the proximal femoral axis differs depending on the degree of stifle flexion. The degree of stifle flexion should be considered in the preoperative planning and intraoperatively when using the patella as a surgical landmark in the sagittal plane for femoral canal broaching in canine total hip replacement.

Résumé

L'objectif de cette étude était d'évaluer la position de la rotule par rapport à l'axe fémoral proximal dans le plan sagittal et d'évaluer sa fiabilité en tant que repère chirurgical pour le placement du composant fémoral dans le remplacement de la hanche canine. La relation entre la rotule et l'axe fémoral proximal a été évaluée en définissant l'angle fémoro-patellaire proximal dans des projections radiographiques médio-latérales avec trois angles de grasset différents (flexion complète, 90°, extension complète) chez des chiens de race moyenne à grande (N = 14). Les mesures de l'angle fémoro-patellaire proximal ont été comparées entre les trois groupes différents de position de grasset en utilisant l'ANOVA pour l'analyse statistique. Les mesures moyennes de l'angle fémoro-patellaire proximal étaient de −7,4° (± 1,3°) dans le groupe flexion, −1,6° (± 1,5°) dans le groupe 90° et 2,1° (± 1,8°) dans le groupe extension. Des différences statistiquement significatives ont été observées dans l'angle fémoro-patellaire proximal entre les groupes ($P \leq 0{,}001$). Ces résultats confirment que la position de la rotule par rapport à l'axe fémoral proximal diffère selon le degré de flexion du grasset. Le degré de flexion du grasset doit être pris en compte dans la planification préopératoire et peropératoire lors de l'utilisation de la rotule comme repère chirurgical dans le plan sagittal pour la présentation du canal fémoral dans le cadre d'une arthroplastie totale de hanche canine.

(Traduit par Docteur Serge Messier)

Introduction

Total hip replacement (THR) is a common surgical procedure in dogs and cats for the treatment of hip pathologies such as hip dysplasia, coxofemoral luxation, femoral head and neck fractures, and Legg-Calvé-Perthes disease (1–6).

Canine THR can either be performed with cemented or cementless components (7). BioMedtrix is one of the most commonly used THR systems (Biomedtrix; Boonton, New Jersey, USA) (8–10). The femoral components used with this system achieve stability through a cement mantle or through initial press-fit and subsequent osteointegration in the CFX and in the BFX models, respectively (9,11,12).

The implant size related to the femoral canal and implant coaxial alignment in both the sagittal and coronal planes are 2 important factors to evaluate adequate femoral component implantation in BFX THR models. The largest stem that can fit between the endosteal femoral surfaces with a minimum of 85% fill of the femoral canal was recommended in previous studies (9,13,14). However, canal fill under 85% was not associated with complications in a recent study (15), and the percentage of canal fill was considered a poor

Pride Veterinary Referrals, IVC Evidensia, Riverside Road, Derby, DE24 8HX United Kingdom (Camarasa, Vallefuoco); Veterios. C/ Arrastaria, 23. 28022. Madrid, Spain (De Vicente).

Address all correspondence to Dr. Juan José Camarasa; telephone: +447568984120; email: juanjocamarasa@gmail.com

Author contributions:
Camarasa JJ: Study design, acquisition of data, data analysis and interpretation, and drafted, revised, and approved the submitted manuscript; Vallefuoco R: data analysis and interpretation, and drafted, revised, and approved the submitted manuscript; De Vicente F: conception of study, study design, data analysis and interpretation, and drafted, revised, and approved the submitted manuscript.

Received July 18, 2022. Accepted November 20, 2022.

FOR PERSONAL USE ONLY

indicator of optimal stem size (15). Because the femoral component relies on initial press-fit stability, precise femoral canal broaching is mandatory to achieve this stability. Femoral component alignment in the femoral canal should be coaxial, matching the long axis of the femur in both the sagittal and coronal planes (4,14). Malalignment during femoral canal preparation may have detrimental biomechanical consequences and can lead to intra-surgical complications such as femoral fissures or fractures (4,15–18). The position of the patella has been proposed as an valuable intraoperative landmark for femoral canal broaching in order to achieve an adequate stem alignment in the proximal femoral axis (4,19). During surgery, the broaching angle and alignment could be determined using the cranial or proximal patella as an orientation landmark (4,9,14). The position of the patella and its relation to the femoral axis, as well as the distal femoral conformation must be assessed in the lateral radiographic views during preoperative planning (4,9,14). Because the patella kinematics are related to the femoral-tibial flexion angle, the patella is more proximal in the femoral trochlea when the stifle is fully extended and it translates caudally and distally when the stifle is flexed (20,21). Therefore, using the patella as an intraoperative orientation landmark during femoral canal preparation could be misleading if the stifle angle is obviated, as patellar position varies depending on the degree of joint flexion.

The objective of this study was to evaluate the relationship between the position of the patella and the proximal femoral axis in the sagittal plane during stifle range of motion, to assess the suitability of the patella as surgical landmark in dogs without anatomical variations in the femur. Our hypothesis was that there would be a significant variation in the position of the patella related to the proximal femoral long axis during stifle range of motion so that the degree of stifle flexion should be taken into consideration when using the patella as a reference for femoral canal broaching in the sagittal plane.

Materials and methods

Study design

A prospective clinical study was performed once ethical approval had been obtained at the authors' institution. Inclusion criteria were medium to large breed skeletally mature dogs (weighing over 15 kg) which underwent pelvic limb radiographs as part of their lameness investigations, with additional radiographs performed for the purpose of this study. Mediolateral open leg radiographic views of the femur and tibia were obtained in 3 different positions: maximum stifle flexion, maximum stifle extension, and 90° of stifle flexion. The correct positioning of the stifle joint at 90° of stifle flexion was determined by using an orthopedic goniometer and measured values of 90° ± 5° were considered acceptable (22). Specific stifle angles were not pursued in the maximum stifle flexion and maximum stifle extension radiographic views; these were taken with the maximum degree of stifle flexion and extension that the patient could have under sedation. The full length of the femur and tibia were included in each radiographic view by including the coxofemoral and the talocrural joints. Radiographic positioning was considered satisfactory if both femoral condyles were superimposed (23). Only dogs with grossly normal femoral anatomy were included based on measurements of the mechanical caudal distal femoral angle (24). Dogs with severe stifle osteoarthritis and dogs with femoral-tibial subluxation due to cranial cruciate ligament disease were excluded from the study. In addition, condrodystrophic breeds and dogs with femoral or tibial angular limb deformities were also excluded from the study.

Measurement technique

All measurements were performed using digital image software (OsiriX MD; Pixmeo, Bernex, Switzerland) on the 3 different mediolateral radiographic views (Figure 1). The proximal femoral axis (PFA) in the sagittal plane was calculated as previously described by drawing a line bisecting the femoral diaphysis at 50% and the proximal 25% of the total femoral length (25). The intersection of the PFA with the radiopaque line that delineates the intertrochanteric fossa, from the greater trochanter to the third trochanter, was considered the vertex point from which all angles would be determined. A second line was drawn between this vertex point and the cranial aspect of the patella, which was named the "patellofemoral orientation line" (PFOL). The exact ending point of the PFOL in the cranial aspect of the patella was defined by tracing a line from the proximal to the distal edge of the patella at its maximum length. A second perpendicular line at the 50% of the maximum patellar proximal-distal length was traced. The cranial end of this line at the patella was considered the landmark for the PFOL.

The angle created between the PFA and the PFOL was considered the proximal patellofemoral angle (PPFA). The PPFA was calculated in the 3 radiographic views for every animal included in this study (Figure 1). The PPFA was considered positive when the position of the patella was cranial to the PFA and negative when the position of the patella was caudal to the PFA. Proximal patellofemoral angles were measured 5 times by the same investigator for each radiograph and measurements were recorded for statistical analysis.

Statistical analysis

Intraclass correlation coefficient was calculated to assess PPFA measurements repeatability. Descriptive statistics were calculated for continuous variables. Normality of the data was evaluated by using the Shapiro-Wilk test and results were reported as mean and standard deviation (SD). A Kruskal-Wallis analysis of variance (ANOVA) on ranks was used to compare PPFA between groups. A Spearman's *rho* correlation coefficient was performed on the interpolated patellofemoral and femoral-tibial data to determine the extent of a linear relationship between stifle angle and PPFA. The data was considered as strongly correlated if the $r > 0.8$ and weakly correlated in $r < 0.3$. For all statistical analyses performed, $P < 0.05$ was considered statistically significant.

Results

Fourteen animals were included in the study. Dogs included in the study belonged to the following breeds: Staffordshire bull terrier ($n = 3$), Labrador retriever ($n = 3$), golden retriever ($n = 2$), German shepherd ($n = 1$), Rottweiler ($n = 1$), springer spaniel ($n = 1$), cocker spaniel ($n = 1$), whippet ($n = 1$), and a cross breed ($n = 1$). The mean age of dogs included in the study was 5.5 y (± 3.5 y), and the mean

FOR PERSONAL USE ONLY



Figure 1. Example of proximal patellofemoral angle (PPFA) in 3 different stifle positions. (PFOL: patellofemoral orientation line).

Table I. Results of PPFA in the different stifle angle positions.

	Full flexion	90°	Full extension
Stifle angle	44.3 (± 4.2)	89.7 (± 2.7)	130 (± 11.2)
Proximal patellofemoral angle (PPFA)	−7.4 (± 1.3)	−1.6 (± 1.5)	2.1 (± 1.8)

Note: Values are expressed as mean degrees ± standard deviation.

weight was 27.2 kg (± 9.8 kg). The mean stifle positioning angles in the flexion, 90° and extension groups were 44.3° (± 4.2°), 89.7° (± 2.7°), and 130° (± 11.2°), respectively (Table I).

In total, 14 stifles and 42 radiographs were assessed. The mean measurements of PPFA were −7.4° (± 1.3°) for the full stifle flexion group, −1.6° (± 1.5°) for the 90° group, and 2.1° degrees (± 1.8°) for the full stifle extension group. There was a mean variation in PPFA angle during full stifle range of movement of 9.5° (± 1.5°). Although there was a smaller variation in PPFA between stifle extension and stifle 90° positions, with a difference of 3.8° (± 1.0°), there was a more pronounced difference between the 90° and flexion position with a difference of 5.8° (± 0.9°). Intra-class correlation coefficient (ICC = 0.893) indicated good agreement of the measurements within the groups.

Statistically significant differences were determined between the PPFA in flexion and 90° position ($P \leq 0.001$), flexion and extension ($P \leq 0.001$), and 90° and extension ($P \leq 0.001$). Total stifle angle measurements were linearly strongly correlated with PPFA (Spearman's *rho* correlation coefficient = 0.904, $P < 0.01$, 95% CI).

Discussion

Results from this study have shown that the relation between the patella position and the PFA in the sagittal plane, measured by the PPFA, is dependent on the degree of extension-flexion of the stifle, and that the difference in the PPFA between the stifle angles evaluated in this study was statistically significant. The stifle angle and PPFA correlation coefficient indicated a strong linear association.

To the authors' knowledge, this is the first study that has investigated the relationship of the position of the patella related to the PFA in the sagittal plane during stifle range of motion. Moore *et al* (21) investigated the normal *in vivo* sagittal plane patellofemoral kinematics in dogs during daily activities using horizontal-beam flat-panel imaging. The results of these investigations concluded that patellofemoral alignment in the sagittal plane was correlated with the femoral-tibial flexion angle. Similar conclusions were drawn by Pozzi *et al* (26) in a cadaveric model, in which passive patellofemoral joint motion was described over a smaller range of femoral-tibial motion. Both studies demonstrated a relation of the proximal-distal position of the patella in relation to the stifle flexion angle. In our study, we identified this movement of the patella in the trochlear groove during stifle range of motion as previously described, but this was not further analyzed as this was beyond the scope of this study.

Achieving coaxial alignment is one of the goals when placing the femoral component in a BFX THR procedure. A misalignment in femoral canal preparation can lead to intraoperative complications during femoral broaching or can potentially lead to postsurgical complications due to stem malalignment (4). During femoral canal preparation for THR, forces resulting from impaction of the broach are distributed uniformly outward provided the broach is aligned parallel with the femoral long axis and enters the canal over the central axis (17). Misdirected forces and encroachment of the broach on the bone generate a consequent increase in bone strain that may result in a fissure or fracture (4,15). Femoral fissures that are not identified intraoperatively may propagate and manifest later as a complete femoral fracture during the terminal stages of broaching or stem insertion (27). In human medicine, Sakai *et al* (28) postulated that imperceptible microfractures occur during femoral canal preparation prior to noticeable intraoperative fracture, which highlights the significance of minimizing energy transmission in undesirable directions during femoral canal preparation.

It has been suggested that malalignment during femoral canal broaching in the sagittal plane could be prevented by aiming the

FOR PERSONAL USE ONLY

instruments just proximal to the patella, and cranial to it when there is caudal angulation of the femoral shaft (4). However, references regarding the degree of stifle flexion during femoral preparation for THR are lacking.

Our study has shown a statistical difference between the PPFA at 3 determined positions of stifle flexion. Due to the large proximal femoral fill required for the femoral component in press-fit with THR systems, it seems logical to assume that small variations in PPFA when broaching the femoral canal can have a clinical consequence. Although full stifle flexion during femoral canal broaching is unlikely in the clinical scenario, it is possible to position the stifle in any degree of extension between 90° and full extension, with a PPFA difference between these 2 stifle positions of 3.8° (± 1.0°). Therefore, neglecting the degree of stifle flexion during femoral canal preparation may result in broaching malalignment and, depending on the desired femoral canal stem filling, may result in encroachment which could increase the risk of intraoperative complications. The results from this study translate also to the clinical scenario and the average 3.8° increases in PPFA between the 90° and flexed stifle positions, and the 9.5° difference seen in PPFA in stifle range of motion could be clinically relevant. Consequently, the exactitude of the patella as anatomic reference during the surgical procedure should be assessed for every individual by measuring the PPFA during radiographic preoperative planning. Considering the degree of stifle flexion when using the patella as an intra-surgical landmark in femoral canal preparation should lead to a more accurate coaxial stem placement. Information related to the effect of the stem malalignment in the perioperative period has conflicting results. One study has shown that dogs with varus angulation of the stem ≥ 5° on postoperative radiographs were 12.5 times more likely to have concurrent intraoperative fissures, whereas malalignment of the stem in other orientations, including craniocaudal tipping, was not associated with fissure or fracture formation (15). Other studies have failed to associate stem positioning with risk of femoral fractures (29–31). In the long-term, misalignment of the prosthetic stem may result in an unnatural load transfer pattern, also defined as "stress shielding" that may lead to periprosthetic fractures, prosthetic loosening, and pain due to postoperative bone atrophy and resorptive bone remodelling (17,32).

Femoral fractures following THR have been reported in up to 13% of patients, but more recent reports have indicated an incidence of 6.8% (30,31). The authors from the later study suggested that their femoral preparation technique with improved femoral component coaxial alignment might be the reason for this lower complication rate. Stems placed in a neutral position allow the most even distribution of strain to provide the initial stability necessary to achieve bone osseointegration and consequently long-term stability (15,16,33,34).

Limitations to this study include the relatively small population of dogs and the potential anatomical differences among the breeds. Although sufficient statistical power was achieved, the different anatomy and size between individuals along with the small sample size may be a limitation and PPFA values may be different in a more homogeneous sample of dogs. The results of this study are based entirely on radiograph observations but results from the test of repeatability suggest that the method of measurement of PPFA is reliable given the high level of correlation.

As a final potential limitation, animals included in this study were presented for investigation of lameness and some had suspected partial cranial cruciate ligament rupture. In a recent study, the patella was noted to be more distal and positioned in greater flexion relative to the femoral trochlear in dogs with cranial cruciate ligament complete rupture during kinematic analyses (34). In a cadaveric experiment, cranial cruciate ligament transection resulted in a proximal shift of the patellofemoral joint contact area (35). In our population of dogs, it is unlikely that the presence of cranial cruciate rupture in some animals could have altered the patellofemoral position, as those patients with a positive cranial drawer test or with femoral-tibial subluxation were excluded from this study.

In summary, results from this study have confirmed our hypothesis, proving a significant difference in PPFA with different degrees of stifle flexion. Not considering this variability when using the patella position as a surgical guideline for femoral canal preparation might predispose to intra-surgical or postsurgical complications during THR due to broaching technique or stem malalignment. Performing preoperative mediolateral radiographs with the degree of stifle flexion which will be expected during surgery is recommended during surgical planning to achieve a correct stem alignment in the sagittal plane when using the patella position as intra-surgical landmark for THR.

Acknowledgments

The authors thank Dr. Muñoz-Prieto for his assistance with the statistical analyses of this report. This research was supported by the IVC Evidensia research grant.

References

1. Pozzi A, Kowaleski MP, Dyce J, Johnson KA. Treatment of traumatic coxo-femoral luxation by cemented total hip arthroplasty. Vet Comp Orthop Traumatol 2004;17:198–203.
2. Jankovits DA, Liska WD, Kalis RH. Treatment of avascular necrosis of the femoral head in small dogs with micro total hip replacement. Vet Surg 2012;41:143–147.
3. Kalis RH, Liska WD, Jankovits DA. Total hip replacement as a treatment option for capital physeal fractures in dogs and cats. Vet Surg 2012;41:148–155.
4. Peck JN, Liska WD, DeYoung DJ, Marcellin-Little DJ. Clinical application of total hip replacement. In: Advances in Small Animal Total Joint Replacement. John Wiley & Sons, 2013: 69–107.
5. Fitzpatrick N, Law AY, Bielecki M, Girling S. Cementless total hip replacement in 20 juveniles using BFX™ arthroplasty. Vet Surg 2014;43:715–725.
6. Gemmill TJ, Pink J, Clarke SP, McKee WM. Total hip replacement for the treatment of atraumatic slipped femoral capital epiphysis in dogs. J Small Anim Pract 2012;53:453–458.
7. Conzemius MG, Vandervoort J. Total joint replacement in the dog. Vet Clin North Am Small Anim Pract 2005;35:1213–1231.
8. Henderson ER, Wills A, Torrington AM, *et al.* Evaluation of variables influencing success and complication rates in canine total hip replacement: Results from the British Veterinary Orthopaedic

FOR PERSONAL USE ONLY

Association Canine Hip Registry (collation of data: 2010–2012). Vet Rec 2017;181:18.
9. Schiller TD. BioMedtrix total hip replacement systems: An overview. Vet Clin North Am Small Anim Pract 2017;47:899–916.
10. Liska WD, Israel SK. Morbidity and mortality following total hip replacement in dogs. Vet Comp Orthop Traumatol 2018;31: 218–221.
11. Schiller TD, DeYoung DJ, Schiller RA, Aberman HA, Hungerford DS. Quantitative ingrowth analysis of a porous-coated acetabular component in a canine model. Vet Surg 1993;22:276–280.
12. DeYoung DJ, DeYoung BA, Aberman HA, Kenna RV, Hungerford DS. Implantation of an uncemented total hip prosthesis technique and initial results of 100 arthroplasties. Vet Surg 1992;21:168–177.
13. Rashmir-Raven AM, DeYoung DJ, Abrams CF, Aberman HA, Richardson DC. Subsidence of an uncemented canine femoral stem. Vet Surg 1992;21:327–331.
14. BioMedtrix Inc. Canine Modular Total Hip Replacement System, Surgical Protocol for BFXTM Cementless Application. Boonton, New Jersey: BioMedtrix, 2008.
15. Townsend S, Kim SE, Pozzi A. Effect of stem sizing and position on short-term complications with canine press fit cementless total hip arthroplasty. Vet Surg 2017;46:803–811.
16. Pernell RT, Gross RS, Milton JL, *et al.* Femoral strain distribution and subsidence after physiological loading of a cementless canine femoral prosthesis: The effects of implant orientation, canal fill, and implant fit. Vet Surg 1994;23:503–518.
17. Pernell RT, Milton JL, Gross RS, *et al.* The effects of implant orientation, canal fill, and implant fit on femoral strain patterns and implant stability during catastrophic testing of a canine cementless femoral prosthesis. Vet Surg 1995;24:337–346.
18. Liska WD. Femur fractures associated with canine total hip replacement. Vet Surg 2004;33:164–172.
19. Hummel D. Zurich cementless total hip replacement. Vet Clin North Am Small Anim Pract 2017;47:917–934.
20. Johnson AL, Probst CW, DeCamp CE, Rosenstein DS, Hauptman JG, Kern TL. Vertical position of the patella in the stifle joint of clinically normal large-breed dogs. Am J Vet Res 2002;63:42–46.
21. Moore EJ, Kim SE, Banks SA, Pozzi A, Coggeshall JD, Jones SC. Normal patellofemoral kinematic patterns during daily activities in dogs. BMC Vet Res 2016;12:262.
22. Jaegger G, Marcellin-Little DJ, Levine D. Reliability of goniometry in Labrador Retrievers. Am J Vet Res 2002;63:979–986.
23. Reif U, Dejardin LM, Probst CW, DeCamp CE, Flo GL, Johnson AL. Influence of limb positioning and measurement method on the magnitude of the tibial plateau angle. Vet Surg 2004;33:368–375.
24. Peterson JL, Torres BT, Hutcheson KD, Fox DB. Radiographic determination of normal canine femoral alignment in the sagittal plane: A cadaveric pilot study. Vet Surg 2020;49:1230–1238.
25. Mostafa AA, Cunningham DP, Boudrieau RJ, Kowaleski MP, Griffon DJ. Influence of radiographic techniques on the measurement of femoral anteversion angles and a conformation score of pelvic limbs in Labrador retrievers. Vet Surg 2018;47:421–430.
26. Pozzi A, Dunbar NJ, Kim SE. Effect of tibial plateau leveling osteotomy on patellofemoral alignment: A study using canine cadavers. Vet J 2013;198:98–102.
27. Jasty M, Bragdon CR, Rubash H, Schutzer SF, Haire T, Harris W. Unrecognized femoral fractures during cementless total hip arthroplasty in the dog and their effect on bone ingrowth. J Arthroplasty 1992;7:501–508.
28. Sakai R, Kikuchi A, Morita T, *et al.* Hammering sound frequency analysis and prevention of intraoperative periprosthetic fractures during total hip arthroplasty. Hip Int J Clin Exp Res Hip Pathol Ther 2011;21:718–723.
29. Kidd SW, Preston CA, Moore GE. Complications of porous-coated press-fit cementless total hip replacement in dogs. Vet Comp Orthop Traumatol 2016;29:402–408.
30. Ganz SM, Jackson J, VanEnkevort B. Risk factors for femoral fracture after canine press-fit cementless total hip arthroplasty. Vet Surg 2010;39:688–695.
31. Weinans H, Huiskes R, Rietbergen BV, Sumner DR, Turner TM, Galante JO. Adaptive bone remodeling around bonded noncemented total hip arthroplasty: A comparison between animal experiments and computer simulation. J Orthop Res 1993;11: 500–513.
32. Mostafa AA, Wefstaedt P. Radiographic evaluation of early periprosthetic femoral bone contrast and prosthetic stem alignment after uncemented and cemented total hip replacement in dogs. Vet Surg 2012;41:69–77.
33. Monotti IC, Preston CA, Kidd SW. Treatment outcomes for periprosthetic femoral fractures in cementless press-fit total hip replacement. Vet Comp Orthop Traumatol 2020;33:370–376.
34. Kim SE, Zann GJ, Tinga S, Moore EJ, Pozzi A, Banks SA. Patellofemoral kinematics in dogs with cranial cruciate ligament insufficiency: An in-vivo fluoroscopic analysis during walking. BMC Vet Res 2017;13:250.
35. Guerrero TG, Pozzi A, Dunbar N, *et al.* Effect of tibial tuberosity advancement on the contact mechanics and the alignment of the patellofemoral and femorotibial joints. Vet Surg 2011;40:839–848.

FOR PERSONAL USE ONLY

Article

Iliopsoas strain demographics, concurrent injuries, and grade determined by musculoskeletal ultrasound in 72 agility dogs

Danny Sack, Debra Canapp, Sherman Canapp, Stephanie Majeski, Jeff Curry, Angela Sutton, Robert Cullen

Abstract

The objective of this study was to describe patient demographics associated with iliopsoas strains, frequency of common concurrent injuries, and associated strain grades based on musculoskeletal ultrasound.

The medical records of 72 client-owned agility dogs that had an iliopsoas musculoskeletal ultrasound (MSK-US) between 2009 and 2015 were retrospectively reviewed. Analyses included patient signalment, physical examination, and diagnostic findings.

Twenty-four breeds of canine athletes from 1.5 to 10 y old (median: 5 y, SD: 2.2 y) were included in the study. Of the 72 records reviewed, border collies were the most common breed (27.8%, 20/72) reported. Isolated iliopsoas strains occurred in 26.4% (19/72) of cases. Concurrent pathology was noted in 73.6% (53/72) of cases. Cranial cruciate ligament (CCL) instability was the most common concurrent pathology, representing 27.8% (20/72) of all cases, with hip (8.3%, 6/72), lumbosacral (23.6%, 17/72), other non-CCL hind limb (6.9%, 5/72), and forelimb (6.9%, 5/72) pathologies making up the remainder of cases with concurrent pathology. In patients with a concurrent hind limb injury, 96.7% (30/31) of dogs had their most severe iliopsoas strain grade on the same limb.

MSK-US revealed Grade I strains in 54.2%, Grade II strains in 22.2%, Grade III strains in 5.2%, and chronic changes in 18.1% of cases. There were no statistically significant associations between iliopsoas strain grade and age, body weight, sex, breed, concurrent pathology, anatomic location of concurrent pathology, or sidedness of concurrent pathology.

Iliopsoas strains are one of the most common agility dog injuries; however, patient demographics, prevalence of concurrent injury and correlation with MSK-US findings have not been previously reported. To the authors' knowledge, this is the first retrospective analysis reporting iliopsoas strain demographics, concurrent injury frequency and correlation with MSK-US evaluation in agility dogs. Although 26.4% of iliopsoas strains occurred as isolated injuries, 73.6% had concurrent injuries, with CCL instability present most commonly, occurring in 27.8% of cases.

Dogs should be thoroughly evaluated for concurrent injuries when presenting with an iliopsoas strain.

Résumé

L'objectif était de décrire les données démographiques des patients associées aux douleurs de l'iliopsoas, la fréquence des blessures concomitantes courantes et les degrés de douleur associés sur la base d'une échographie musculosquelettique.

Les dossiers médicaux de 72 chiens d'agilité appartenant à des clients qui ont subi une échographie musculosquelettique de l'iliopsoas (MSK-US) entre 2009 et 2015 ont été examinés rétrospectivement. L'analyse comprenait le signalement du patient, l'examen physique et les résultats de diagnostic.

Vingt-quatre races d'athlètes canins âgés de 1,5 à 10 ans (médiane 5, SD 2,2) ont été incluses dans l'étude. Sur les 72 enregistrements examinés, les border collies étaient la race la plus fréquemment signalée (27,8 %, 20/72). Des douleurs isolées du psoas iliaque sont survenues dans 26,4 % (19/72) des cas. Une pathologie concomitante était notée dans 73,6 % (53/72) des cas. L'instabilité du ligament croisé crânien (CCL) était la pathologie concomitante la plus fréquente, représentant 27,8 % (20/72) de tous les cas, avec hanche (8,3 %, 6/72), lombo-sacrée (23,6 %, 17/72), autres pathologies des membres postérieurs du CCL (6,9 %, 5/72) et des membres antérieurs (6,9 %, 5/72) constituent le reste des cas avec une pathologie concomitante. Chez les patients présentant une lésion concomitante du membre postérieur, 96,7 % (30/31) des chiens présentaient leur degré de douleur de l'iliopsoas le plus grave sur le même membre. MSK-US a révélé des douleurs de grade I dans 54,2 %, des douleurs de grade II dans 22,2 %, des douleurs de grade III dans 5,2 % et des modifications chroniques dans 18,1 % des cas. Aucune association statistiquement significative n'a été trouvée entre le degré de douleur de l'iliopsoas et l'âge, le poids corporel, le sexe, la race, la pathologie concomitante, la localisation anatomique de la pathologie concomitante ou le caractère latéral de la pathologie concomitante.

Veterinary Orthopedic and Sports Medicine Group, 10975 Guilford Road Ste B, Annapolis Junction, Maryland 20701, USA (Sack, Canapp D, Canapp S, Majeski, Curry, Cullen); Canapp Sports Medicine, 6030 Daybreak Circle, Clarksville, Maryland 21029, USA (Canapp D, Canapp S, Sutton).

Address all correspondence to Dr. Danny Sack; email: Dsack16@gmail.com

Received December 27, 2022. Accepted January 9, 2023.

FOR PERSONAL USE ONLY

Les douleurs d'iliopsoas sont l'une des blessures les plus courantes chez les chiens d'agilité; cependant, la démographie des patients, la prévalence des blessures concomitantes et la corrélation avec les résultats MSK-US n'ont pas été rapportées auparavant. À la connaissance de l'auteur, il s'agit de la première analyse rétrospective faisant état de la démographie de la douleur de l'iliopsoas, de la fréquence des blessures concomitantes et de la corrélation avec l'évaluation MSK-US chez les chiens d'agilité. Bien que 26,4 % des douleurs de l'iliopsoas se soient produites sous forme de blessures isolées, 73,6 % avaient des blessures concomitantes. L'instabilité du CCL était présente le plus souvent, survenant dans 27,8 % des cas.

Les chiens doivent être soigneusement évalués pour les blessures concomitantes lorsqu'ils présentent une douleur de l'iliopsoas.

(Traduit par les auteurs)

Introduction

Iliopsoas injury is a common cause of hind limb lameness in dogs and has been investigated at an increased frequency in recent years (1–4). In a study by Nielson and Pluhar (3), the iliopsoas muscle was the most common hind limb muscle strain, primarily affecting 32% of cases. In addition, in that study, 95% of all hind limb muscle strains were localized to the hip adductor muscle group, comprised of iliopsoas and/or pectineus muscles, and dogs were markedly uncomfortable on simultaneous hind limb extension and internal rotation (but with pain unable to be isolated to either the iliopsoas or pectineus muscles). In a more recent study by Markley *et al* (5) that surveyed 4197 agility dog owners, iliopsoas strain was the second most often reported condition, occurring in 19.4% of the 1958 canine athletes included.

The iliopsoas muscle is comprised of the iliacus and psoas major muscles. The psoas major originates from the transverse processes of lumbar vertebrae 2 and 3, with additional connections to lumbar vertebrae 3 through 7 *via* an aponeurosis with the quadratus lumborum muscle. The iliacus muscle arises from the ventral ilium. The 2 muscles course caudoventrally with a conjoined insertion on the lesser trochanter of the femur. The major function of the iliopsoas is hip flexion. In addition, the iliopsoas aids in hip joint and vertebral column stabilization, flexion of the vertebral column when the femur is in a fixed position and produces adduction and external rotation of the femur (6,7).

The frequency of muscle injury in dogs is presumed to be underdiagnosed due to the often self-limiting nature of the injury and the patient not being presented to a veterinarian (2,3,6,8). Likewise, an iliopsoas strain may also act as a "red herring," and be implicated as the suspected primary cause of discomfort, when comorbidities may be present, such as a cranial cruciate ligament rupture, underlying hip dysplasia, or lumbosacral pathology. Orthopedic or neurologic causes of lameness, such as cranial cruciate ligament injury (CCL), hip dysplasia (HD), lumbosacral (LS) disease, or spinal myelopathy, may confound the diagnosis and occur concurrently with an iliopsoas strain (1,3,9,10).

Acute iliopsoas strains occur when external forces applied to the muscle overload its contractile force during eccentric contraction (3,4,8,11,12). Strains commonly occur at the muscle-tendon junction as this is the weakest portion of the myotendinous unit. This results in muscle fiber disruption and loss of continuity, disruption in vascular supply, and subsequent interstitial hemorrhage and inflammation (3,13). Patients with acute iliopsoas injury may have an identifiable preceding traumatic event such as jumping, slipping into a splay-legged position in the hind limbs, or strenuous hiking, and are often associated with athletic events such as agility (1). Chronically affected patients typically have a history of recurrent or progressive hind limb lameness (2). Furthermore, a patient with iliopsoas injury may ambulate with a shortened stride length and decreased hip extension (2). Agility dogs may exhibit decreased hind limb extension when jumping, decreased drive in their hind limbs when weaving, and decreased weight bearing in the affected limb. Pain and/or spasm may be appreciated on palpation of the lumbar muscles, ventromedial to the ilium at the lesser trochanter, and on transrectal palpation of the pubic rim in small dogs. They also may be resistant to hip extension with simultaneous internal rotation (iliopsoas muscle maneuver test), or hip abduction (1,3,4).

The structures evaluated during musculoskeletal ultrasound (MSK-US) of the iliopsoas include the region of insertion on the lesser trochanter and its associated bursa, the muscle belly, and muscle origins. Examination allows for grading of the strain and subsequent categorization, according to a 3-tiered grading system based on structural abnormalities and strain severity (4,14,15). Muscle and tendon injury are graded according to the same scheme.

Ultrasonographically, acute strains appear as hypoechoic lesions within the belly of the muscle, or within the tendon, and there is evidence of fiber disruption. Chronic strains appear hyperechoic, indicative of fibrosis or scar tissue, presumably a consequence of a historic acute strain, acute on chronic injury or repetitive microtrauma (4). Grade I strains have focal edema or hemorrhage with $< 5\%$ muscle or tendon involvement. Grade II strains have increased muscle and tendon involvement, with mild disruption of muscle fibers, and increased presence of edema and/or hemorrhage. In Grade III strains, there is marked fascial tearing, muscle and tendon fiber rupture, edema and/or hemorrhage. In instances of chronic injury, similar degrees of fiber disruption and muscle involvement are present as seen in Grade II strains, but with hyperechoic fiber changes within the muscle/tendon and/or fibrous change/debris within the iliopsoas bursa (4,12,16). Dogs with injuries containing properties of 2 grades are given an intermediate grade (*i.e.*, Grade I–II or II–III) (4).

Iliopsoas strains are a common injury in agility dogs, yet there is a paucity of literature on the topic. The goals of this study were to describe the demographics and frequency of concurrent injuries with iliopsoas strains in agility dogs. We hypothesized that dogs with iliopsoas strains have concurrent musculoskeletal pathology in $> 50\%$ of cases.

Materials and methods

Medical records of 72 agility dogs that were presented to Veterinary Orthopedic and Sports Medicine Group between 01/2009 and 7/2015 with pain on iliopsoas palpation, iliopsoas stretch

FOR PERSONAL USE ONLY

(*i.e.,* hip extension with internal rotation) and a confirmed iliopsoas strain based on MSK-US were reviewed. The present study is a follow-up to a study performed by Cullen *et al* (4) that used the same patient population and described the ultrasound findings in agility dogs with iliopsoas strains and proposed a 3-tier grading scheme for iliopsoas strain characterization based on MSK-US findings. The owner of 1 of the initial 73 patients included in the initial study had requested to be excluded in subsequent research studies; the remaining 72 patients were included in the present report. Items reviewed included patient demographics, concurrent musculoskeletal conditions noted on physical examination, as well as diagnostics pursued based on examination findings. Concurrent injuries were categorized based on physical examination and diagnostic imaging findings. All patients were sedated for MSK-US evaluation with a combination of butorphanol 0.2 mg/kg and dexmedetomidine 3 μg/kg IV or IM. All ultrasound examinations were performed by a single observer (Debra Canapp 'DC'). MSK-US findings were used to grade iliopsoas strains into 4 categories (I, II, III, and chronic) as previously described, and are summarized in Table I (10). Iliopsoas strains with characteristics overlapping 2 grade categories (*i.e.,* Grade I–II strain) were rounded to the nearest grade (*i.e.,* a Grade II–III rounded to a Grade III lesion) based on discussion with the ultrasonographer (DC) to facilitate analysis. Patients were allocated into 6 categories: no concurrent injury (isolated iliopsoas strain), concurrent CCL instability, hip pathology, LS disease, forelimb pathology, and other non-CCL hind limb injury. Cranial cruciate ligament pathology was diagnosed on physical examination based on palpable tibial thrust or cranial drawer, or *via* arthroscopy. Hip pathology was diagnosed based on laxity appreciated while performing an ortolani maneuver, or if there was a radiographic diagnosis of hip dysplasia with concurrent pain on hip extension. Lumbosacral pathology was suspected when there was significant discomfort appreciated on palpation of the LS junction on physical examination. Magnetic resonance imaging reports from patients that had undegone LS imaging were reviewed to determine if LS discomfort was a result of spinal cord compression, nerve compression, or referred pain from the iliopsoas origin along the lumbar vertebrae. All patients received a static position MRI.

Statistical analyses were used to identify potential relationships between selected parameters and iliopsoas injury grade. Categorical data including sex, breed, concurrent injury diagnosis, anatomic location of concurrent injury (*i.e.,* hind limb, forelimb, or LS), and sidedness of concurrent injury diagnosis, compared to the iliopsoas injury, were evaluated using a Pearson's Chi square. Continuous data (age and body weight) were assessed using Pearson's correlation. Statistical significance was set at $P \leq 0.05$ for all analyses. Analyses were performed using NCSS 2022, v22.0.3 (NCSS 2022 Statistical Software (2022). NCSS, LLC. Kaysville, Utah, USA, ncss.com/software/ncss).

Table I. Musculotendinous grading scheme for dogs.

Grade	Description
I	"Mild strain," < 5% muscle involvement, focal edema/hemorrhage
II	"Moderate strain," > 5% muscle involvement, mild fiber tearing, increased edema/hemorrhage
III	"Severe strain," significant fascial tearing, marked to complete muscle fiber disruption, marked edema/hemorrhage
Chronic	Hyperechoic fiber pattern, hyperechoic changes and/or debris within bursa, > 5% muscle involvement, mild fiber tearing

Results

All canine athletes were from 1.5 to 10 y old, with a mean age of 5.0 y (SD = 2.2 y). Twenty-four dog breeds were represented. The border collie was the most common purebred dog (n = 20), followed by the Australian shepherd (n = 8), Shetland sheepdog (n = 5), and golden retriever, Labrador retriever, and the Welsh corgi (n = 4 each) with various other purebred dogs reported in fewer numbers (< 4 individuals each). The average dog weight was 20.2 kg, with 56 patients weighing from 10 to 30 kg (78%). Spayed females were most common in this group representing 32 of 72 (44.4%) participants. Neutered males accounted for 18 (25%) dogs, and there were 8 intact females (11%) and 14 intact males (19.4%).

Of the 72 patients examined, a concurrent, non-iliopsoas injury was diagnosed in 53 dogs. Distributions of the suspected concurrent musculoskeletal conditions based on physical examination are summarized in Table II. In 19 (26.4%) dogs, the only source of discomfort was pain on palpation of the iliopsoas insertion. In all 19 cases, the iliopsoas strain was confirmed to be the only musculoskeletal pathology, and therefore determined to be a primary iliopsoas strain. Cranial cruciate ligament instability was present in 20 dogs (27.8% of cases). Lumbosacral discomfort was noted on palpation in 22 patients but was considered the primary source of pain based on reactivity during lumbosacral palpation in 17 patients (23.6% of all cases). Magnetic resonance imaging of the LS spine was performed in 14 of the 17 patients in which the LS region was localized as the primary source of pain. Of the 14 patients, MRI revealed LS pathology in 5 patients and was normal in 6 patients. Reports were unavailable in 3 patients at the time of the present study. The distribution of confirmed injuries (n = 66), considering MRI findings, is shown in Figure 1. In this subset of data, dogs with a normal LS scan were considered to have a primary iliopsoas strain, except for 1 dog with very mild concurrent CCL pathology (but no appreciated instability), with significant lumbosacral pain on initial physical examination. Dogs with significant LS discomfort without an MRI performed, or dogs with unavailable MRI reports, were not included in this data subset. Radiographically diagnosed hip pathology and pain and/or instability was noted in 6 dogs (8.3% cases). An injury to the forelimb was noted in 5 dogs (6.9% of cases), and a non-CCL injury to the hind limb was diagnosed in 5 dogs (6.9% of cases). Forelimb injuries consisted of medial shoulder instability (n = 2), supraspinatus and biceps tendinopathy (n = 2), and fragmented medial coronoid process (n = 1). Non-CCL hind limb injuries included a sartorius strain (n = 1), and medial patellar luxation with marked stifle osteoarthritis (n = 4).

In all patients, MSK-US of the iliopsoas was performed bilaterally. Distribution of all iliopsoas strain grades is illustrated in

FOR PERSONAL USE ONLY

Table II. Anatomic distribution of injury based on physical examination (*n* = 72).

Anatomic location	
Iliopsoas insertion	19 (26.4%)
Iliopsoas plus:	
CCL	20 (27.8%)
Hip	6 (8.3%)
Lumbosacral	17 (23.6%)
Forelimb	5 (6.9%)
Non-CCL hind limb	5 (6.9%)

Figure 2. MSK-US examination of the iliopsoas revealed Grade I strains most often in 39 cases (54.2%). Grade II strains were present in 16 cases (22.2%), Grade III strains in 4 cases (5.6%), and chronic changes in 13 cases (18.1%). Bilateral ultrasonographic iliopsoas changes were noted in 52/72 (72.2%) of dogs. Although frequently occurring, contralateral ultrasonographic findings in unilaterally lame dogs were thought to be less significant and were considered a compensatory, non-clinical finding. In dogs with concurrent pathology, the most significant iliopsoas injury, determined by both reactivity on physical examination and MSK-US findings, occurred on the same hind limb as the concurrent pathology most seen in 30 cases (41.7%). The concurrent pathology occurred in the contralateral hind limb in 1 (1.4%) case, the ipsilateral forelimb in 3 (4.2%) cases, and the contralateral forelimb in 2 cases (2.8%), as illustrated in Figure 3. In 17 cases (23.6%), pain was localized to the LS region on spinal palpation, and therefore was not a lateralizing physical examination finding. Of the 31 patients in which the primary injury was localized to the hind limb, 30 (96.8%) of patients had their most significant iliopsoas strain on the same limb of their concurrent injury. Of the 14 patients that had an MRI of the LS spine, 11 reports were available for review. The primary source of LS pain was attributed to an isolated iliopsoas strain in 6/11 cases (54.5%) as no nerve or spinal cord compression was noted. In the 5 (45.5%) remaining MRI cases, iliopsoas pain was deemed secondary to underlying intervertebral disc disease or nerve impingement.

Grade I iliopsoas strains were most common in patients with isolated iliopsoas strains, and concurrent CCL, hip, LS pathology, or other non-CCL hind limb injuries. In the studied sample population, Grade I strains were equally as frequent in those with concurrent forelimb pathology as Grade II strains. Grade II strains were diagnosed in 16 dogs, with 7/16 (43.8%) occurring in dogs with isolated iliopsoas strains. Grade III strains were the least frequently confirmed strain in all categories. Chronic changes to the iliopsoas occurred most frequently in dogs with concurrent CCL instability 4/13 (30.8%). These findings are summarized in Table III and illustrated in Figure 4.

There were no significant differences amongst sex, breed, or concurrent injury type, anatomic location of concurrent injury, or sidedness of concurrent injury between the 4 iliopsoas injury categories in this dataset. Likewise, there were no significant correlations between age or body weight, and any of the 4 iliopsoas injury categories, or between sidedness of iliopsoas injury and concurrent injuries in cases in which those were present.

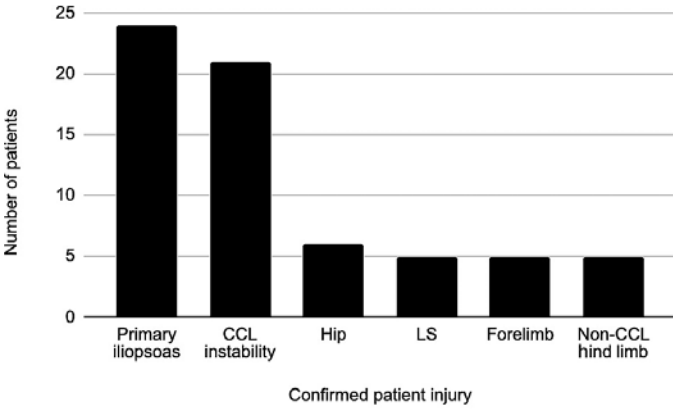


Figure 1. Distribution of confirmed primary injuries (*n* = 66). Note, 6 cases were removed due to no MRI report (*n* = 3) or not pursuing MRI (*n* = 3) despite LS pain on physical examination.

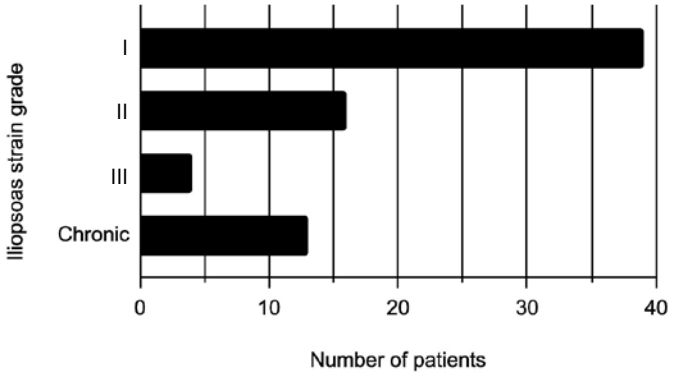


Figure 2. Distribution of all iliopsoas pathology noted on musculoskeletal ultrasound (*n* = 72).

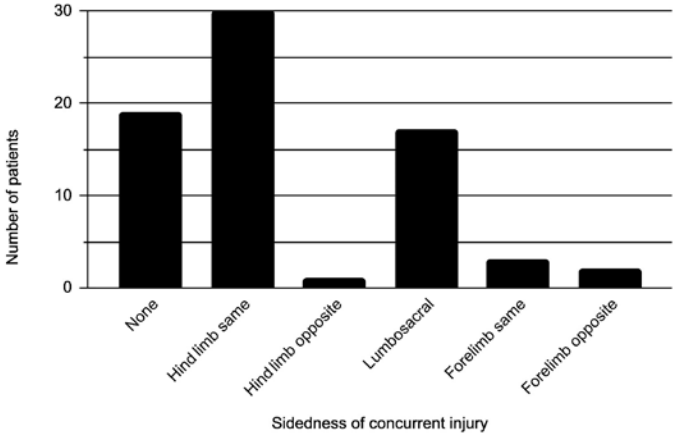


Figure 3. Sidedness of concurrent injury relative to the primary iliopsoas strain (*n* = 72).

FOR PERSONAL USE ONLY

Table III. Distribution of iliopsoas strain grade based on primary injury on physical examination (*n* = 72 dogs).

	Isolated iliopsoas	CCL	Hip	Lumbosacral	Forelimb	Other non-CCL hind limb
I	8	13	4	9	2	3
II	7	2	0	4	2	1
III	1	1	1	1	0	0
Chronic	3	4	1	3	1	1

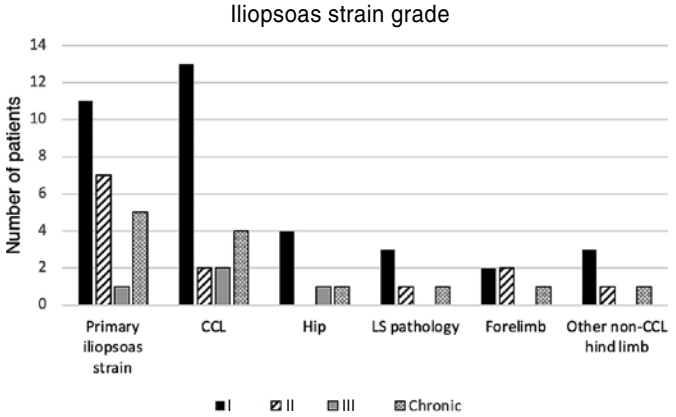


Figure 4. Distribution of iliopsoas strain grade based on isolated or concurrent injury on physical examination (*n* = 72).

Discussion

Results of this study confirmed that most agility dogs with iliopsoas strains had concurrent injuries. Of the concurrent injuries noted on physical examination, CCL injury was the most common, closely followed by LS disease. Pathology associated with the hip, forelimbs and other hind limb and non-CCL injuries were also reported, but less frequently. Notably, LS pain was reported in 17 cases; however, in only 5 cases of the 14 that received an MRI, was pathology of the spine or nerves diagnosed. This is likely underdiagnosed in the studied population as an LS MRI was not performed in all patients and is a limitation of this study. In addition, all patients received a static MRI. Perhaps subclinical lumbosacral pathology was present in some dogs whose lumbosacral region was deemed normal on MRI, whereas pathology may have been diagnosed had a dynamic MRI been performed (17). Further research is warranted to evaluate the frequency of these 2 concurrent pathologies due to the overlap in physical examination findings and relatively low number of cases for these injuries.

Consistent with previous studies and breed popularity in agility, the border collie was the most common purebred dog in this study (5,18,19). The 2021 report by Markley *et al* (5) highlighted the iliopsoas muscle as a common injury amongst agility dogs. In that study, the iliopsoas was the second most frequently reported injury, behind shoulder injury, accounting for 19.4% of injuries sustained. In a report by Nielsen *et al* (3), the iliopsoas was the most common pelvic limb muscle strain location. Iliopsoas strains had been reported to occur concurrently with other concurrent orthopedic and neurologic diseases (1,3), and as reported in a study by Ragetly *et al* (8). Despite the common nature of this disease in agility dogs, there is a dearth of studies investigating iliopsoas strains. To the authors' knowledge, this is the first report investigating the frequency of iliopsoas strains as either an isolated or concurrent injury in canine athletes, as well as the distribution of iliopsoas strain grades relative to concurrent injury, or lack thereof.

Treatment and recovery of iliopsoas strains was outside the scope of this report due to the frequency of concurrent injury and frequent loss of follow-up after diagnosis of a concurrent injury. Treatment and management of iliopsoas strains is variable, based on both strain grade and clinician preference, and the timeline to recovery is often confounded by concurrent injuries. Accordingly, further research is warranted regarding the ideal treatment for this condition.

A limitation of the present study was the retrospective nature and reliance on accuracy and completeness of medical records. Data included in this study was between 7 and 13 y old at the time of this report; therefore, diagnostic techniques and interpretation may have been altered based on continued clinical experience, advancements in research, and diagnostic technologies. Additional limitations included lack of blinding, randomization, control group, and MRI verification of iliopsoas strain diagnosis. In addition, there is risk of bias as data were collected by the principal investigator, who was not the same investigator who obtained all ultrasound images. For the purposes of this study, injury grades were divided into 4 categories (I, II, III, and chronic). As previously reported, intermediate grades (*i.e.*, I–II) for iliopsoas strains have historically been assigned to facilitate analysis with the selected population (4). To facilitate statistical analysis, grades were rounded up to the nearest grade (*i.e.*, a Grade II–III rounded to a Grade III lesion) for all injuries originally classified as an intermediate grade, based on discussion with the ultrasonographer (DC). Therefore, the resulting grades in this study were slightly more severe from what truly occurred in the studied population. Classification of strain chronicity was based on ultrasonographic appearance, correlated with clinical experience and previous retrospective studies, including timeline of injury, muscle/tendon fiber pattern, and presence of edema on ultrasound. No histologic testing was performed to corroborate MSK-US findings. All these factors could have contributed to the lack of statistically significant associations between iliopsoas injury grade and the parameters examined in this dataset, although it is also important to note that some of the comparisons made were underpowered. Additional work in larger groups of dogs is needed to confidently determine if any of these parameters are significantly associated

FOR PERSONAL USE ONLY

with grade of iliopsoas strain in the dog, and whether any of these relationships are clinically relevant.

Another significant limitation to this study was case selection. Despite no available data on the overall percentages of iliopsoas strain grades in companion animals, there may be an increased frequency of high-grade strains in canine athletes due to frequent microtrauma related to their high activity. All cases were obtained from a single facility; therefore, most cases were from a relatively similar geographic region within the United States. As described by Markley *et al* (5), iliopsoas injury is significantly more common in the US and Canada than in dogs of the UK, Ireland, and continental Europe. This may have further implications in distribution of iliopsoas strain severity and correlation with concurrent injuries. In addition, the reported concurrent injuries are not isolated to only those participating in agility. Data are lacking in the reported injury rates within the overall canine population. The present study did not compare the frequency of concurrent injuries as related to that of the general population.

Findings of this study highlighted the complicated nature of diagnosing iliopsoas strains on physical examination only, and the importance of utilizing advanced imaging techniques such as MSK-US to confirm and grade an iliopsoas strain. In addition, the high frequency of concurrent injuries indicated the importance of screening for other concurrent pathology when iliopsoas pain is noted on physical examination.

Acknowledgments

The authors thank Drs. Glenna Mauldin and Neal Mauldin for assistance with statistical analyses.

References

1. Johnston SA, Tobias KM. Veterinary Surgery: Small Animal Expert Consult. St. Louis, Missouri: Saunders, 2017.
2. Breur GJ, Blevins WE. Traumatic injury of the iliopsoas muscle in three dogs. J Am Vet Med Assoc 1997;210:1631–1634.
3. Nielsen C, Pluhar GE. Diagnosis and treatment of hind limb muscle strain injuries in 22 dogs. Vet Comp Orthopaed 2005;18: 247–253.
4. Cullen R, Canapp D, Dycus D, Carr B, Ibrahim V, Canapp S. Clinical evaluation of iliopsoas strain with findings from diagnostic musculoskeletal ultrasound in agility performance canines — 73 cases. Vet Évid 2017:2.
5. Markley AP, Shoben AB, Kieves NR. Internet-based survey of the frequency and types of orthopedic conditions and injuries experienced by dogs competing in agility. J Am Vet Med Assoc 2021;259:1001–1008.
6. Cabon Q, Bolliger C. Iliopsoas muscle injury in dogs. Compendium 2019:35. Available from: https://www.vetfolio.com/learn/article/iliopsoas-muscle-injury-in-dogs Last accessed June 1, 2023.
7. Evans HE, Lahunta A de. Miller's Anatomy of the Dog. St. Louis, Missouri: WB Saunders, 1993.
8. Ragetly GR, Griffon DJ, Johnson AL, Blevins WE, Valli VE. Bilateral iliopsoas muscle contracture and spinous process impingement in a German Shepherd dog. Vet Surg 2009;38: 946–953.
9. Garrett WE. Muscle strain injuries. Am J Sports Med 1996;24: S2–S8.
10. Kraus-Hansen AE. Trigger points in 48 dogs with myofascial pain syndromes. Vet Surg 1992;21:87.
11. Anderson K, Strickland SM, Warren R. Hip and groin injuries in athletes. Am J Sports Med 2001;29:521–533.
12. Johnston CAM, Wiley JP, Lindsay DM, Wiseman DA. Iliopsoas bursitis and tendinitis. Sports Med 1998;25:271–283.
13. Cook CR. Ultrasound imaging of the musculoskeletal system. Vet Clin North Am Small Animal Pract 2016;46:355–371.
14. Peetrons P. Ultrasound of muscles. Eur Radiol 2002;12:35–43.
15. Takebayashi S, Takasawa H, Banzai Y, *et al.* Sonographic findings in muscle strain injury: Clinical and MR imaging correlation. J Ultrasound Med 1995;14:899–905.
16. Laor T. Hip and groin pain in adolescents. Pediatr Radiol 2010; 40:461–467.
17. Lampe R, Foss KD, Hague DW, Oliveira CR, Smith R. Dynamic MRI is reliable for evaluation of the lumbosacral spine in healthy dogs. Vet Radiol Ultrasound 2020;61:555–565.
18. Levy I, Hall C, Trentacosta N, Percival M. A preliminary retrospective survey of injuries occurring in dogs participating in canine agility. Vet Comp Orthop Traumatol 2009;22:321–324.
19. Cullen KL, Dickey JP, Bent LR, Thomason JJ, Moëns NMM. Internet-based survey of the nature and perceived causes of injury to dogs participating in agility training and competition events. J Am Vet Med Assoc 2013;243:1010–1018.

FOR PERSONAL USE ONLY

Long-term outcomes after arthroscopic treatment of dogs affected by osteochondrosis dissecans of the humeral trochlea, with or without medial coronoid disease: 23 cases (2012–2020)

Joachim Lahiani, Antoine Dunié-Mérigot, Alexandre Caron, Kevin Le Boedec, Guillaume Ragetly

Abstract

The objective of this study was to report long-term clinical and radiographic outcomes following arthroscopic reparative treatment — flap removal, curettage, and osteostixis of subchondral bone — in dogs with humeral trochlea osteochondritis dissecans (OCD). Dogs were included in this retrospective multicenter case series if they had a computed tomography diagnostic of humeral trochlear OCD, with or without medial coronoid disease, that was treated by arthroscopic reparative technique, and a detailed follow-up at least 6 mo postoperatively. The latter included a clinical examination, assessment of lameness, measurement of the brachial circumference and elbow amplitude, International Elbow Working Group (IEWG) radiographic score, owner-completed canine brief pain inventory (CBPI) score, and visual analogue scale (VAS) rating. A generalized linear model and tests for symmetry and marginal homogeneity were used to compare data. Twenty-three dogs (30 affected elbows) were included. Long-term (median: 22 mo; range: 6 to 98 mo) postoperative lameness, CBPI, VAS, joint distension, and pain scores were significantly improved compared with the preoperative values. Long-term postoperative range of motion and brachial circumference did not reveal any significant difference between OCD-affected and unaffected elbows. Long-term IEWG scores were similar to preoperative values in 56% of elbows and had progressed by 1 grade in 44%. Long-term complications included persistent Grade-1 lameness and occurred in 23% of dogs. Long-term outcomes based on lameness and CBPI scores were considered excellent in 67% of dogs, good in 27%, and intermediate in 6%. Arthroscopic treatment is thus a suitable surgical procedure for OCD of the humeral trochlea in dogs and provides good long-term results.

Résumé

Cette étude rapporte les résultats cliniques et radiographiques à long terme après un traitement arthroscopique chez des chiens atteints d'ostéochondrite disséquante (OCD) de la trochlée humérale. Les chiens inclus ont reçu un diagnostic d'OCD de la trochlée humérale par tomographie, un traitement réparateur par arthroscopie et un suivi post-opératoire d'au moins 6 mois. Ce dernier comprenant un examen clinique et orthopédique, la mesure de la circonférence brachiale et de l'amplitude du coude, le score radiographique de l'International Elbow Working Group (IEWG), le score Canine Brief Pain Inventory (CBPI) et l'échelle visuelle analogique (EVA). Un modèle linéaire généralisé et des tests de symétrie et d'homogénéité marginale ont permis de comparer les données. Vingt-trois chiens (30 coudes affectés) ont été inclus. Les scores postopératoires à long terme (médiane, 22 mois), de boiterie, de CBPI, d'EVA, de distension articulaire et de douleur étaient significativement améliorés. L'amplitude de mouvement et la circonférence brachiale postopératoires à long terme entre les coudes affectés et non affectés n'ont pas révélé de différence significative. Les scores IEWG à long terme étaient similaires aux valeurs préopératoires dans 56 % des coudes et avaient progressé d'un grade dans 44 %. Les résultats à long terme basés sur la boiterie et les scores CBPI ont été considérés comme excellents chez 67 % des chiens, bons chez 27 % et intermédiaires chez 6 %. Le traitement arthroscopique est donc une procédure chirurgicale appropriée pour l'OCD de la trochlée humérale chez le chien et donne de bons résultats à long terme.

(Traduit par les auteurs)

Centre Hospitalier Vétérinaire Frégis, Arcueil, France (Lahiani, Le Boedec, Ragetly); Centre Hospitalier Vétérinaire Languedocia, Montpellier, France (Dunié-Mérigot); Clinique Vétérinaire AniCura TRIOVet, Rennes, France (Caron).

Address all correspondence to Dr. Guillaume Ragetly; telephone: +33 1 49 85 83 03; email: gragetly@fregis.com

This paper was accepted for a poster presentation at the 2021 European College of Veterinary Surgeons (ECVS) Congress.

Conflict of interest

None of the authors of this article has a financial or personal relationship with other people or organizations that could inappropriately influence or bias its content.

Received November 13, 2022. Accepted February 13, 2023.

FOR PERSONAL USE ONLY

Introduction

Osteochondrosis dissecans (OCD) of the humeral trochlea affects mostly young dogs of medium to large breeds (1). Several treatments have been suggested. Initially, reparative techniques were carried out by arthrotomy, which consisted of excision of the cartilage flap with or without underlying bone marrow stimulation (2). These initial open approaches have not shown better results than conservative management, based on exercise restriction for 6 wk with or without injection of pentosan polysulfate once a week for 4 wk (3,4). Arthroscopic reparative techniques have later been described, including flap removal, curettage of any diseased cartilage surrounding the defect, and subchondral osteostixis to promote fibrocartilage growth (5).

Osteochondral autograft transplants (OAT) have more recently been described for treating humeral trochlear OCD lesions in dogs (6,7). Although technically feasible, this restorative technique has raised some major concerns, including donor site morbidity, invasiveness, significant revision challenges after graft or implant failure, quality of the grafted material, difficulty in restoring elbow congruity, and lack of described long-term follow-up (6,8). Synthetic osteochondral resurfacing, allografts, and xenografts have been mentioned to mitigate some of these concerns but have not been described in the canine elbow. In human orthopedics, despite many advanced reparative techniques, debridement and microfracture remain a gold standard in the surgical treatment of elbow OCD (9,10).

We are not aware of any study evaluating dogs with OCD of the humeral trochlea, including a long-term standardized postoperative assessment of this arthroscopic reparative technique based on clinical, radiographic, and owner-questionnaire scorings. The objective of this study was to determine whether arthroscopic debridement and microfracture is a suitable treatment for humeral trochlear OCD. Our hypothesis was that this minimally invasive technique allows long-term clinical improvement in canine patients, despite the development of osteoarthritis over time.

Materials and methods

This retrospective multicenter case series included dogs from 3 veterinary referral hospitals that were operated on by 3 experienced arthroscopic, Board-certified surgeons from 2012 to 2020. Data for each case, collected during preoperative and postoperative assessment, are listed in Table I. The inclusion criteria were the presence of a humeral trochlear OCD, among other elbow dysplasia components, diagnosed by computed tomography and treated by arthroscopic reparative technique, as well as a detailed long-term follow-up at least 6 mo after the surgery.

Follow-up included a clinical examination, assessment of lameness, measurement of the brachial circumference and maximal elbow range of motion, International Elbow Working Group (IEWG) radiographic score, owner-completed canine brief pain inventory (CBPI) score, and visual analogue scale (VAS) score.

A complete orthopedic examination was carried out on each dog and no other abnormalities of the forelimb were identified. Dogs with other concurrent components of elbow dysplasia were not excluded from the study. Elbow incongruity was diagnosed when greater than 2 mm. For each dog, the breed, sex, age, and duration of lameness were recorded. All dogs were in good health overall. A client consent form was signed by each owner prior to enrolment in the study. Surgery and postoperative follow-up were carried out by the same surgeon.

Table I. Summary of data collected during preoperative and postoperative assessment.

Preoperative assessment	• Breed, sex, age, BCS, weight, and duration of lameness • Clinical and orthopedic examination, lameness score, search for palpable elbow distension and pain in flexion, extension, pronation, or supination • Preoperative elbow radiographs and IEWG score when available
Long-term follow-up (At least 6 mo postoperatively)	Same clinical assessment as in preoperative, in addition to: • brachial circumference and elbow range of motion measurement; • postoperative elbow radiographs and IEWG score; and • owner-completed CBPI and VAS scores.

BCS — Body condition score; IEWG — International Elbow Working Group; CBPI — Canine brief pain inventory; VAS — Visual analogue scale.

A preoperative clinical assessment was carried out in all dogs, including a lameness score, as described in Table II (11), search for palpable subjective elbow distension and pain in maximal flexion or extension, and evaluation of the presence of pain on pronation and flexion. The same clinical assessment was repeated at a long-term postoperative evaluation at least 6 mo after surgery, in addition to an evaluation of brachial circumference and maximal elbow range of motion measurements. The brachial circumference was measured halfway between the acromion and the lateral humeral epicondyle using a calibrated spring tension Gulick II measuring tape, with the dog awake and in the standing position. This process was repeated 3 times by the same surgeon on both front limbs and the mean of the 3 values was retained.

The maximal elbow range of motion was measured in maximum flexion and extension of the elbow using a universal plastic goniometer. With the dog awake and in lateral recumbency, the pivot point of the goniometer was placed over the lateral humeral epicondyle and the goniometer's arms were aligned with the long axis of the humerus and radius. In the unilaterally affected dogs, the same data were recorded for the unaffected elbow. The body condition score (BCS) ranged from 1 to 9 and weight was recorded at admission.

Preoperative calibrated radiographs of the affected elbow were collected in standard craniocaudal and mediolateral views when available. All dogs underwent a preoperative computed tomography (CT) examination (16-slices, 0.625-mm thickness, Optima CT Scanner; General Electric, Coventry, England) of both elbows under

FOR PERSONAL USE ONLY

Table II. Subjective numeric lameness scoring system at walk (11).

Lameness grade	Description
0	Normal
I	Slightly noticeable, intermittent lameness
II	Obvious weight-bearing lameness
III	Severe weight-bearing lameness
IV	Intermittent non-weight-bearing lameness
V	Continuous non-weight-bearing lameness

general anesthesia. A long-term postoperative radiographic assessment was carried out on each dog, under sedation. Radiographic evidence of elbow dysplasia was recorded, including disruption of subchondral bone, flattening or concavity of the bone contour, sclerotic margins, presence of an articular bone fragment, irregularity of the medial coronoid process, articular incongruity greater than 2 mm or anconeal process fracture. Radiographic periarticular elbow osteophytosis was scored using the IEWG scoring system outlined in Table III (12).

The following protocol was used for anesthesia: premedication with morphine (Lavoisier, Paris, France) or methadone (Dechra, Bladel, Netherlands), 0.2 to 0.3 mg/kg body weight (BW), intravenously (IV), followed by induction for endotracheal intubation with either propofol (Fresenius Kabi, Uppsala, Sweden) IV to effect or alfaxalone (Jurox, Worcestershire, UK), 2 mg/kg BW IV, and midazolam (Roche, Bale, Switzerland) or diazepam (Roche, Boulogne Billancourt, France), 0.2 mg/kg BW, IV. Anesthesia was maintained using isoflurane (Virbac, Carros, France) in oxygen. Lactated Ringer's solution at 5 mL/kg BW per hour was administered IV for the duration of the surgery. The dogs were placed in lateral or dorsal recumbency and routinely prepared for aseptic elbow surgery by clipping and disinfecting the skin area extending from the shoulder to the carpus.

An arthroscopic exploration was carried out using a 30° 2.7-mm arthroscope in standard medial portal placement (13). The presence of an OCD lesion and evidence of concomitant elbow joint pathology, such as medial coronoid process disease (MCD), was assessed. The modified Outerbridge classification, as outlined in Table IV, was used to grade articular cartilage lesions in the humeral trochlea, radius, and ulna (14).

The OCD flap was removed using arthroscopic grasping forceps and the cartilage bed was gently debrided with a curette or shaver. The edges of the lesion were palpated using a right-angle probe or a small curette to remove any remaining diseased cartilage and create edges that were relatively perpendicular to the joint surface. To promote cartilage growth, osteostixis of the subchondral bone was carried out using an 18-gauge, 1.5-inch needle until subchondral bone bleeding was observed. When a concomitant fissured or fragmented medial coronoid process was identified, it was treated by arthroscopic removal of the fragment or partial or subtotal coronoidectomy. The joint was lavaged and the portal incisions were closed (13).

Postoperative analgesia was titrated to the individual dog's requirements with morphine (Lavoisier), 0.2 mg/kg BW, IV every 4 to 6 h, or buprenorphine (Virbac), 0.02 mg/kg BW, IV every 6 to 8 h

Table III. Classification of elbow arthrosis according to the International Elbow Working Group (IEWG) (12).

Degree	Definition
0	Normal elbow joint No evidence of incongruence, sclerosis, or arthrosis
1	Presence of osteophytes < 2 mm high Subtrochlear sclerosis, but trabecular pattern still visible
2	Presence of osteophytes 2 to 5 mm high Obvious subtrochlear sclerosis (no trabecular pattern) Radioulnar step of 3 to 5 mm Indirect signs of a primary lesion (OCD, MCD, ununited anconeal process)
3	Presence of osteophytes > 5 mm high Radioulnar step of > 5 mm Obvious presence of a primary lesion (OCD, MCD, ununited anconeal process)

OCD — Osteochondrosis dissecans; MCD — Medial coronoid process disease.

for the first 24 h. Non-steroidal anti-inflammatory medication with meloxicam (Boehringer Ingelheim, Ingelheim Am Rhein, Germany), 0.02 mg/kg BW, was administered IV at the induction of anesthesia and was subsequently administered at 0.1 mg/kg BW, PO, q24h for 20 d.

Strict rest was recommended for 4 wk, followed by a gradual increase in the duration of leash-only walking for 4 wk. Omega-3 fatty acids and chondroitin sulfate were prescribed for life.

Owner appreciation was quantified using the CBPI and VAS scores before surgery and at the time of the postoperative long-term evaluation (15). To complete the VAS score, owners were presented with a 10-cm line, one end of which corresponded to a healthy dog with no lameness and the other to a dog with constant non-weight-bearing lameness.

Surgical outcomes were considered excellent in dogs with no lameness at the long-term postoperative examination and a CBPI score of ≤ 20. The outcome was considered good when Grade-1 lameness persisted or when the CBPI score was 20 to 30 and intermediate when Grade-2 lameness persisted or when the CBPI score was 30 to 50. Poor outcome was defined as Grades 3 to 5 persistent lameness or a CBPI score of > 50.

The following outcome variables were compared before and after surgical treatment: lameness score, subjective presence of joint distension, presence of pain on pronation and flexion, presence of pain at maximal elbow flexion and extension, radiographic IEWG score, CBPI score, and VAS score.

A 2-level, random intercept, mixed-effects generalized linear model (GLM) was used to consider the repeated measures for each dog: linear regression for CBPI and VAS values (continuous variables), logistic regression for pain at elbow maximal flexion and extension (binary variable), and ordered logistic regression for the IEWG score (ordinal variable). For each model, the independent fixed-effects variables included the evaluation time (*i.e.,* pre- *versus* postoperative), age, body weight, BCS, lameness duration, follow-up duration, bilateral elbow involvement, IEWG score, presence of

FOR PERSONAL USE ONLY

Table IV. Modified-Outerbridge classification (14).

Grade	Description
0	Normal cartilage
1	Chondromalacia (evaluated using an arthroscopic probe)
2	Partial-thickness fibrillation
3	Deep fibrillation/incomplete cartilage loss (subchondral bone still covered)
4	Penetrating, full-thickness cartilage fissure (subchondral bone visible)
5	Eburnated subchondral bone

concurrent MCD, and radial and ulnar modified Outerbridge score. The random-effects variable was the individual dog.

When it was not possible to use the generalized linear model (GLM) for variables that were often 0, the results of symmetry and marginal homogeneity tests were compared. For maximal flexion and extension angles and the brachial circumference, a 2-level, random intercept, mixed-effects regression model was used to consider the lack of independence of the 2 elbows in the same dog. For each model, the independent fixed-effects variables included the elbow (*i.e.,* affected or unaffected) and the same potential confounding variables as previously mentioned. The random effects variable was the individual dog.

For regression models, assumptions of Gaussianity and homoscedasticity of the fixed residuals were checked graphically and by the Shapiro-Wilk and Breusch-Pagan and Cook-Weisberg tests, respectively. The goodness-of-fit of the logistic regressions was assessed using the Hosmer–Lemeshow test. All analyses were conducted using STATA, version 14.2 software (StataCorp, College Station, Texas, USA). The level of significance was set at $P < 0.05$.

Results

Twenty-three dogs (30 elbows) were included in the study. Seven had bilateral humeral trochlear OCD. The breeds included Australian shepherds ($n = 5$), Labrador retrievers ($n = 5$), golden retrievers ($n = 3$), Dogues de Bordeaux ($n = 3$), Newfoundland dogs ($n = 2$), and 1 each of chow chow, Shar pei, American Staffordshire terrier, American Akita, and crossbreed. The male:female ratio was 4.75:1. The median age at admission was 8 mo (range: 6 to 47 mo) and the median age at lameness onset was 5 mo (range: 3 to 41 mo). The median duration of preoperative lameness was 3 mo (range: 1 to 9 mo). The median body weight was 28 kg (range: 16 to 68 kg) and the median BCS was 6 (range: 4 to 7).

Preoperative and long-term (median: 22 mo) postoperative outcomes are listed in Table V and Table VI. A comparison of long-term postoperative outcome measurements between the OCD-affected and unaffected elbows is presented in Table VII. The range of elbow motion was not significantly associated with the IEWG score. At long-term postoperative follow-up, 70% of operated elbows had a normal extension angle and 43% had a normal flexion angle.

Preoperative radiographs were obtained for 18 affected elbows, 93% of which had preoperative radiographic evidence of humeral trochlear OCD. Based on the findings of the computed tomography examination, 90% of the elbows had a concomitant MCD and 30% had a subjective articular incongruity, either humeroradial or humeroulnar, none of which was > 2 mm, and 10% had evidence of ulnar panosteitis.

Table V. Preoperative and long-term postoperative values of continuous outcome variables.

	Preoperative		Postoperative		
	Median	Range	Median	Range	*P*-value
Lameness score	3	1 to 4	0	0 to 1	< 0.01
CBPI score	61	28 to 84	15	10 to 49	< 0.01
VAS	68.5	20 to 87	10	0 to 60	< 0.01
IEWG score	1	0 to 2	2	0 to 3	0.03

CBPI — Canine brief pain inventory; VAS — Visual analogue scale; IEWG — International Elbow Working Group.

Table VI. Preoperative and long-term postoperative values of binary outcome variables.

	Preoperative	Postoperative	*P*-value
Presence of joint distension	100% (30/30)	23% (7/30)	< 0.01
Pain on pronation and flexion	100% (30/30)	17% (5/30)	< 0.01
Pain on maximal flexion	93% (28/30)	10% (3/30)	0.01
Pain on maximal extension	90% (27/30)	7% (2/30)	0.02

The preoperative and long-term postoperative radiographic IEWG scores are listed in Table V. These scores were stable in 56% of elbows and had progressed by 1 grade in 44% of the others; none had progressed by > 1 grade. IEWG scores were significantly positively associated with body weight ($P = 0.02$), the duration of lameness ($P < 0.01$), and bilateral elbow involvement ($P = 0.05$).

In all cases, arthroscopy confirmed the presence of humeral trochlear OCD lesions. All humeral trochlear modified Outerbridge scores were 5; the median radial score was 0.5 (range: 0 to 3) and ulnar score was 3.5 (range: 0 to 5). Ninety percent of the elbows had a concomitant MCD. None of the patients showed evidence of joint incongruity or ununited anconeal process. In all cases, arthroscopy allowed for reparative treatment of the OCD lesion.

No difficulties were experienced in flap removal, curettage of the cartilage bed, or osteostixis of the subchondral bone (Figure 1). Of the 30 operated elbows, none developed short-term complications from the procedure, except for lameness. Long-term complications consisted of persistent Grade-1 lameness and occurred in 23% of dogs ($n = 5$).

As shown in Table V, postoperative CBPI and VAS scores were significantly lower than preoperative scores ($P < 0.01$) and were not significantly affected by the IEWG score, body weight, duration of lameness, or bilateral involvement. Based on the previously mentioned classification, long-term clinical outcomes were rated as excellent in 67% of the dogs, good in 27%, and intermediate in 6%. No outcome was classified as poor.

Discussion

The main finding of this study was that long-term outcomes after arthroscopic reparative treatment of humeral trochlear OCD were good to excellent in most dogs. There were no short- or long-term

FOR PERSONAL USE ONLY

Table VII. Comparison of long-term postoperative evaluation criteria between affected and unaffected elbows (*n* = 16 dogs).

	Unaffected limb		Affected limb		
	Median	Range	Median	Range	*P*-value
Brachial circumference (cm)	26.3	20 to 35	25.8	20 to 38	0.18
Maximal flexion angle (°)	45	20 to 100	50	20 to 95	0.07
Maximal extension angle (°)	160	140 to 170	160	140 to 170	0.75

complications as a result of this treatment, except for mild persistent lameness in a minority of cases. Based on postoperative lameness and CBPI scores, arthroscopic reparative treatment of OCD led to good to excellent clinical results in 94% of dogs at a median of 22 mo.

The results of the CBPI scores showed that the owners perceived an improvement in the quality of life of their dogs. The CBPI score is a validated outcome measurement that provides evidence of the actual positive impact perceived by owners after reparative arthroscopic treatment (16). It is not known whether the dogs would have improved without surgery, however, and this could only have been determined by adding a control group to the study.

The 47-month-old dog included in the study had an early diagnosis of bilateral OCD that resulted in unilateral lameness and led to unilateral surgery at 13 mo of age. In this case, the second elbow did not show clinical signs until almost 3 y later and was then operated on and included in this study.

The 2 main studies available that include cases of humeral trochlear OCD treated arthroscopically revealed good results in all 8 dogs and in 71% of 38 elbows with long-term follow-up (5,17). Both studies lacked detailed outcomes and quantified evaluation criteria. The results of the present study reinforce the findings of these studies.

Dogs with higher body weight, longer duration of lameness, or bilateral OCD had significantly higher IEWG scores than their counterparts, although these parameters did not significantly affect the CBPI and VAS scores. Similarly, there was no significant association between range of motion and the IEWG score. Despite these results, it seems advisable to operate on OCD lesions as early as possible since the absence of a correlation between the IEWG score, which is greater for dogs undergoing surgical treatment later in life, and clinical outcome could be related to a Type-II error.

Most dog breeds affected by OCD of the humeral trochlea included in this study have already been reported in the literature, except for the Australian shepherd and Dogue de Bordeaux (18,19). The Australian shepherd, which has recently become a very popular breed, has only been officially recognized since 2007, which may explain its absence in previous reports. It was the most affected breed in this study, accounting for 22% of all cases.

All but one of the dogs included in this study had a concomitant disease in addition to OCD, most often an MCD, which is a limitation of this study. This limitation is inherent in the frequent association between these 2 diseases. The high incidence of their co-occurrence supports the hypothesis that the aetiopathogenesis of OCD includes dynamic incongruity. The complexity of these lesions and their frequent association is an additional argument in favor of arthroscopy to treat elbow OCD, as OCD and MCD lesions can be accurately evaluated and treated using the same minimally invasive approach.

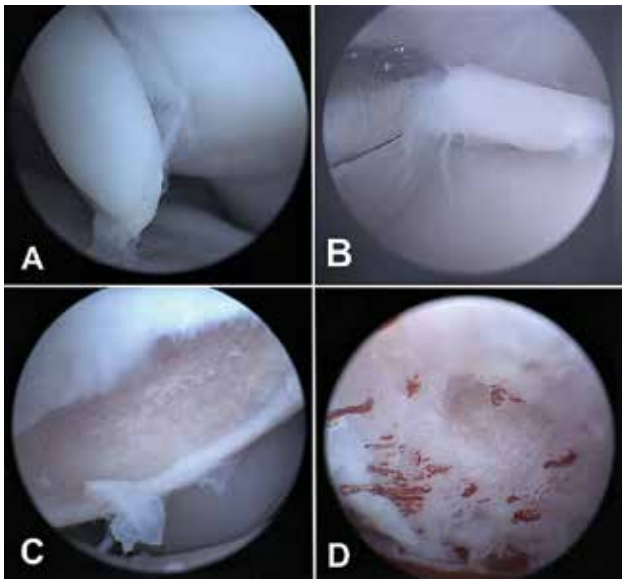


Figure 1. Intraoperative photographs of arthroscopic treatment based on flap removal for humeral trochlear osteochondrosis dissecans (OCD). A — OCD flap. B — Grasping forceps removing the flap. C-Underlying subchondral bone after curettage of the OCD bed. D — Underlying subchondral bone after osteostixis of the OCD bed.

This limitation may play a confounding role in the interpretation of our results, but it also represents the complex pathology of these dogs and their response to treatment.

Although quantifiable, some evaluation criteria used in this study were subjective. The CBPI score has been validated by gait analysis and has been shown to reliably quantify the owner's assessment of chronic pain in dogs in their usual environment over a 1-week period (16). The VAS has also been shown to be repeatable, valid, and efficient in measuring pain and assessing lameness in dogs (20,21). Among the various methods used to objectively assess elbow function, goniometric assessment of range of motion has been proven reliable in both sedated and awake dogs (22).

The bilateral condition of the dogs included in this study may also have influenced the scoring of their lameness, resulting in difficulty in correctly assessing lameness in their forelimbs. Finally, as the same investigator carried out the surgery and measured the outcome, this person was not blinded to the severity of the disease identified on arthroscopy, which could have biased the results. Force plate gait analysis would have been a useful tool to objectively quantify postoperative outcomes at a given time.

The impact of the retrospective multicenter nature of this study was probably limited, given the similar level of experience of the

FOR PERSONAL USE ONLY

surgeons and the similar operating conditions in the veterinary hospitals participating in this study. A larger number of cases could have allowed the subgrouping of concomitant diseases or preoperative clinical or radiographic status.

Furthermore, a controlled study would have permitted a better investigation of the therapeutic benefits of arthroscopic treatment for OCD of the humeral trochlea, compared with medically managed dogs and dogs undergoing treatment with alternative surgical techniques. Given the low prevalence of the disease, however, it may be difficult to conduct such a study (1).

In conclusion, arthroscopic treatment of humeral trochlear OCD provided good long-term results in the 23 dogs included in this study. This outcome was mainly characterized by a good to excellent return to function perceived by the owners and the veterinarians and a low evolution of periarticular osteophytosis. Owing to its low complication rate, especially compared to more advanced but invasive procedures such as resurfacing techniques, arthroscopic reparative techniques remain an appropriate approach for the treatment of elbow OCD.

Acknowledgments

The authors thank M. Hauducoeur, Dr. C. Bismuth, and Y. Lahiani for their scientific advice, as well as IVC Evidensia for the funding of this study.

References

1. Nečas A, Dvořák M, Zatloukal J. Incidence of osteochondrosis in dogs and its late diagnosis. Acta Vet Brno 1999;68:131–139.
2. Johnston SA. Osteochondritis dissecans of the humeral head. Vet Clin North Am Small Anim Pract 1998;28:33–49.
3. Bennett D, Duff SR, Kene RO, Lee R. Osteochondritis dissecans and fragmentation of the coronoid process in the elbow joint of the dog. Vet Rec 1981;109:329–336.
4. Bouck GR, Miller CW, Taves CL. A comparison of surgical and medical treatment of fragmented coronoid process and osteochondritis dissecans of the canine elbow. Vet Comp Othop Traumatol 1995;8:177–183.
5. van Ryssen B. Arthroscopy in the diagnosis and treatment of osteochondrosis in the dog [PhD dissertation]. Gent, Belgium: University of Ghent, 1996.
6. Böttcher P, Zeissler M, Winkels P, Ludewig E, Maierl J, Grevel V. Mosaicplasty in the elbow of a dog: Instrumentation and evaluation of achieved joint congruency by computed tomography and computed tomographic osteoabsorptiometry. Tierärzti Prax Ausg K Kleintiere Heimtiere 2007;4:253–260.
7. Fitzpatrick N, Yeadon R, Smith TJ. Early clinical experience with osteochondral autograft transfer for treatment of osteochondritis dissecans of the medial humeral condyle in dogs. Vet Surg 2009;38:246–260.
8. Böttcher P, Zeissler M, Maierl J, Grevel V, Oechtering G. Mapping of split-line pattern and cartilage thickness of selected donor and recipient sites for autologous osteochondral transplantation in the canine stifle joint. Vet Surg 2009;38:696–704.
9. Sayani J, Plotkin T, Burchette DT, Phadnis J. Treatment strategies and outcomes for osteochondritis dissecans of the capitellum. Am J Sports Med 2021;49:4018–4029.
10. McLaughlin RJ, Leland DP, Bernard CD, *et al.* Both debridement and microfracture produce excellent results for osteochondritis dissecans lesions of the capitellum: A systematic review. Arthrosc Sports Med Rehabil 2023;3:e593–e603.
11. Millis D, Levine D. Assessing and measuring outcomes. In: Canine Rehabilitation and Physical Therapy. 2nd ed. St. Louis, Missouri: Elsevier, 2014:221.
12. Ohlerth S, Tellhelm B, Amort K, Ondreka N. Explanation of the IEWG grading system. Proc 30th Annu Meet IEWG. Vienna, Austria, 2016:14–16.
13. Beale B, Hulse D, Schulz K, Whitney W. Arthroscopically assisted surgery of the elbow joint. In: Small Animal Arthroscopy. Philadelphia, Pennsylvania: WB Saunders, 2003:51–70.
14. Krotscheck U, Böttcher P. Developmental elbow disease. In: Johnston SA, Tobias KM, eds. Veterinary Surgery: Small Animal. 2nd ed. St. Louis, Missouri: Elsevier, 2017:848–885.
15. Ragetly GR, Massey L, Brown DC. Initial psychometric testing and validation of the French version of the canine brief pain inventory. Vet Anaesth Analg 2019;46:667–672.
16. Brown DC, Boston RC, Farrar JT. Comparison of force plate gait analysis and owner assessment of pain using the canine brief pain inventory in dogs with osteoarthritis. J Vet Intern Med 2013; 27:22–30.
17. Meyer-Lindenberg A, Langhann A, Fehr M, Nolte I. Arthrotomy versus arthroscopy in the treatment of the fragmented medial coronoid process of the ulna in 421 dogs. Vet Comp Othop Traumatol 2003;16:204–210.
18. LaFond E, Breur GJ, Austin CC. Breed susceptibility for developmental orthopedic diseases in dogs. J Am Anim Hosp Assoc 2002;38:467–477.
19. Slater MR, Scarlett JM, Kaderly RE, Bonnett BN. Breed, gender, and age as risk factors for canine osteochondritis dissecans. Vet Comp Orthop Traumatol 1991;4:100–106.
20. Hielm-Björkman AK, Kapatkin AS, Rita HJ. Reliability and validity of a visual analogue scale used by owners to measure chronic pain attributable to osteoarthritis in their dogs. Am J Vet Res 2011;72:601–607.
21. Hudson JT, Slater MR, Taylor L, Scott HM, Kerwin SC. Assessing repeatability and validity of a visual analogue scale questionnaire for use in assessing pain and lameness in dogs. Am J Vet Res 2004;65:1634–1643.
22. Jaegger G, Marcellin-Little DJ, Levine D. Reliability of goniometry in Labrador Retrievers. Am J Vet Res 2002;63:979–986.

FOR PERSONAL USE ONLY

Comparison of rostral spread of lumbosacral epidural volume calculated by body weight or length of the vertebral column in small-sized anesthetized dogs

Flavio A.V. Freitag, Alexander Valverde, Monica Jensen, Andrea Sanchez, Diego E. Gomez, Craig Bailey

Abstract

The first objective of this prospective, randomized, crossover experimental trial was to compare the rostral spread of lumbosacral epidural volume calculated by body weight (BW) or vertebral column length (LE) in 6 small, isoflurane-anesthetized female beagle dogs (BW: 7.5 to 10.2 kg; LE measured from the occipital crest to the sacrococcygeal space: 46 to 56 cm). The second objective was to assess the response to a noxious stimulus once the dogs recovered from anesthesia and to determine the effects of the injection on cardiopulmonary variables. While in sternal position, dogs were injected through an epidural catheter with a volume mixture of bupivacaine 0.25% and iopamidol 15% based on BW: 0.2 mL/kg or LE: 0.05 mL/cm (< 50 cm) or 0.07 mL/cm (50 to < 70 cm). Rostral spread was determined by counting the number of vertebrae reached by iopamidol using computed tomography. After anesthesia, cardiopulmonary variables, motor function, and responses to nociceptive stimuli were evaluated. Comparisons were completed with mixed linear models and 2-way analysis of variance (ANOVA) ($P < 0.05$). The volume of injectate (3.29 ± 0.74 *versus* 1.81 ± 0.21 mL; mean ± SD) and the number of vertebrae (22 ± 2 *versus* 19 ± 2 vertebrae) reached by iopamidol were significantly greater for LE than for BW. Response to nociception, time to return of pain sensation, motor function, and cardiopulmonary variables were similar between groups. In conclusion, dosing based on LE resulted in larger rostral spread than when based on BW in dogs of small size.

Résumé

Le premier objectif de cet essai expérimental croisé prospectif randomisé était de comparer la propagation rostrale du volume épidural lombo-sacré calculé en fonction du poids corporel (PC) ou de la longueur de la colonne vertébrale (LE) chez 6 petites chiennes beagle anesthésiées à l'isoflurane (PC : 7,5 à 10,2 kg; LE mesuré de la crête occipitale à l'espace sacro-coccygien : 46 à 56 cm). Le deuxième objectif était d'évaluer la réponse à un stimulus nocif une fois que les chiens se sont remis de l'anesthésie et de déterminer les effets de l'injection sur les variables cardiopulmonaires. En position sternale, les chiens ont reçu une injection *via* un cathéter péridural d'un mélange volumique de bupivacaïne à 0,25 % et d'iopamidol à 15 % basé sur le poids corporel : 0,2 mL/kg ou LE : 0,05 mL/cm (< 50 cm) ou 0,07 mL/cm (50 à < 70 cm). La propagation rostrale a été déterminée en comptant le nombre de vertèbres atteintes par l'iopamidol en utilisant la tomodensitométrie. Après l'anesthésie, les variables cardiopulmonaires, la fonction motrice et les réponses aux stimuli nociceptifs ont été évaluées. Les comparaisons ont été complétées avec des modèles linéaires mixtes et une analyse de variance à 2 facteurs (ANOVA) ($P < 0,05$). Le volume d'injectat (3,29 ± 0,74 *versus* 1,81 ± 0,21 mL; moyenne ± SD) et le nombre de vertèbres (22 ± 2 *versus* 19 ± 2 vertèbres) atteints par l'iopamidol étaient significativement plus élevés pour LE que pour BW. La réponse à la nociception, le temps de retour de la sensation de douleur, la fonction motrice et les variables cardiopulmonaires étaient similaires entre les groupes. En conclusion, le dosage basé sur LE a entraîné une plus grande propagation rostrale que lorsqu'il était basé sur BW chez les chiens de petite taille.

(Traduit par Docteur Serge Messier)

Department of Clinical Studies (Freitag, Valverde, Jensen, Sanchez, Gomez) and Department of Biomedical Sciences (Bailey), Ontario Veterinary College, University of Guelph, Guelph, Ontario, N1G 2W1.

Address all correspondence to Dr. Alexander Valverde; telephone: (519) 824-4120; email: valverde@uoguelph.ca

Author contributions

FAVF: Data collection, statistical analysis, and interpretation, manuscript preparation, and approval of final version. AV: Funding and design, data collection, statistical analysis, and interpretation, manuscript preparation, and approval of final version. MJ: Data collection, imaging interpretation, manuscript preparation, and approval of final version. AS, DG, and CB: Design, manuscript preparation, data interpretation, approval of final version.

Received February 7, 2023. Accepted March 29, 2023.

FOR PERSONAL USE ONLY

Introduction

Epidural lumbosacral (LS) injection of a local anesthetic with or without an opioid is one of the most common regional techniques used in dogs in clinical practice to provide anesthesia and/or analgesia to the pelvic limb, pelvic area, and abdomen (1–3). The rostral spread of a local anesthetic drug injected into the LS space allows the drug to interact with the spinal cord and emerging spinal nerves in order to exert its analgesic/anesthetic effects (4–7).

For a local anesthetic, the relationship between volume of injectate and rostral spread is linear (8–11) and determines the extent of blockade. A small volume of injectate at the LS space acts close to the site of injection and may only involve sensory blockade of the pelvic area, whereas a larger volume of injectate can be adjusted to reach higher lumbar and lower thoracic segments of the spinal cord to include the abdomen (8,11,12).

In addition to volume of injectate, the degree of epidural rostral spread is influenced by two physical factors: gravity and friction (13). Gravity and friction forces in the epidural space are influenced by inherent factors of the animal, such as body condition score (BCS) and size, position at the time of injection and thereafter, injection at the site of entry of the needle or in a more rostral position with an epidural catheter, and whether the animal is conscious, sedated, or under general anesthesia (8,10–12,14–16).

The epidural volume of injectate can be calculated by two methods, either using body weight (BW; mL/kg) or length of the vertebral column (LE; mL/cm) from the occipital crest to the sacrococcygeal space (8–11,13–16). It has not yet been determined in live dogs whether these methods are interchangeable.

In a recent study, the comparison of both methods of calculation in a hypothetical situation determined that they are not interchangeable in small- and medium-sized dogs (< 25 kg) since larger calculated volumes were obtained based on LE when compared to BW. This difference tended to disappear or revert as size increased (≥ 25 kg) and with higher BCS (obesity) (13). It has not yet been determined whether the methods of calculation result in different volumes of injectate, which could in turn result in different analgesic and cardiopulmonary effects from epidural spread.

Therefore, the objectives of this study were i) to compare in small, anesthetized dogs (≤ 10 kg) the rostral spread of an LS epidural injection volume of bupivacaine–contrast medium calculated by LE or BW using computerized tomography (CT); and ii) to assess the response to a noxious stimulus once the dogs recovered from anesthesia as well as to determine the effects of the injection on cardiopulmonary variables.

We hypothesized that epidural volume calculated using recommended doses based on LE would be greater than that based on BW in small-sized dogs and result in higher rostral spread and desensitization of a greater number of dermatomes, but that cardiopulmonary variables would remain similar in both groups.

Materials and methods

Animals

A total of 6 purpose-bred research, ovariohysterectomized female beagle dogs, aged 5.3 to 8.3 y and weighing 7.5 to 10.2 kg, with the same BCS (3 of 5 = moderate) (17) were studied and considered healthy based on physical examination, complete blood (cell) count, and biochemistry profile. The study was carried out in accordance with the guidelines of the Canadian Council on Animal Care and was approved by the Institutional Animal Care Committee at the University of Guelph (AUP #4347).

Study

Dogs were used in a prospective, randomized, crossover study design, in which each received two treatments, with a washout period of at least 5 d between treatments. On the first occasion, 3 dogs received Treatment 1 (epidural volume based on LE) and the other 3 dogs received Treatment 2 (epidural volume based on BW), followed by the reversed order on the second occasion (http://www.random.org).

Volumes of injectate for the epidural injection consisted of 0.2 mL/kg calculated according to BW and 0.05 mL/cm (< 50 cm) or 0.07 mL/cm (50 to < 70 cm) according to LE (13). On each occasion, the dogs were fasted for 12 h for food, but water was available. Body weight was recorded each day before the experiment and LE was recorded under anesthesia while dogs were in sternal recumbency and with pelvic limbs extended caudally, using a metric tape, during the first occasion.

Epidural injection and evaluation

General anesthesia was induced on the CT table by delivering 5% isoflurane (Aerrane; Baxter Corporation, Mississauga, Ontario) in oxygen at 4 to 5 L/min *via* facemask with a circle system. The trachea was intubated and dogs were connected to an electronically controlled, volume-cycled ventilator (S/5 Aespire 7900 Ventilator; GE Healthcare, Madison, Wisconsin, USA) at a rate of 10 breaths/min, a tidal volume of 15 mL/kg, and an inspiration-to-expiration ratio of 1:3.

The dogs were positioned in sternal recumbency with the pelvic limbs extended caudally and anesthesia maintained with isoflurane in $> 95\%$ oxygen with a fresh gas flow of 1 to 2 L/min at an initial end-tidal isoflurane concentration (F_E'Iso) of 1.5%; adjusted accordingly for depth during placement of the epidural catheter. The F_E'Iso was measured from the connection of the endotracheal tube with the circle system using a multiparameter monitor (Datex-Ohmeda S/5 Anesthesia Monitor; GE Healthcare Finland, Helsinki, Finland), calibrated before each experiment with a standardized calibration gas mixture designed for the analyzer (755571-HEL, Calibration gas mixture; GE Healthcare Finland).

In addition, dogs were instrumented for non-invasive oscillometric arterial blood pressure using a cuff width size of approximately 40% of the limb circumference above the tarsal joint on the right pelvic limb (Size 2), rectal thermometer, capnography, pulse oximetry, and side-stream end-tidal CO_2 ($P_E'CO_2$). These variables were recorded at 5 to 10 min intervals throughout anesthesia during the CT.

A 5- $\times$ 5-cm area over the LS space was clipped and aseptically prepared. A stab incision was made over the LS space and a 24-gauge, 25-cm epidural catheter was advanced through a 20-gauge, 4.5-cm Tuohy needle (Epidural Pain Management Kit; MILA, Florence, Kentucky, USA), 1 to 2 cm into the epidural space from the tip of the needle.

FOR PERSONAL USE ONLY



Figure 1. Diagram used to determine the number of vertebrae reached by iopamidol after lumbosacral epidural injection. A maximum of 27 vertebrae was possible (7 lumbar + 13 thoracic + 7 cervical).

The Tuohy needle was left in place and the catheter flushed with 0.1 mL of sterile saline, followed by injection of a test dose of a 1:1 mixture of preservative-free bupivacaine 0.5% (Bupivacaine Injection BP; SteriMax, Oakville, Ontario) and iopamidol contrast medium (IsoVue–300; Bracco Imaging, Anjou, Quebec), 0.2 to 0.3 mL, resulting in a solution of bupivacaine 0.25% and iopamidol 15%.

An initial CT scan (16-slice detector, BrightSpeed CT Scanner; GE Healthcare, USA) was conducted to confirm the correct placement of the epidural catheter and presence of the iopamidol. The remaining final volume was then injected by hand over 20 s and a CT scan of the entire spine was completed within 5 min of the injection.

Images from the CT were acquired and evaluated from the cranial aspect of the cervical spine to just caudal to the LS space, in both soft tissue (standard) and bone windows, by a Board-certified radiologist (MJ) who was unaware of the treatment. Assessment included the most cranial spread of positive contrast medium to determine the number of vertebrae reached by the iopamidol from the LS space. A maximum of 27 vertebrae was possible (7 lumbar + 13 thoracic + 7 cervical) and was always inclusive of the vertebra the iopamidol reached, regardless of being whole or a fraction of it (Figure 1).

Following the CT, the epidural catheter and needle were removed, isoflurane administration was discontinued, and dogs were transported to a different room and maintained in the same sternal position during recovery until full display of normal conscious behavior. Dogs were extubated when spontaneous breathing returned.

Total anesthesia time, from intubation to extubation, was recorded. During recovery, dogs were assessed for 30 min for post-anesthesia sedation by a blinded investigator (FF) using a recovery score of 0 to 3, with 0 indicating no sedation and 3 indicating profound sedation (see Appendix A) (18). Heart rate, assessed by auscultation, oscillometric blood pressure (Cardell Veterinary Vital Signs Monitor, Model 9403; Midmark Corporation, Versailles, Ohio, USA), and rectal temperature were measured at 10 and 30 min during this period.

At 30, 45, and 60 min post-extubation and every 30 min thereafter, dogs were assessed for ambulation by the same blinded investigator using a score from 0 to 3, with 0 indicating normal ambulation and 3 indicating unable to stand and/or ambulate (see Appendix B), until a score of 0 was achieved. Time to full recovery was recorded as time from extubation to a score of 0 for both the sedation and ambulation scores.

Analgesia assessments were aimed at detecting the return of pain and were completed by the same blinded investigator and started when the post-anesthesia sedation score was 0, but not before 30 min post-extubation. The assessment consisted of applying a noxious stimulus to 11 dermatomes, starting at the tail and moving cranially to the thoracic limb paw. These included the base of the tail (AN1), the pelvic limb paw (AN2), the area surrounding the iliac crest (AN3), the inguinal area near the femoral nerve (AN4), the area close to the transverse process of L_3 and flank (AN5), the paramedian area next to the umbilicus (AN6), along the thirteenth rib (AN7), the paramedian area to the xyphoid (AN8), along the ninth rib (AN9), along the second rib (AN10), and the thoracic limb paw (AN11).

Noxious stimulation consisted of clamping the tail or paws with 24-cm sponge forceps with protective plastic tubing on each jaw (Robbins Instruments, Deptford, New Jersey, USA) or the use of a 12.5-cm hemostat for the remaining dermatomes. The anatomical region was clamped with the instrument, without reaching the first notch, for a period of < 3 s. A positive response to pain consisted of gross purposeful movement or a vocal response elicited during the period of stimulation.

If the evaluator was uncertain of the response, electrical current was applied using alligator clips 5 cm apart in the anatomical area tested with the surgical instrument and consisted of 1 to 3 single stimuli of 30 to 40 volts at 50 cycles/s for 10 ms (S48 Stimulator; Astro-Med, West Warwick, Rhode Island, USA). If gross purposeful movement or a vocal response was elicited before the cycle was completed, the electrical stimulus was discontinued immediately and the response assessed as positive.

A second positive response obtained in the following assessment time indicated complete sensory recovery and the time to a positive response to noxious stimulation was recorded as the time when the first assessment was completed. All dermatomes were assessed until 2 consecutive positive responses were obtained and were no longer stimulated subsequently.

Dogs were administered meloxicam (Metacam; Boehringer Ingelheim Canada, Burlington, Ontario), 0.1 mg/kg subcutaneously (SC), at the end of each experiment and were monitored for normal behavior. Dogs were returned to the supplier when the last dog had completed the study.

Statistical analysis

All data were tested for normality using Shapiro-Wilk, Kolmogorov-Smirnov, Cramer-von Mises, and Anderson-Darlin procedures. UNIVARIATE and PLOT procedures were used to detect unequal variances, outliers, and other non-random patterns within the data for each group (SAS Version 9.4; SAS Institute, Cary, North Carolina, USA).

A mixed model of residual maximum likelihood was used to compare the effect of the method (LE *versus* BW dosing) and the period of administration (first and second time) on the number of vertebrae

FOR PERSONAL USE ONLY

Table I. Demographic data of female beagle dogs after a lumbosacral epidural injection of 0.2 mL/kg body weight (BW) and 0.05 mL/cm (< 50 cm) or 0.07 mL/cm (50 to < 70 cm) based on length of the vertebral column (LE) in a randomized crossover fashion of a volume mixture of bupivacaine 0.25% and iopamidol 15%.

Dog number	FT	Age (years)	LE (cm)	BW1 (kg)	BW2 (kg)	Volume for BW (mL)	Volume for LE (mL)
1	LE	5.3	52	10.2	10.2	2.04	3.64
2	BW	7.1	52	9.6	9.5	1.92	3.64
3	LE	5.3	46	7.5	7.5	1.50	2.30
4	LE	5.3	48	7.6	8	1.60	2.40
5	BW	8.3	55	9.6	9.6	1.92	3.85
6	BW	5.3	56	9.4	9.4	1.88	3.92
Mean ± SD		6.1 ± 1.30	51.5 ± 3.9	9.0 ± 1.1	9.0 ± 1.0	1.81 ± 0.21	3.29* ± 0.74

FT — First assigned treatment; BW1 — First occasion; BW2 — Second occasion.

* Significantly different than volume for BW (P = 0.0012).

reached by iopamidol. Presence of pain was analyzed with a mixed model of residual maximum likelihood that considered the method and dermatome, with time as the independent variable.

The error structure was selected based on the Akaike Information Criteria among structures offered by SAS using a random effect for each treatment. Cardiopulmonary and temperature variables and sedation and ambulation scores for both methods were analyzed with a mixed model if there were missing values or a 2-way analysis of variance (ANOVA) with repeated measures when all values were recorded and multiple comparisons within treatments were carried out with a Šidák test (GraphPad, Version 9.3.1 for MacOS; GraphPad Software, San Diego, California, USA). Significance was set at $P < 0.05$.

The sample size was calculated based on the mathematical model for the different methods of calculating the epidural volume (13), using the small-sized (< 10 kg) dog category data. Therefore, to compare the mean volume of injection of 2.2 mL (LE dose) and 1.1 mL (BW dose) with a standard deviation of 0.5, a power of 0.8 (Type-II error) and *alpha* of 0.05 (Type I-error) required at least 5 dogs.

Results

All 6 dogs completed the study without complication (Table I). One of the dogs weighed 10.2 kg but was kept in the study because the data from this dog was consistent with dogs < 10 kg. Total anesthesia time from intubation until extubation was 24.2 ± 2.1 min in the LE group and 23.7 ± 6.5 min in the BW group.

During the epidural injection and CT under anesthesia, as well as during the assessment of the presence of pain after anesthesia, cardiopulmonary values and rectal temperature were not significantly different between groups (Figure 2).

Epidural volume and rostral spread

The volume of injectate was significantly greater for LE than for BW (3.29 ± 0.74 mL *versus* 1.81 ± 0.21 mL; P = 0.0012), which resulted in a significantly larger (P = 0.0488) rostral spread for LE [22 ± 2 vertebrae; 20, 24 (95% confidence intervals)] than for BW (19 ± 2; 17, 21) (Figure 3). The range of vertebrae reached with the LE dose was C4 to T1 and with the BW dose was C5 to T5.

Response to noxious stimulation

Sedation scores of 0 (no sedation) were present in all dogs at 30 min post-extubation and were not significantly different between groups (P = 0.8833). Ambulation scores were not significantly different between groups at any of the periods of assessment (P = 0.4582) and times for a score of 0 for both sedation and ambulation scales were 48.2 ± 18.8 min in the LE group and 35.5 ± 28.6 min in the BW group (P = 0.2904).

The time from recovery until the first assessment for the presence of pain was 36.3 ± 0.8 min in the LE group and 37.7 ± 1.9 min in the BW group and not significantly different (P = 0.2065). Time to positive response to the presence of pain was similar between individual dermatomes and groups (P = 0.1440) and overall time to the presence of pain (37.7 ± 20.4 min for LE and 49.0 ± 20.4 min for BW) was also similar (P = 0.3591). The times for detection to positive response to nociception for each dermatome are shown in Table II.

Discussion

The rostral spread of an LS injectate volume based on LE or BW was successfully determined in small-sized dogs (≤ 10.2 kg). The doses used for LE and BW resulted in a volume of epidural injectate 1.82-fold greater for LE than for BW, which resulted in a larger rostral spread for LE (22 ± 2 vertebrae *versus* 19 ± 2 vertebrae, respectively).

A greater volume for LE than BW was also determined in another study in small- (< 10 kg) and medium-sized (10 to < 25 kg) dogs with a body condition score (BCS) of 2 to 5 in a mathematical model and the difference for the small-dog category in that study was 2.18-fold (13). The dose for LE and BW should therefore not be considered interchangeable in small-sized dogs.

The rostral spread of any substance in the epidural space is the result of dynamic forces that affect cerebral spinal fluid (CSF) motion and pressures in that space. These forces include compliance of the spinal canal; physical activity and position of the individual; the cardiovascular system (blood pressure, cardiac output, and heart rate); the respiratory system (rate and effort of breathing); and systemic absorption of the substance (16,19,20).

Several studies have determined a time-dependent behavior of rostral epidural spread of contrast medium for up to 45 min using

FOR PERSONAL USE ONLY

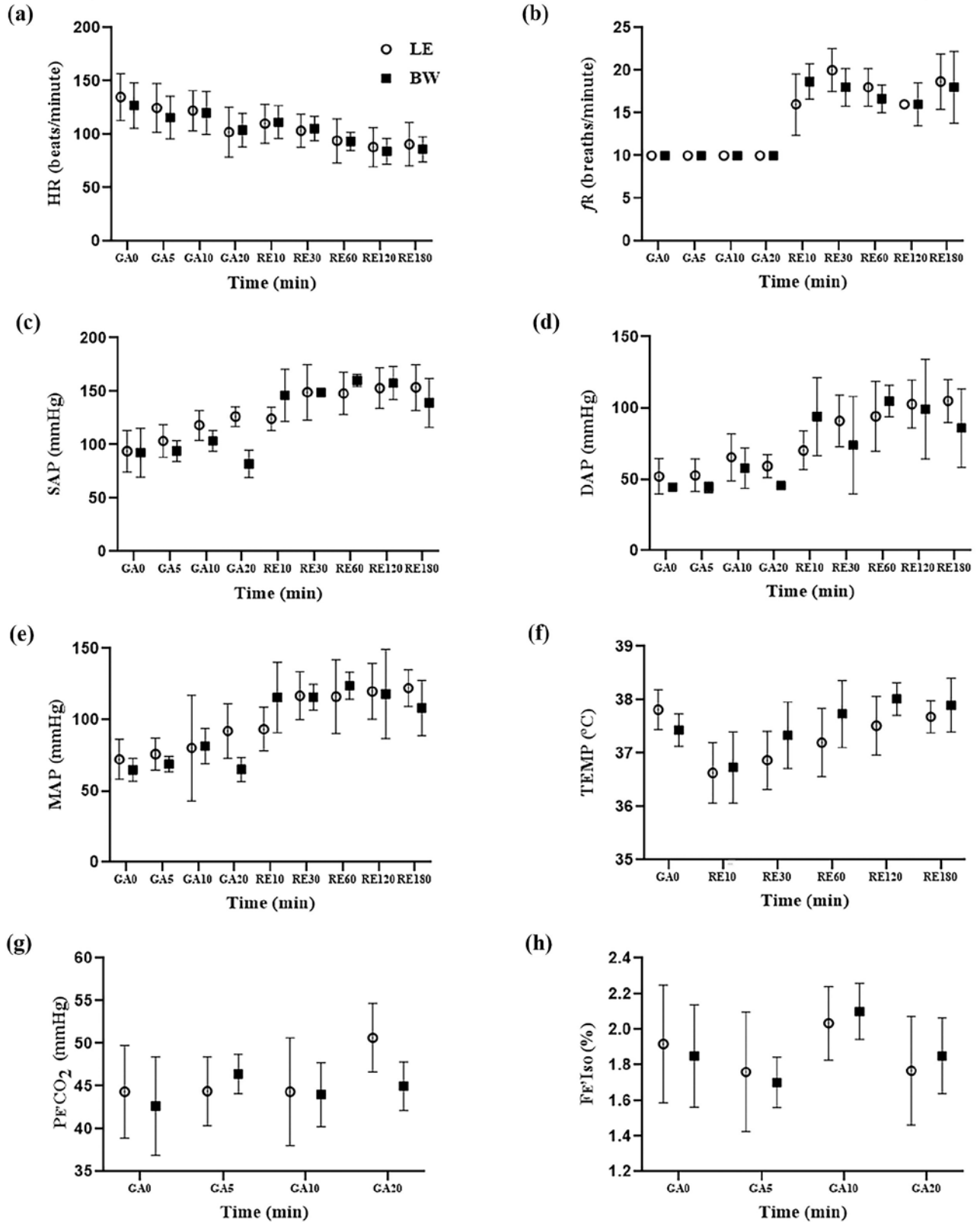


Figure 2. a — Heart rate (HR); b — Respiratory rate (f_R); c — Systolic arterial pressure (SAP); d — Diastolic arterial pressure (DAP); e — Mean arterial pressure (MAP); f — Rectal temperature (TEMP); g — End-tidal CO_2 ($P_{E'}CO_2$); and h — End-tidal isoflurane concentration ($F_{E'}Iso$) in 6 dogs initially under general anesthesia (GA) for placement of an epidural lumbosacral catheter and injection of a volume mixture of bupivacaine 0.25% and iopamidol 15% and after anesthesia (RE). The injection consisted of 0.2 mL/kg based on body weight (BW; solid black square) on one occasion or 0.05 mL/cm (< 50 cm) or 0.07 mL/cm (50 to < 70 cm) based on length of the vertebral column (LE; open circle) on a different occasion in a randomized crossover fashion. Data are presented as mean ± standard deviation.

FOR PERSONAL USE ONLY

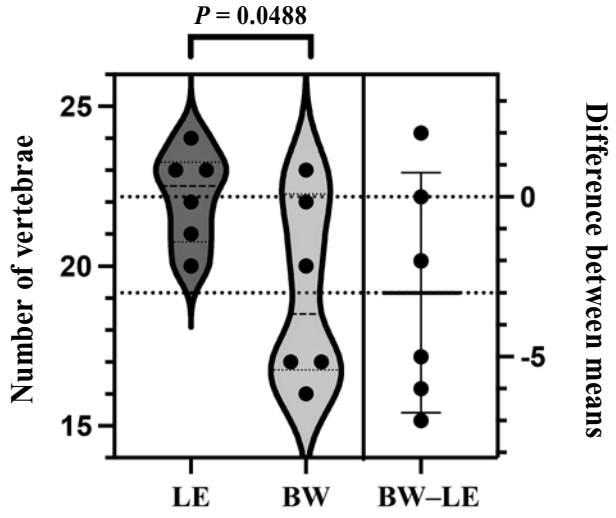


Figure 3. Comparison of number of vertebrae reached by a volume mixture of bupivacaine 0.25% and iopamidol 15% in 6 dogs administered a lumbosacral epidural injection of 0.2 mL/kg based on body weight (BW) and 0.05 mL/cm (< 50 cm) or 0.07 mL/cm (50 to < 70 cm) based on length of the vertebral column (LE) in a randomized crossover fashion. Each violin plot depicts the frequency distribution of the data, with lines at the median (dashed line) and quartiles (smaller dotted lines) for each group (LE, BW). The larger dotted lines across both violin plots indicate the mean of each group and the difference between the 2 means, and standard deviation is depicted with solid lines on the right axis (3 ± 3.6 vertebrae).

Table II. Time to presence of a positive response to noxious stimulation of different dermatomes starting from caudal to cranial in 6 female beagle dogs that received a lumbosacral epidural injection of 0.2 mL/kg based on body weight (BW) and 0.05 mL/cm (< 50 cm) or 0.07 mL/cm (50 to < 70 cm) based on the length of the vertebral column (LE) in a randomized crossover fashion of a volume mixture of bupivacaine 0.25% and iopamidol 15%.

	Time to presence of pain (min)	
Dermatome	LE	BW
AN1	46.3 ± 23.4	55.2 ± 23.4
AN2	38.8 ± 23.4	52.7 ± 23.4
AN3	38.8 ± 23.4	52.7 ± 23.4
AN4	36.3 ± 23.4	52.7 ± 23.4
AN5	36.3 ± 23.4	52.7 ± 23.4
AN6	36.3 ± 23.4	52.7 ± 23.4
AN7	36.3 ± 23.4	52.7 ± 23.4
AN8	36.3 ± 23.4	52.7 ± 23.4
AN9	36.3 ± 23.4	40.2 ± 23.4
AN10	36.3 ± 23.4	37.7 ± 23.4
AN11	36.3 ± 23.4	37.7 ± 23.4
Mean ± SD	37.7 ± 20.4	49.0 ± 20.4

AN1 — Base of the tail; AN2 — Pelvic limb paw; AN3 — Area surrounding the iliac crest; AN4 — Inguinal area near the femoral nerve; AN5 — Area surrounding the transverse process of L_3 and flank; AN6 — Paramedian area next to the umbilicus; AN7 — Along the 13th rib; AN8 — Paramedian area to the xyphoid; AN9 — Along the 9th rib; AN10 — Along the 2nd rib; AN11 — Thoracic limb paw.

radiographic imaging (16) or for up to 20 to 30 min using CT (15,21). The number of vertebrae reached gradually increases in the first 20 to 30 min post-injection (15,16,21) and then decreases 30 min after injection due to systemic absorption of the contrast medium (16).

The LE doses used in this study were based on studies in pigs and dogs in which a linear regression equation was generated by injecting the contrast diatrizoate mixed with lidocaine 2% in 2-mL increments at the LS to determine the rostral spread radiographically immediately after the injection to help predict the volume of injectate needed to reach T10 (vertebra 11) (8), which represents dermatomes that include abdominal analgesia/anesthesia in addition to the pelvis and pelvic limb.

In contrast, for pelvis and pelvic limb, the inclusion of up to L3 (vertebra 5) is all that is required (22). In the present study, in both the LE and BW groups, the iopamidol spread exceeded the predicted site (T10) by reaching C4 to T1 with the LE dose and C5 to T5 with the BW dose. This extent of rostral spread did not correspond to the sensory block elicited by bupivacaine 0.25% in this study.

This study demonstrated similar rostral spread to that obtained in medium-sized dogs injected with 0.2 mL/kg of contrast medium in other studies, 12.8 kg (10 to 15 kg) (15) and 12.0 kg (10.9 to 14.0 kg) (21), but less rostral spread than that obtained in small-sized dogs of 7.6 ± 1.1 kg in another study (16). It is difficult to draw comparisons between studies as different methodologies are used to determine the speed of injection, time to imaging, use or not of epidural catheter, and the method for counting the number of vertebrae.

In the present study, dogs were injected faster (over 20 s) using an epidural catheter and assessed sooner (within 5 min) than in other studies (0.6 to 1.0 mL/min for injection and imaging at 20 to 45 min). In addition, only one other study used an epidural catheter (21) and different methods for counting the number of vertebrae reached were used in all studies (15,16,21).

The epidural distribution of the indicator (contrast medium or dye) is not always uniform around the spinal cord. In some studies, including this one, the number of vertebrae reached was based on the presence of the indicator without regard for uniform spread (14,15). In other studies, this was calculated as the mean of the dorsal and ventral spread (10,16) or by approximating the number to the nearest half vertebral body (21,23), the number corresponding to the ventral column (8), or the number according to a set percentage of coverage around the spinal cord, *e.g.*, 90% (11).

In the present study, 11 dermatomes were used to assess the analgesic effects of epidural bupivacaine. The methods for assessing analgesia used herein have also been used in other studies (10,24). In certain dermatomes, it was easier to use electrical current to interpret when responses to the mechanical stimulation were not definitive. This occurred in very few instances and in anatomical areas that were more diffusely innervated, such as the flank and the inguinal area.

The main difference in assessment of the response to nociception in this study and in other studies was that the observer was blinded to the treatments, and it was an all-or-none response, which is more

FOR PERSONAL USE ONLY

representative of detecting the presence of pain perception than the degree of analgesia.

Depending on the type of indicator used, it has been shown that the number of analgesic dermatomes did not correspond to the rostral spread of that indicator (10,16). A 1:1 mixture of bupivacaine 0.5% with methylene blue 1% dosed at 0.2, 0.4, 0.6, and 0.8 mL/kg resulted in a larger rostral spread of dye of 18 ± 7 (T3), 22 ± 2 (C6), 26 ± 2 (C2), and 26 ± 1 (C2) vertebrae, respectively, than for analgesia, which was assessed for 30 min post-injection and resulted in a maximum of 5.0 ± 3.3 vertebrae (L3), 14.2 ± 4.2 (T7), 20.2 ± 1.3 (T1), and 21.0 ± 0 (C7), respectively (10).

The need to dilute the bupivacaine 0.5% by adding an equal volume of the contrast medium and the resulting reduction in concentration to 0.25% was a limitation of this study and of other studies. It is most likely associated with the incomplete and short-lasting sensory block, despite the extensive rostral spread of iopamidol with doses calculated based on both LE and BW. In humans, the contrast medium used was highly correlated ($r = 0.97$) with analgesic spread when effective concentrations of local anesthetic were used (25).

The effectiveness of sensory and motor block with an LS epidural local anesthetic depends on both volume and concentration of the anesthetic. Although volumes of 0.2, 0.4, and 0.6 mL/kg of bupivacaine 0.25% resulted in more rostral sensory blockade, sensory responses to noxious stimulation were never absent due to the diluted form of the bupivacaine (10).

Increasing concentrations from 0.25% to 0.5% and 0.75% resulted in faster onset and duration, as well as a higher degree of sensory and motor block (24,26), which demonstrates that bupivacaine 0.25% does not cause a complete sensory block. Epidural bupivacaine 0.25% is commonly administered to women to provide analgesia during labor, although frequent top-ups are required to maintain the degree of analgesia (27), whereas epidural bupivacaine 0.5% can be used alone to provide anesthesia for caesarean section (28).

Bupivacaine concentrations of at least 0.5% result in effective motor and sensory block (24,29). Motor block assessed in humans by a quantitative method using isometric measurements of force of extension and flexion of the leg joints to 90% of the control value (before epidural) demonstrated no difference in the return to sensory and motor function for bupivacaine (29).

In the present study, the duration of block with bupivacaine 0.25% was determined by the return of complete motor function (score of 0 for ambulation). During the recovery phase in our study, the effects of isoflurane anesthesia could have influenced the coordination of the dogs and prolonged the duration of motor block. Times of motor block in this study, however, were shorter than those in other studies using the same dose and bupivacaine concentration (10,24). Differences in these times are also due to the endpoints for assessing motor block in those other studies in which ataxia was considered part of the motor block *versus* complete inability to ambulate as was used in the present study.

Dogs were fully ambulatory at 48.2 ± 18.8 min in the LE group and 35.5 ± 28.6 min in the BW group post-extubation. Although not significant, this difference was most likely related to the higher volume of bupivacaine administered in the LE group. In another study, 0.2 mL/kg of bupivacaine 0.25% caused complete motor block in only 33% of the dogs at 10 min post-injection and the duration of the motor block (from ataxia to complete paralysis) was 72 ± 55 min (24).

In the present study, the use of general anesthesia to facilitate placement of the epidural catheter and carry out CT scanning was a major limitation to our objective of determining cardiopulmonary effects and the degree of motor and sensory block. This meant that the immediate post-injection assessments had to be delayed until the dog had fully recovered. As a result, analgesia was assessed approximately 35 min post-extubation in both the LE and BW group, which meant not earlier than 40 min after the epidural injection of bupivacaine 0.25%. Due to the design of the present study, the onset and immediate effects on sensory and motor function post-extubation were missed since positive responses to nociceptive stimulation were already present at 37.7 ± 20.4 min for LE and 49.0 ± 20.4 min for BW post-extubation.

Despite a high rostral spread with either dosing method, cardiopulmonary variables and rectal temperature values were within acceptable limits (30,31) and were similar in both groups. In one study, rectal temperature was lower in a group of conscious dogs dosed based on LE than in dogs dosed based on BW, although rectal temperature was still ≥ 37°C, which was assumed to be the result of sympathetic block and vasodilation (32). In dogs (18.9 ± 3.3 kg) administered LS bupivacaine 0.25% at 0.2 or 0.4 mL/kg under isoflurane anesthesia, mean arterial pressure and cardiac output values were acceptable with both doses for up to 60 min (33).

In this study, pulmonary function was only assessed by respiratory rate and none of the dogs appeared to have negative effects of the rostral spread of bupivacaine 0.25%. This was most likely because, at this concentration and these doses (BW: 0.2 mL/kg, LE: 0.37 mL/kg), the effect on motor fibers to the respiratory muscles is minimal (10,33).

In conclusion, this study demonstrated that volumes of epidural injectate in small-sized dogs were greater when doses are calculated based on LE than when based on BW. As this results in more rostral spread of the anesthesia, the methods cannot be considered interchangeable. Cardiopulmonary function was similar regardless of the method used to calculate epidural volume. Due to the design of this study, however, it was not possible to demonstrate whether the difference in epidural volume had an impact on the immediate assessment of analgesia because recovery from anesthesia delayed the start of this assessment.

FOR PERSONAL USE ONLY

Appendix A. Sedation recovery score used during the first 30 min (recovery period) after epidural injection in dogs anesthetized with isoflurane.

Sedation score	
0	Bright and alert, no apparent sedation
1	Calm, minimal sedation (quiet but still alert and aware of surroundings, mild resistance to restraint for lateral recumbency, moderate response to voices and touch)
2	Very calm, with moderate sedation (quiet, relaxed, minimal restraint required for lateral recumbency, mild response to voices or touch)
3	Profound sedation (quiet, very relaxed, no restraint necessary for lateral recumbency, does not respond to voices or touch)

Modified from Skelding *et al* (18).

Appendix B. Ambulation score used at the end of recovery period (30 min) after epidural injection in dogs anesthetized with isoflurane.

Ambulation score	
0	Normal ambulation
1	Able to walk but shows ataxia and mild proprioceptive deficit of hind limbs
2	Drags one or both hind limbs when walking; marked proprioceptive deficit
3	Unable to stand and/or ambulate

Acknowledgments

The authors thank William Sears for statistical analysis and advice and the Ontario Veterinary College Pet Trust for funding this project.

References

1. Valverde A. Epidural analgesia and anesthesia in dogs and cats. Vet Clin North Am Small Anim Pract 2008;38:1205–1230.
2. Garcia-Pereira F. Epidural anesthesia and analgesia in small animal practice: An update. Vet J 2018;242:24–32.
3. Martin-Flores M. Epidural and spinal anesthesia. Vet Clin North Am Small Anim Pract 2019;49:1095–1108.
4. Bromage PR. Physiology and pharmacology of epidural analgesia. Anesthesiology 1967;28:592–622.
5. Li YM, Wingrove DE, Too HP, *et al.* Local anesthetics inhibit substance P binding and evoked increases in intracellular Ca^{2+}. Anesthesiology 1995;82:166–173.
6. Nagy I, Woolf CJ. Lignocaine selectively reduces C fibre-evoked neuronal activity in rat spinal cord in vitro by decreasing N-methyl-D-aspartate and neurokinin receptor-mediated postsynaptic depolarization: Implications for the development of novel centrally acting analgesic. Pain 1996;64:59–70.
7. Furutani K, Ikoma M, Ishii H, Baba H, Kohno T. Bupivacaine inhibits glutamatergic transmission in spinal dorsal horn neurons. Anesthesiology 2010;112:138–143.
8. Strande A. Epidural anaesthesia in young pigs, dosage in relation to the length of the vertebral column. Acta Vet Scand 1968;9:41–49.
9. Johnson RA, Lopez MJ, Hedrickson DA, Kruse-Elliott KT. Cephalad distribution of three different volumes of new methylene blue injected into the epidural space in adult goats. Vet Surg 1996;25:448–451.
10. Freire CD, Torres MLA, Fantoni DT, Cavalcanti RL, Noel-Morgan J. Bupivacaine 0.25% and methylene blue spread with epidural anesthesia in dog. Vet Anaesth Analg 2010;37:63–69.
11. Vesovski S, Makara M, Martinez-Taboada F. Computer tomographic comparison of cranial spread of contrast in lumbosacral and sacrococcygeal epidural injections in dog cadavers. Vet Anaesth Analg 2019;46:510–515.
12. Bromage PR. Spread of analgesic solutions in the epidural space and their site of action: A statistical study. Br J Anaesth 1962;34:161–178.
13. Valverde A, Skelding A. Comparison of calculated lumbosacral epidural volumes of injectate using a dose regimen based on body weight versus length of the vertebral column in dogs. Vet Anaesth Analg 2019;46:135–140.
14. Gorgi AA, Hofmeister EH, Higginbotham MJ, Kent M. Effect of body position on cranial migration of epidurally injected methylene blue in recumbent dogs. Am J Vet Res 2006;67:219–221.
15. Iseri T, Nishimura R, Nagahama S, *et al.* Epidural spread of iohexol following the use of air or saline in the 'loss of resistance' test. Vet Anaesth Analg 2010;37:526–530.
16. Son W, Kim J, Seo J, *et al.* Cranial epidural spread of contrast medium and new methylene blue dye in sternally recumbent anaesthetized dogs. Vet Anaesth Analg 2011;38:510–515.
17. Baldwin K, Bartges J, Buffington T, *et al.* AAHA nutritional assessment guidelines for dogs and cats. J Am Anim Hosp Assoc 2010;46:285–296.
18. Skelding A, Valverde A, Aguilera R, Moens NM, Sinclair M, Thomason JJ. Comparison of three blind brachial plexus block techniques during maintenance of anesthesia and postoperative pain scores in dogs undergoing surgical procedures of the thoracic limb. Can J Vet Res 2019;83:197–205.
19. Higuchi H, Adachi Y, Kazama T. Effects of epidural saline injection on cerebrospinal fluid volume and velocity waveform. Anesthesiology 2005;102:285–292.
20. Sánchez AL, Martínez-Bazán C, Gutiérrez-Montes C, *et al.* On the bulk motion of the cerebrospinal fluid in the spinal canal. J Fluid Mech 2018;841:203–227.
21. Zhang D, Fujiwara R, Iseri T, *et al.* Distribution of contrast medium epidurally injected at thoracic and lumbar vertebral segments. J Vet Med Sci 2013;75:663–666.
22. Bailey CS, Kitchell RL. Cutaneous sensory testing in the dog. J Vet Intern Med 1987;1:128–135.
23. Kawalilak LT, Tucker RL, Greene SA. Use of contrast-enhanced computed tomography to study the cranial migration of a lumbosacral injectate in cadaver dogs. Vet Radiol Ultrasound 2015;56:570–574.

FOR PERSONAL USE ONLY

24. Gómez de Segura IA, Vazquez I, De Miguel E. Antinociceptive and motor-blocking action of epidurally administered IQB-9302 and bupivacaine in the dog. Reg Anesth Pain Med 2000;25: 522–528.
25. Yokoyama M, Hanazaki M, Fujii H, *et al.* Correlation between the distribution of contrast medium and the extent of blockade during epidural anesthesia. Anesthesiology 2004;100:1504–1510.
26. Duke T, Caulkett NA, Ball SD, Remedios AM. Comparative analgesic and cardiopulmonary effects of bupivacaine and ropivacaine in the epidural space of the conscious dog. Vet Anaesth Analg 2000;27:13–21.
27. Eddleston JM, Holland JJ, Griffin RP, Corbett A, Horsman EL, Reynolds F. A double-blind comparison of 0.25% ropivacaine and 0.25% bupivacaine for extradural analgesia in labour. Br J Anaesth 1996;76:66–71.
28. Crosby E, Sandler A, Finucane B, *et al.* Comparison of epidural anaesthesia with ropivacaine 0.5% and bupivacaine 0.5% for caesarean section. Can J Anaesth 1998;45:1066–1071.
29. Axelsson K, Nydahl PA, Philipson L, Larsson P. Motor and sensory blockade after epidural injection of mepivacaine, bupivacaine, and etidocaine — A double blind-study. Anaesth Analg 1989;69:739–747.
30. Haskins S, Pascoe PJ, Ilkiw JE, Fudge J, Hopper K, Aldrich J. Reference cardiopulmonary values in normal dogs. Comp Med 2005;55:156–161.
31. Merin RG, Bernard JM, Doursout MF, Cohen M, Chelly CE. Comparison of the effects of isoflurane and desflurane on cardiovascular dynamics and regional blood flow in the chronically instrumented dog. Anesthesiology 1991;74:568–574.
32. Leite GM, Augusto LEF, Pereira VG, Cunha AF, Pontes KCS, Santana JLP. Comparative study of epidural anesthesia in dogs by weight or occipito-coccygeal distance. Rev Ceres 2017;64: 12–17.
33. Dias RSG, Soares JHN, Castro DSE, *et al.* Cardiovascular and respiratory effects of lumbosacral epidural bupivacaine in isoflurane-anesthetized dogs: The effects of two volumes of 0.25% solution. PLoS One 2018;13:1–16.

FOR PERSONAL USE ONLY

Rostral spread of lumbosacral epidural volumes of dye and contrast medium calculated using body weight or length of the vertebral column in dog cadavers

Flavio A.V. Freitag, Alexander Valverde, Monica Jensen, Andrea Sanchez, Diego E. Gomez, Craig Bailey

Abstract

The objective of this study was to compare the rostral spread of lumbosacral epidural volumes of a mixture of dye and contrast medium, calculated using body weight (BW) or vertebral column length (LE), in 22 dog cadavers. The dogs weighed 4.6 to 52.0 kg. Dogs were paired within a < 10% difference for BW and LE and with the same body condition score (BCS). Pairs of dogs were injected while in sternal recumbency through an epidural catheter with a volume mixture of iopamidol and dye, calculated based on BW: 0.2 mL/kg in one of the cadavers and based on LE: 0.05 mL/cm (< 50 cm), 0.07 mL/cm (50 to < 70 cm), 0.08 mL/cm (70 to < 80 cm), and 0.11 mL/cm (≥ 80 cm) in the other cadaver. The extent of rostral spread was determined using computed tomography for iopamidol and anatomical dissection for dye. Comparisons for dye and iopamidol within each dog, and for BW and LE within matched pairs, were completed with mixed linear models ($P < 0.05$). The number of vertebrae reached by dye was greater than the number reached by iopamidol in both BW and LE, but the rostral spread was not significantly different between BW and LE for all pairs. In conclusion, dye tends to spread further than iopamidol and therefore, these two methods should not be considered interchangeable when used in research studies.

Résumé

L'objectif de cette étude était de comparer l'étalement rostral des volumes épiduraux lombo-sacrés d'un mélange de colorant et de produit de contraste, calculé en utilisant le poids corporel (PC) ou la longueur de la colonne vertébrale (LE), chez 22 cadavres de chiens. Les chiens pesaient de 4,6 à 52,0 kg. Les chiens ont été appariés avec une différence < 10 % pour PC et LE et avec le même score d'état corporel (PCS). Des paires de chiens ont reçu une injection alors qu'ils étaient en décubitus sternal à travers un cathéter péridural avec un mélange volumique d'iopamidol et de colorant, calculé sur la base du poids corporel : 0,2 mL/kg dans l'un des cadavres et sur la base de la LE : 0,05 mL/cm (< 50 cm), 0,07 mL/cm (50 à < 70 cm), 0,08 mL/cm (70 à < 80 cm) et 0,11 mL/cm (≥ 80 cm) dans l'autre cadavre. L'étendue de la propagation rostrale a été déterminée par tomodensitométrie pour l'iopamidol et dissection anatomique pour le colorant. Les comparaisons pour le colorant et l'iopamidol au sein de chaque chien, et pour PC et LE au sein de paires appariées, ont été complétées avec des modèles linéaires mixtes ($P < 0,05$). Le nombre de vertèbres atteintes par le colorant était supérieur au nombre atteint par l'iopamidol dans PC et LE, mais la propagation rostrale n'était pas significativement différente entre PC et LE pour toutes les paires. En conclusion, le colorant a tendance à se propager plus loin que l'iopamidol et, par conséquent, ces deux méthodes ne doivent pas être considérées comme interchangeables lorsqu'elles sont utilisées dans des études de recherche.

(Traduit par Docteur Serge Messier)

Department of Clinical Studies (Freitag, Valverde, Jensen, Sanchez, Gomez) and Department of Biomedical Sciences (Bailey), Ontario Veterinary College, University of Guelph, Guelph, Ontario N1G 2W1.

Address all correspondence to Dr. Alexander Valverde; telephone: (519) 824-4120; email: valverde@uoguelph.ca

Author contributions

FAVF: Data collection, statistical analysis and interpretation, manuscript preparation, and approval of final version. AV: Funding and design, data collection, statistical analysis and interpretation, manuscript preparation, and approval of final version. MJ: Data collection, imaging interpretation, manuscript preparation, and approval of final version. AS, DG, and CB: Design, manuscript preparation, data interpretation, and approval of final version.

Received February 7, 2023. Accepted March 29, 2023.

FOR PERSONAL USE ONLY

Introduction

Lumbosacral (LS) epidural injections with local anesthetics result in a blockade of all types of nerve fibers, including nociceptive fibers. The extent of sensory block depends on the rostral spread and contact time of the anesthetic with dural cuffs surrounding the nerve roots of spinal nerves, as well as with nociceptive fibers within the spinal cord, in the epidural space (1–3). A linear relationship has been established between the LS epidural volume of local anesthetics and the extent of rostral spread (4–8). Therefore, the higher the volume, the more dermatomes a local anesthetic can block due to its greater rostral spread.

The degree of rostral spread is influenced by gravity and friction (9). Studies assessing the rostral spread of local anesthetics have used different methodologies and lack uniformity for factors that can influence forces of gravity and friction. These factors include body condition score (BCS) of the sample population; position of the dog during the epidural injection; advancing an epidural catheter or use of a needle; conscious state (awake, sedation, anesthesia); use of cadavers or live dogs; and use of dye or contrast medium or local anesthetic and their combinations (1,4,7,8,10–13).

The combination of a dye or contrast medium with a local anesthetic has been used in different studies to visualize the extent of rostral spread using necropsy dissection for dye or computed tomography (CT) or radiographs for contrast medium. These findings are then correlated with the sensory block from the local anesthetic. This correlation is not always accurate, however, and often results in discrepancies between the extent of rostral spread of the substances and the method of visualization. For example, rostral spread of dye was of greater magnitude than contrast medium in one study (12) and did not match the degree of sensory block by bupivacaine in other studies (7,14).

This study compares the rostral spread of LS epidural volumes of a mixture of dye and contrast medium, calculated based on body weight (BW) and vertebral column length (LE; from the sacrococcygeal space to the occipital crest) in pairs of similarly matched dog cadavers. These are the 2 common methods used to calculate epidural volumes in dogs.

Assessments were completed with computed tomography for contrast medium and necropsy dissections for dye in order to determine whether rostral spread is similar for both methods of volume calculation. We hypothesized that rostral spread of dye would be greater than that of contrast medium, regardless of the method used to calculate epidural volume.

Materials and methods

Animals

A total of 22 dog cadavers were used (6 mixed breeds, 4 hounds, 3 German shepherds, 2 poodles, 2 Shih tzus, and 1 each of Chihuahua, beagle, Rottweiler, mastiff, and Great Dane). The dogs were clinical cases that were euthanized and donated for teaching laboratories. The dogs were divided into 11 pairs according to body weight: small ($<$ 10 kg; 4 pairs), medium (10 to $<$ 25 kg; 3 pairs), large (25 to $<$ 45 kg; 3 pairs), and giant ($\geq$ 45 kg; 1 pair). All cadavers were kept frozen until the day before the study. The approval of the institutional Animal Care Committee was not required for use of the cadavers.

Within each body weight category, cadavers were paired according to BW (kg) and LE measured in centimeters using a metric tape. Both cadavers in a pair were within $<$ 10% difference for BW and LE and with the same BCS (1 to 5) in which 1 = emaciated; 2 = thin; 3 = moderate; 4 = stout; and 5 = obese (15). Each matched pair within each category was then randomized (http://www.random.org) for an epidural injection calculated according to BW (0.2 mL/kg) in one of the cadavers or according to LE [0.05 mL/cm ($<$ 50 cm), 0.07 mL/cm (50 to $<$ 70 cm), 0.08 mL/cm (70 to $<$ 80 cm), and 0.11 mL/cm ($\geq$ 80 cm)] in the other cadaver (9).

Epidural injection and evaluation

Matched pairs of cadavers were thawed completely prior to the day of the experiment. With the cadaver in sternal recumbency with the pelvic limbs extended caudally, a Tuohy needle was inserted at the LS space and an epidural catheter advanced rostrally into the epidural space beyond the tip of the needle 1 cm for $<$ 10 kg, 2 cm for 10 to $<$ 25 kg, 3 cm for 25 to $<$ 45 kg, and 4 cm for $\geq$ 45 kg. Verification consisted of ease of advancement of the catheter and later identification in the epidural space with computed tomography (CT).

The epidural catheter used for dogs of $<$ 10 kg in the BW category consisted of a 24-gauge, 25-cm catheter advanced through a 20-gauge, 4.5-cm Tuohy needle (Epidural Pain Management Kit; MILA, Florence, Kentucky, USA). A 19-gauge, 90-cm catheter and 17-gauge, 8.9-cm Tuohy needle were used in the other 3 BW categories (FlexTip Plus Epidural Catheter; Arrow International, Reading, Pennsylvania, USA). Once the epidural catheter was in place, the Tuohy needle was removed, and the catheter was flushed with 0.1 to 0.2 mL of saline and secured in place with squared gauze fixed to the skin with a towel clamp.

Cadavers remained in sternal recumbency for the CT (16-slice detector, Brightspeed CT Scanner; GE Healthcare, Madison, Wisconsin, USA). The injection consisted of a solution of iopamidol contrast medium (IsoVue–300; Bracco Imaging, Anjou, Quebec), 300 mg/mL, diluted to a final concentration of 240 mg/mL (5:1) by adding yellow tissue-marking dye (Cancer Diagnostics Inc, Durham, North Carolina, USA).

To prime the catheter, the injectate volume included an additional 0.1 mL of the solution for small epidural catheters and 0.2 mL for large epidural catheters. An initial test injection of 0.3 mL of the solution was scanned to confirm correct placement of the epidural catheter. After confirmation, the remaining volume of solution was injected by hand over 20 s and CT images of the entire spine were acquired within 5 min of the injection and assessed from the cranial aspect of the cervical spine to just caudal to the LS space, in both soft tissue (standard) and bone windows, by a Board-certified radiologist (MJ) who was unaware of the treatment.

The number of vertebrae and the distance (measured in centimeters) reached by iopamidol was determined as the most cranial spread from the LS space and was always inclusive of the vertebra it reached, regardless of whether the whole vertebra had been reached or only a fraction of it. The distance was obtained after

FOR PERSONAL USE ONLY

Table I. Demographic data for 22 dog cadavers divided into pairs matched by < 10% difference in body weight (BW) and length of the vertebral column (LE) and with the same body condition score (BCS), in which one cadaver received an epidural injection of 0.2 mL/kg for BW and the other cadaver received 0.05 mL/cm (< 50 cm), 0.07 mL/cm (50 to < 70 cm), 0.08 mL/cm (70 to < 80 cm), or 0.11 mL/cm (≥ 80 cm mL/cm) for LE of a 5:1 volume mixture of iopamidol 30% and yellow tissue-marking dye, respectively.

Size	Pair	Treatment	Breed	BW (kg)	LE (cm)	BCS	Volume (mL)
Small	1	BW	Mixed breed	4.6	39	3/5	0.92
(< 10 kg)		LE	Mixed breed	4.6	39	3/5	1.95
	2	BW	Chihuahua	4.8	42	3/5	0.96
		LE	Mixed breed	4.6	41	3/5	2.05
	3	BW	Poodle	6.8	46	2/5	1.40
		LE	Poodle	6.7	48	2/5	2.40
	4	BW	Shih tzu	8.0	46	5/5	1.60
		LE	Shih tzu	8.0	44	5/5	2.20
Medium	1	BW	Mixed breed	11.0	51	3/5	2.20
(10 to < 25 kg)		LE	Beagle	11.5	55	3/5	3.85
	2	BW	Hound	19.5	70	3/5	3.90
		LE	Hound	20.5	73	3/5	5.84
	3	BW	Hound	23.5	71	3/5	4.70
		LE	Hound	21.5	73	3/5	5.84
Large	1	BW	German shepherd	25.0	75	3/5	5.00
(25 to < 45 kg)		LE	German shepherd	25.1	79	3/5	6.32
	2	BW	Mixed breed	33.0	79	3/5	6.60
		LE	Mixed breed	34.0	80	3/5	8.80
	3	BW	Rottweiler	40.0	91	3/5	8.00
		LE	German shepherd	37.0	91	3/5	10.01
Giant	1	BW	Mastiff	52.0	90	3/5	10.40
(> 45 kg)		LE	Great Dane	48.0	99	3/5	10.89

the transverse images had been reconstructed into a sagittal plane using multiplanar reformatting to make the spine as straight as possible.

Following the CT scan, cadavers were kept in sternal position and transferred immediately to the necropsy room and dissected in this position, avoiding changes in the horizontal position during this phase. A longitudinal skin incision was made along the spinous processes of the vertebral column and all anatomical layers above the spinous processes were reflected on each side until the vertebrae were exposed below the vertebral arches.

A laminectomy was carried out by removing each arch from the C1 vertebra to the sacrum, until the entire extent of the spinal cord was exposed. The most cranial spread of dye was also assessed by recording the number of vertebrae and the distance to each specific vertebra from the LS space using a metric measuring tape. Necropsies were completed within 60 min of the CT assessments.

Statistical analysis

All data were tested for normality using Shapiro-Wilk, Kolmogorov-Smirnov, Cramer-von Mises, and Anderson-Darlin procedures. UNIVARIATE and PLOT procedures were used to detect unequal variances, outliers, and other non-random patterns within the data for each group (SAS Version 9.4; SAS Institute, Cary, North Carolina, USA).

A mixed model of residual maximum likelihood was used for comparisons between pairs of dogs (LE *versus* BW dosing) for each weight category for the use of contrast (CT) and dye (necropsy) and the number of vertebrae reached by each substance. When appropriate, multiple pairwise comparisons in the mixed model were done by use of the Tukey-Kramer test. Comparisons between the number of vertebrae reached by the contrast and dye in all dogs were completed with an unpaired *t*-test and correlations were determined between contrast and dye with the number of vertebrae or distance reached by them (GraphPad Software, Version 9.3.1 for MacOS; GraphPad, San Diego, California, USA).

Results

Demographic data for the dog cadavers and the volume of injectate administered are provided in Table I. All pairs were within the established limits of < 10% difference in BW and LE and both dogs had the same BCS.

FOR PERSONAL USE ONLY

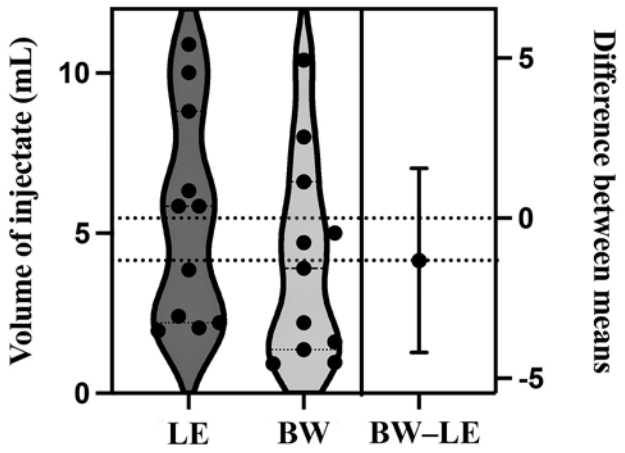


Figure 1. Volume of lumbosacral epidural injectate in 22 dog cadavers matched by < 10% difference in body weight (BW) and length of the vertebral column (LE) and with the same body condition score, in which one cadaver received an epidural injection of 0.2 mL/kg based on BW and the paired cadaver received 0.05 mL/cm (< 50 cm), 0.07 mL/cm (50 to < 70 cm), 0.08 mL/cm (70 to < 80 cm), or 0.11 mL/cm (≥ 80 cm) based on LE, of a 5:1 volume mixture of iopamidol 30% and yellow tissue-marking dye. Each violin plot depicts the frequency distribution of the data with lines at the median (dashed line) and quartiles (smaller dotted lines) for each group (LE, BW). The larger dotted lines across both violin plots indicate the mean of each group and the difference between the two means and standard deviation is depicted with solid lines on the right axis (1.32 ± 1.38 mL).

For all 11 pairs of dogs, the volume of injectate was always greater for LE than for BW, but not significantly different (5.47 ± 3.30 mL *versus* 4.15 ± 3.16 mL, respectively; mean ± standard deviation; $P = 0.3495$) (Figure 1). For each contrast medium and dye, there was no difference in the number of vertebrae or distance reached by the indicator between LE and BW for all size categories included. There was a trend for small- and medium-sized dogs to have more rostral spread with LE than with BW (Table II).

There were strong correlations between volume of injectate and distance reached by iopamidol and dye for all dog categories included and in both the LE and BW groups (r values ≥ 0.92, $P < 0.0001$ for each comparison) (Figure 2 A). This correlation was weaker between the volume of injectate and the number of vertebrae (iopamidol and LE: $r = 0.48$, $P = 0.1335$; iopamidol and BW: $r = 0.83$, $P = 0.0014$; dye and LE: $r = 0.48$, $P = 0.1366$; dye and BW: $r = 0.71$, $P = 0.0136$) (Figure 2 B).

The maximum possible number of vertebrae reached by dye or contrast medium was 27 = 7 lumbar + 13 thoracic + 7 cervical. The number of vertebrae reached by dye (22 ± 6) was greater than for contrast medium (19 ± 5) ($P = 0.0597$), but this data had to be transformed to accept normality, which resulted in a significant difference ($P = 0.0041$).

The distance reached by dye (51.8 ± 23.6 cm) was not significantly greater than for contrast medium (40.0 ± 18.6 cm). There was a strong correlation between dye and contrast medium for all dogs in both the LE and BW groups for the number of vertebrae ($r = 0.92$; $P < 0.0001$) and for distance ($r = 0.99$; $P < 0.0001$) reached by the indicators (Figure 3).

Discussion

In this study, epidural volumes were calculated based on LE or BW, which are the two reported methods used in this technique (4,6,9,12,14,16). The volume of injectate based on LE was greater than for BW, but the two methods did not differ significantly for the range in weight of all 11 pairs of dogs (4.6 to 52 kg). This difference has been shown to be significant in smaller sized dogs (≤ 25 kg), however, and the two methods of volume calculation are therefore not considered to be interchangeable for all sizes of dogs (9,14).

The volume of injectate was strongly correlated with the extent of rostral spread with both the dye and iopamidol, but had a weaker correlation with the number of vertebrae, which is a logical outcome due to the variation in size of vertebrae among the range of body weights and sizes of the dogs in this study. From a clinical point of view, it would be preferable if there was agreement between the volume of injectate and the number of vertebrae in order to accurately predict the dermatomes blocked by the epidural injection.

The most relevant finding of this study was that the number of vertebrae reached by dye was significantly greater than the number reached by iopamidol (22 ± 6 *versus* 19 ± 5), regardless of the method used to calculate volume. Although not significant (14.0 ± 5.4 vertebrae for dye and of 12.7 ± 5.7 vertebrae for iohexol), similar findings of greater rostral spread with methylene blue 1% than with iohexol 30% were obtained in another study in anesthetized small dogs (7.6 ± 1.1 kg) that were also injected with 0.2 mL/kg of the combination (12). Dogs were also injected at the LS space in sternal position, but assessed for 45 min radiographically to determine the spread of iohexol, and then bled out from the carotid artery before euthanasia and necropsy to assess the spread of dye (12). As necropsies were completed within 60 min of the CT assessments in our study, the times for dye assessments were probably similar in both studies, but earlier for contrast medium in our study.

In studies in both live and cadaver dogs, dye attaches to the surface of the spinal cord membranes and continues to spread due to delayed assessment until the time of necropsy (7,12). For this reason, it is likely that the degree of rostral spread was overestimated when dye was injected. In one study, the rostral spread of bupivacaine was assessed by pinching the skin over the spinous processes of vertebrae in conscious dogs (9.9 ± 1.9 kg) 30 min after volumes of 0.2, 0.4, 0.6, and 0.8 mL/kg of a 1:1 mixture of bupivacaine 0.5% and methylene blue 1% were injected through an epidural LS catheter advanced 5 cm into the epidural space (7). Analgesia had spread to vertebrae L3, T7, T1, and C7, respectively, for each volume, whereas it was determined during necropsy of these dogs that the dye was present at T3, C6, C2, and C2, respectively (7). This discrepancy is also partially due to the form of the diluted bupivacaine (0.25%) that results from the mixture, which has been shown to result in incomplete sensory blockade (7,17).

The dye and iopamidol were not distributed uniformly around the spinal cord in dog cadavers in the present study. This finding emphasizes the idiosyncrasy of the epidural space and factors that interfere with the spread of any substance, including anatomical structures, such as meningovertebral ligaments, epidural fat, presence of intervertebral foramens, differences in diameter along the spinal canal,

FOR PERSONAL USE ONLY

Table II. Rostral spread measured by number of vertebrae and distance (cm) from the lumbosacral space (LS) of an LS epidural dose calculated using body weight (BW; 0.2 mL/kg) or length of the vertebral column [LE; 0.05 mL/cm (< 50 cm), 0.07 mL/cm (50 to < 70 cm), 0.08 mL/cm (70 to < 80 cm), or 0.11 mL/cm (≥ 80 cm)] of a 5:1 volume mixture of iopamidol 30% and yellow tissue-marking dye, respectively, in pairs of dog cadavers matched according to < 10% difference in BW and LE and with the same body condition score. Spread of iopamidol was determined by CT imaging and spread of dye by necropsy of the spinal cord.

			Number of vertebrae		Distance from LS (cm)	
Size	Pair	Treatment	CT	Necropsy	CT	Necropsy
Small	1	BW	14	21	19.4	28
(< 10 kg)		LE	21	27	29.8	36
	2	BW	16	19	19.7	25
		LE	23	26	28.9	33
	3	BW	11	10	16.9	19
		LE	10	17	16.9	27
	4	BW	10	12	15.3	22
		LE	19	23	25.4	37.4
Mean ± SD		BW	13 ± 5	16 ± 7	17.8 ± 2.1	23.5 ± 3.9
(range)			(T_5 to T_{11})	(C_7 to T_{11})		
		LE	18 ± 5	24 ± 7	25.3 ± 5.9	33.4 ± 4.6
			(C_5 to T_{11})	(C_1 to T_4)		
Medium	1	BW	9	8	15.5	18
(10 to < 25 kg)		LE	22	23	38.8	47
	2	BW	20	23	36.8	56.6
		LE	22	26	48.2	68.5
	3	BW	20	22	43.6	55
		LE	20	23	43.5	57
Mean ± SD		BW	16 ± 5	18 ± 7	32.0 ± 14.7	43.2 ± 21.8
(range)			(T_1 to T_{12})	(C_6 to T_{13})		
		LE	21 ± 5	24 ± 7	43.5 ± 4.7	57.5 ± 10.8
			(C_6 to T_1)	(C_2 to C_5)		
Large	1	BW	22	24	52.3	66
(25 to < 45 kg)		LE	23	27	56.1	73
	2	BW	21	27	52.7	71
		LE	24	26	55.9	70.3
	3	BW	23	24	59.7	68
		LE	24	27	69.6	87.5
Mean ± SD		BW	22 ± 5	25 ± 7	54.9 ± 4.2	68.3 ± 2.5
			(C_5 to C_7)	(C_1 to C_4)		
		LE	24 ± 5	27 ± 7	60.5 ± 7.9	76.9 ± 9.3
			(C_4 to C_5)	(C_1 to C_2)		
Giant	1	BW	24	27	63.7	81
(≥ 45 kg)		LE	22	27	70.4	94
Overall mean ± SD		BW & LE	19 ± 5	22 ± 6*	40.0 ± 18.6	51.8 ± 23.6

* Significantly different than CT scan ($P = 0.0041$).

FOR PERSONAL USE ONLY

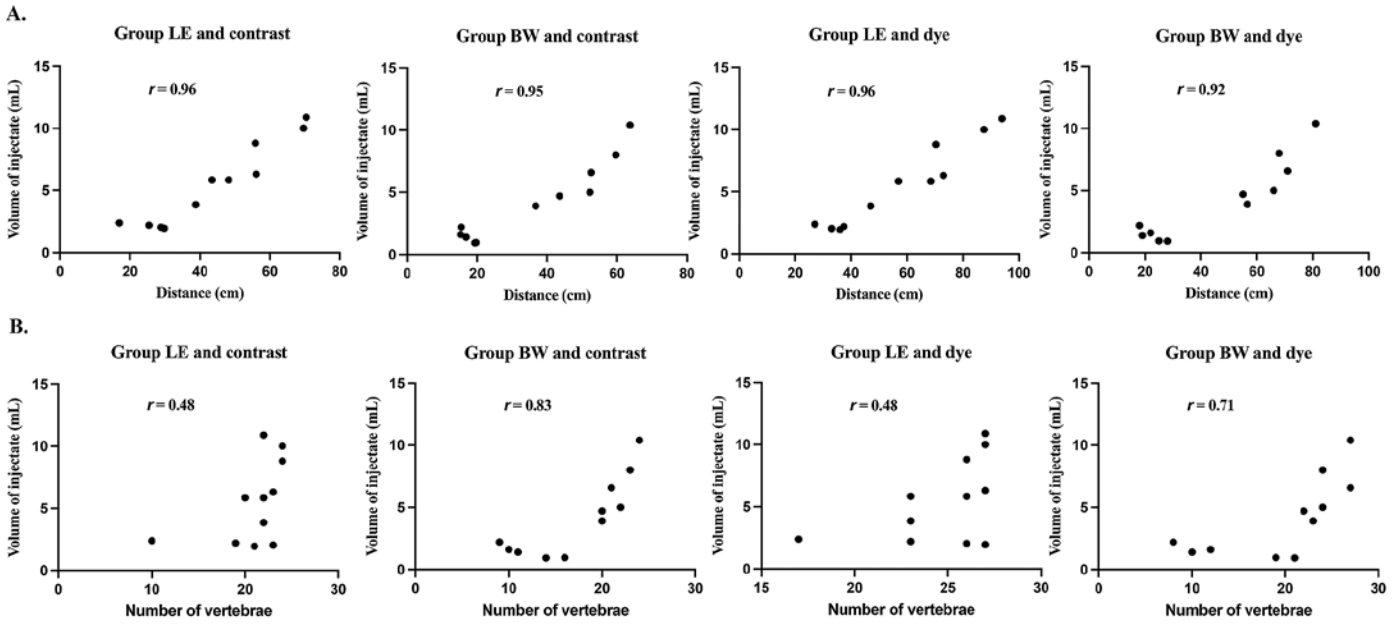


Figure 2. Correlations between distance (cm) (A) or number of vertebrae (B) reached by a volume of injectate of a 5:1 mixture of iopamidol 30% and yellow tissue-marking dye in 22 cadavers matched by < 10% difference in body weight (BW) and length of the vertebral column (LE) and with the same body condition score, in which one cadaver received a lumbosacral epidural injection of 0.2 mL/kg of the mixture for BW and the paired cadaver received 0.05 mL/cm (< 50 cm), 0.07 mL/cm (50 to < 70 cm), 0.08 mL/cm (70 to < 80 cm), or 0.11 mL/cm (≥ 80 cm) for LE.

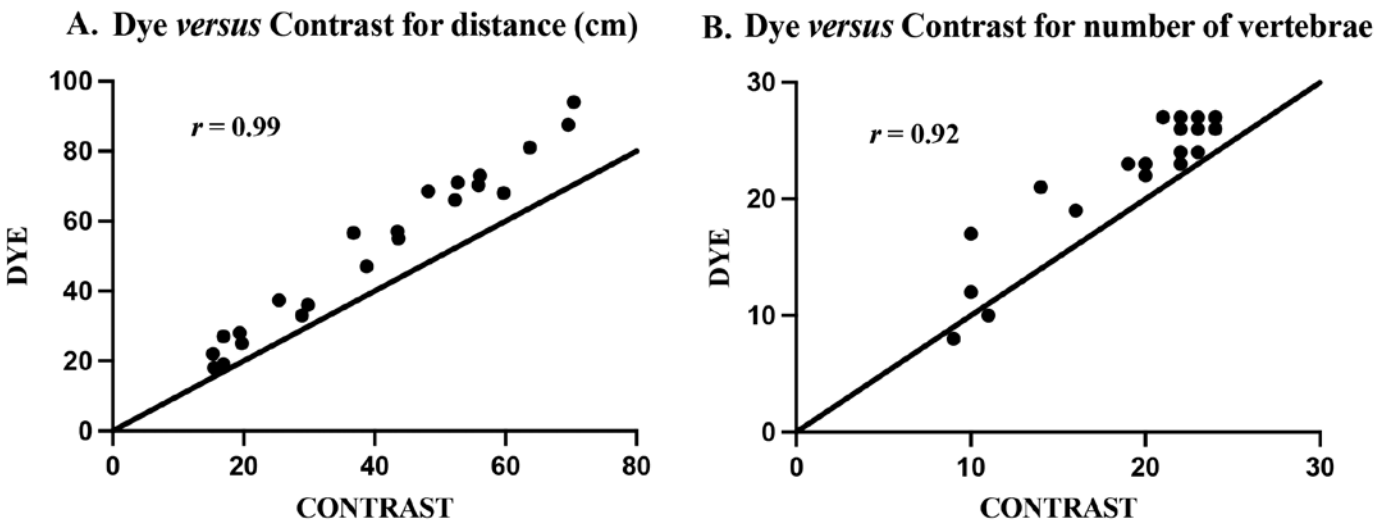


Figure 3. Correlation between distance (cm) (A) and number of vertebrae (B) reached by a volume of injectate of a 5:1 mixture of iopamidol 30% and yellow tissue-marking dye in 22 cadavers matched by < 10% difference in body weight (BW) and length of the vertebral column (LE) and with the same body condition score, in which one cadaver received a lumbosacral epidural injection of 0.2 mL/kg of the mixture for BW and the paired cadaver received 0.05 mL/cm (< 50 cm), 0.07 mL/cm (50 to < 70 cm), 0.08 mL/cm (70 to < 80 cm), or 0.11 mL/cm (≥ 80 cm) for LE.

and differences in the diameter of the spinal cord (18–20). The use of cadavers prevented other factors, such as systemic absorption and motion, which may interfere with or contribute, respectively, to rostral spread of epidural substances (12,21,22).

Rostral spread of an epidural volume of injectate dose based on LE has not been extensively studied. In one study, rostral spread was assessed radiographically 10 min after LS injection of contrast medium in sedated dogs (14.9 ± 5.2 kg) at 0.05, 0.1, or 0.15 mL/cm of iopamidol combined with ropivacaine 0.2% or 0.5% to determine the percentage of the total length of the vertebral column reached by the contrast medium (23). Unfortunately, these results cannot be compared to our study because the number of vertebrae or length of the vertebral column of the dogs were not reported.

The LE doses used in this study ranged from 0.05 to 0.11 mL/cm, according to the increase in vertebral length from < 50 to ≥ 80 cm as body weight (BW) increases. These doses are based on the linear relationship between the LS epidural volume and the extent of rostral spread determined in pigs and dogs to help predict the volume of injectate to reach T10 (vertebra 11) (4). In cadavers used in the present study, LE doses spread the iopamidol contrast beyond T10

FOR PERSONAL USE ONLY

in 10/11 pairs of dogs and from C4 to T1 and to T11 in the other pair of dogs. Interestingly, despite a lower volume of injectate, the spread of iopamidol in dogs given doses based on BW was also beyond vertebra T10 in 9/11 pairs of dogs and from C4 to T5 and to T11 and T12 in the other 2 pairs of dogs.

This study demonstrated that volumes of epidural injectate calculated over a wide range of body weights is not significantly different for BW and LE, despite a trend for a greater volume using LE. The number of vertebrae reached by the dye was significantly greater than the number reached by iopamidol, regardless of the method of volume calculation. Therefore, the results from studies using dye cannot be considered interchangeable with the results of studies using contrast medium.

Acknowledgments

The authors thank William Sears for statistical analysis and advice and the Ontario Veterinary College Pet Trust for funding this project.

References

1. Bromage PR. Spread of analgesic solutions in the epidural space and their site of action: A statistical study. Br J Anaesth 1962;34:161–178.
2. Bromage PR. Physiology and pharmacology of epidural analgesia. Anesthesiology 1967;28:592–622.
3. Furutani K, Ikoma M, Ishii H, Baba H, Kohno T. Bupivacaine inhibits glutamatergic transmission in spinal dorsal horn neurons. Anesthesiology 2010;112:138–143.
4. Strande A. Epidural anaesthesia in young pigs, dosage in relation to the length of the vertebral column. Acta Vet Scand 1968;9:41–49.
5. Johnson RA, Lopez MJ, Hedrickson DA, Kruse-Elliott KT. Cephalad distribution of three different volumes of new methylene blue injected into the epidural space in adult goats. Vet Surg 1996;25:448–451.
6. Li YM, Wingrove DE, Too HP, *et al.* Local anesthetics inhibit substance P binding and evoked increases in intracellular Ca^{2+}. Anesthesiology 1995;82:166–173.
7. Freire CD, Torres MLA, Fantoni DT, Cavalcanti RL, Noel-Morgan J. Bupivacaine 0.25% and methylene blue spread with epidural anesthesia in dog. Vet Anaesth Analg 2010;37:63–69.
8. Vesovski S, Makara M, Martinez-Taboada F. Computer tomographic comparison of cranial spread of contrast in lumbosacral and sacrococcygeal epidural injections in dog cadavers. Vet Anaesth Analg 2019;46:510–515.
9. Valverde A, Skelding A. Comparison of calculated lumbosacral epidural volumes of injectate using a dose regimen based on body weight versus length of the vertebral column in dogs. Vet Anaesth Analg 2019;46:135–140.
10. Gorgi AA, Hofmeister EH, Higginbotham MJ, Kent M. Effect of body position on cranial migration of epidurally injected methylene blue in recumbent dogs. Am J Vet Res 2006;67:219–221.
11. Iseri T, Nishimura R, Nagahama S, *et al.* Epidural spread of iohexol following the use of air or saline in the 'loss of resistance' test. Vet Anaesth Analg 2010;37:526–530.
12. Son W, Kim J, Seo J, *et al.* Cranial epidural spread of contrast medium and new methylene blue dye in sternally recumbent anaesthetized dogs. Vet Anaesth Analg 2011;38:510–515.
13. Kawalilak LT, Tucker RL, Greene SA. Use of contrast-enhanced computed tomography to study the cranial migration of a lumbosacral injectate in cadaver dogs. Vet Radiol Ultrasound 2015;56:570–574.
14. Freitag F. Comparison of rostral spread of lumbosacral epidural volume calculated by body weight or length of the vertebral column in dogs [DVSc dissertation]. Guelph, Ontario: University of Guelph, 2022:70–84.
15. Baldwin K, Bartges J, Buffington T, *et al.* AAHA nutritional assessment guidelines for dogs and cats. J Am Anim Hosp Assoc 2010;46:285–296.
16. Leite GMDP, Augusto LEF, Pereira VG, Cunha AF, Pontes KCS, Santana JLP. Comparative study of epidural anesthesia in dogs by weight or occipito-coccygeal distance. Rev Ceres 2017;64:12–17.
17. Gómez de Segura IA, Vazquez I, De Miguel E. Antinociceptive and motor-blocking action of epidurally administered IQB-9302 and bupivacaine in the dog. Reg Anesth Pain Med 2000;25:522–528.
18. Park WY, Massengale M, Kim SI, Poon KC, Macnamara TE. Age and the spread of local anesthetic solutions in the epidural space. Anesth Analg 1980;59:768–771.
19. Fletcher TF, Kitchell RL. Anatomical studies on the spinal cord segments of the dog. Am J Vet Res 1966;27:1759–1767.
20. Geers C, Lecouvet FE, Behets C, Malghem J, Cosnard G, Lengelé BG. Polygonal deformation of the dural sac in lumbar epidural lipomatosis: Anatomic explanation by the presence of meningovertebral ligaments. Am J Neuroradiol 2003;24:1276–1282.
21. Higuchi H, Adachi Y, Kazama T. Effects of epidural saline injection on cerebrospinal fluid volume and velocity waveform. Anesthesiology 2005;102:285–292.
22. Sánchez AL, Martínez-Bazán C, Gutiérrez-Montes C, *et al.* On the bulk motion of the cerebrospinal fluid in the spinal canal. J Fluid Mech 2018;841:203–227.
23. Otero P, Tarragona L, Ceballos M, Portela D. Epidural cephalic spread of a local anesthetic in dogs: A mathematical model using the column length (abstract). Vet Anaesth Analg 2010;37:35–36.

FOR PERSONAL USE ONLY

Comparison of two ratios of xylazine:ketamine for the anesthesia of free-ranging North American beavers *(Castor canadensis)* in a remote setting

Stéphane Lair, Gregory Bourguelat, Gaétan Fournier

Abstract

The objective of this study was to evaluate and compare 2 different xylazine:ketamine combination anesthetic protocols in free-ranging beavers *(Castor canadensis)*. Twenty-two beavers (weighing 2.5 to 18.5 kg) were equally assigned to one of the following protocols: 1:10 xylazine:ketamine ratio and 3:10 xylazine:ketamine ratio. Using standard metabolic scaling, the following ranges of dosages were calculated and used:

- for the 1:10 xylazine:ketamine group 1.08 to 2.25 mg/kg (median = 1.2 mg/kg) of xylazine + 10.8 to 22.5 mg/kg (median = 12 mg/kg) of ketamine IM; and
- for the 3:10 xylazine:ketamine group 2.04 to 3.67 mg/kg (median = 2.7 mg/kg) of xylazine + 6.81 to 12.25 mg/kg (median = 8.8 mg/kg) ketamine IM.

Measured cardiorespiratory parameters and anesthetic event intervals were compared between protocols. Both protocols rapidly induced levels of anesthesia adequate for minimally invasive procedures of short duration. Durations of immobility ranged from 15 to 35 min and were not significantly different between the protocols ($P = 0.64$). Recovery phases, following the IM administration of 0.2 mg/kg of atipamezole 30 to 65 min post-induction, were usually faster with the 3:10 xylazine:ketamine protocol, but this was not statistically significant ($P = 0.40$). Heart rates were significantly lower with the 3:10 xylazine:ketamine protocol ($P = 0.0002$). $P_{ET}CO_2$ values, measured with a nasal cannula, were similar between protocols and suggestive of hypoventilation. Despite the fact that the 3:10 xylazine:ketamine protocol was associated with a greater cardiac depression, the apparent, even if not statistically significant, faster recovery time with that protocol is definitively an asset for projects occurring in remote locations relying on helicopter transportation.

Résumé

Le but de cette étude était d'évaluer et de comparer 2 protocoles anesthétiques différents combinant xylazine et kétamine chez des castors sauvages (*Castor canadensis*). Vingt-deux castors (2,5-18,5 kg) ont été assignés de manière égale à l'un des protocoles suivants : xylazine:kétamine à un ratio de 1:10 et xylazine:kétamine à un ratio de 3:10. À l'aide d'une échelle métabolique standard, les dosages calculés et utilisés ont été les suivants :

- 1,08 à 2,25 (médiane = 1,2) mg/kg de xylazine + 10,8 à 22,5 (médiane = 12) mg/kg de kétamine IM pour le groupe xylazine:kétamine à un ratio de 1:10; et
- 2,04 à 3,67 (médiane = 2,7) mg/kg de xylazine + 6,81 à 12,25 (médiane = 8,8) mg/kg de kétamine IM pour le groupe xylazine:kétamine à un ratio de 3:10.

Les paramètres cardiorespiratoires et les intervalles anesthésiques mesurés ont été comparés entre les protocoles. Les deux protocoles ont permis d'induire rapidement tous les castors à un niveau d'anesthésie adéquat pour une procédure minimalement invasive de courte durée. Les durées d'immobilité variaient de 15 à 35 minutes et n'étaient pas significativement différentes entre les protocoles ($P = 0{,}64$). Les phases de récupération, après l'administration IM de 0,2 mg/kg d'atipamézole 30 à 65 minutes après l'induction, étaient généralement plus rapides avec le protocole xylazine:kétamine à un ratio de 3:10, mais cela n'était pas statistiquement significatif ($P = 0{,}40$). Les fréquences cardiaques étaient significativement plus basses avec le protocole xylazine:kétamine à un ratio de 3:10 ($P = 0{,}0002$). Les valeurs de $P_{ET}CO_2$, mesurées avec une canule nasale, étaient similaires entre les protocoles et suggéraient une hypoventilation. Malgré le fait que le protocole xylazine:kétamine à un ratio de 3:10 était associé à une dépression cardiaque plus importante, le temps de récupération apparemment plus rapide, même si ce n'était pas statistiquement significatif, avec ce protocole est définitivement un atout pour les projets se déroulant dans des endroits éloignés accessibles uniquement par hélicoptère.

(Traduit par les auteurs)

Centre québécois sur la santé des animaux sauvages/Canadian Wildlife Health Cooperative, Faculté de médecine vétérinaire, Université de Montréal, 3200 rue Sicotte, Saint-Hyacinthe, Québec J2S 7C6, Canada (Lair); Service canadien de la faune/Canadian Wildlife Service — Québec Region, Environment and Climate Change Canada/Government of Canada, 801–1550, avenue D'Estimauville, Québec, Québec G1J 0C3, Canada (Bourguelat); Service de la gestion des espèces et des habitats terrestres, Direction générale de la gestion de la faune et des habitats, Ministère de l'Environnement de la Lutte contre les changements climatiques, de la Faune et des Parcs, 880, chemin Sainte-Foy, 2e étage, Québec, Québec G1S 4X4, Canada (Fournier).

Address all correspondence to Dr. Stéphane Lair; telephone: (514) 343-6111, ext. 8667; email: stephane.lair@umontreal.ca

Received November 26, 2022. Accepted January 29, 2023.

FOR PERSONAL USE ONLY

Introduction

Due to the high demand for its pelt, the North American beaver *(Castor canadensis)*, a key species in the Canadian boreal ecosystem, had been a driving factor in the early establishment of European settlements in North America (1). This Canadian iconic species is also a strong cultural and spiritual figure for members of the North American First Nations and remains a source of revenue for trappers (1,2).

Research and management activities on this large semi-aquatic rodent often involve procedures that require chemical immobilization (3). Different protocols to anesthetize beavers in field settings involving either injectable drugs (4–10), or volatile anesthetics (11), have been described over the last 40 y. The choice of protocol is guided by the invasiveness and length of the procedure performed, and by logistical and economic factors. Protocols allowing for fast recovery and that do not require bulky equipment are preferred for projects taking place in locations only accessible by helicopter.

Anesthetic protocols combining IM injection of ketamine with α-2 adrenergic receptor agonists often meet the above criteria and are frequently used in wild mammals including rodents (12–14). The reversibility of the α-2 adrenergic receptor agonists represents a significant advantage for field procedures for which short recovery times are critical (13). The dosage regimens proposed usually involve a ketamine:α-2 adrenergic ratio which facilitates the use of this combination of drugs in the field since it is possible to premix the drugs together in a single vial.

The goal of this project was to recommend an anesthetic protocol that could be used in free-ranging beavers in remote locations only accessible by helicopter. Based on personal experience with beaver anesthesia in captive settings, it was decided to use a combination of xylazine and ketamine. This combination of drugs has been previously described in free-ranging beavers, but the exact dosage ratio used, and the details of the procedures were not described, and no attempts were made to antagonize the xylazine (7).

The primary objective of the current study was to evaluate and compare 2 dosage regimens of xylazine and ketamine followed by reversal with atipamezole for short-term anesthesia of beavers requiring telemetric implantation in a remote setting. A secondary objective was to evaluate the usefulness of metabolic scaling and its application in extrapolating dosages to fit a wide range of body masses observed in this species. Our hypothesis was that dosage regimens based on metabolic scaling instead of body mass would result in homogenous anesthetic effects for the protocols used in this study.

Materials and methods

This study was performed during a field project on post-translocation survival and dispersal of beavers in the Northern part of the boreal forest. These animals were translocated to adjacent territories from an area designated to be flooded following the development of a hydroelectric power plant reservoir. All procedures were approved by the Faculté de médecine vétérinaire Animal Care and Use Committee, which operates under the auspices of the Canadian Council on Animal Care (project number 03-00-13).

Twenty-two beavers ranging in weight from 2.5 to 18.5 kg were live captured in August 2003 near Eastmain River, James Bay, Québec, Canada (between N52°10′ W76°05′ and N52°11′ W74°38′, altitude ~300 m) (Table I). These beavers were captured using either Hancock traps (Fil-Brown, Sherbrooke, Québec J1L 1M9, Canada) or Ezee Set Live Catch Beaver traps (Les Entreprises Makwa, Wendake, Québec G0A 4V0, Canada) baited with scent lures containing beaver glands extracts and essential oils. Traps were visually inspected daily, within 24 h of their deployments. Following capture, the trap was covered with a thin fabric to minimize visual stress. Tentative weights were obtained on captured animals while still confined to the previously weighed traps. These weights were used to determine the volume to be injected. Anesthetized beavers were re-weighed to obtain accurate weights, which were retrospectively used to calculate the mg/kg of ketamine and xylazine given.

Two different mixtures of xylazine/ketamine were tested. The first mixture (1:10 xylazine:ketamine ratio) was obtained by mixing 2 mL of xylazine hydrochloride (Rompun, 100 mg/mL; Bayer, Toronto, Ontario) with 20 mL of ketamine hydrochloride (Vetalar, 100 mg/mL; Bioniche Animal Health Canada, Belleville, Ontario), rendering final concentrations in solution of 9.1 mg/mL of xylazine and 91 mg/mL of ketamine. For the second mixture (3:10 xylazine:ketamine ratio), 3.96 mL of 100 mg/mL xylazine, 13.2 mL of 100 mg/mL ketamine and 4.84 mL of sterile water were mixed to obtain a final solution of 18 mg/mL of xylazine and 60 mg/mL of ketamine.

Beavers were assigned sequentially to each protocol following control for age group. Each animal was assigned to 1 of the following age classes based on body mass: 0- to 12-month-old kits (< 6.8 kg), 13 to 24 month-old yearlings (6.8 to 10.8 kg), 25 to 36 month-old subadults (10.9 to 16.0 kg), and ≥ 37 month-old adults (> 16 kg) (15).

Eleven of the captured beavers received the 1:10 xylazine:ketamine protocols. The dosage to be given to each animal was calculated using metabolic scaling. Based on clinical experience, the reference dose was set to a total of 7.5 mg of xylazine and 75 mg of ketamine for a 5 kg beaver (equivalent to 1.5 mg/kg of xylazine and 15 mg/kg of ketamine). This reference dose was then transformed to a mg/kcal dosage by dividing the total dose by the theoretical minimum energy cost of a 5 kg beaver using the following equation (16):

$$MEC = 70\ (M)^{0.75}$$

where: MEC is the minimal energy cost in kcal for a 24-hour period, and M is the tentative weight of the animal in kg. The total dose to be administered to each animal was then calculated by multiplying the MEC of each beaver by the mg/kcal dosages obtained (0.032 mg/kcal of xylazine and 0.320 mg/kcal of ketamine). The 3:10 xylazine:ketamine protocol was used on the second group of 11 beavers. For this group, the reference dose for a 5 kg beaver was set to 15 mg of xylazine and 50 mg of ketamine (3 mg/kg of xylazine and 10 mg/kg of ketamine), which is equivalent to a dosage of 0.064 mg/kcal of xylazine and 0.213 mg/kcal of ketamine. Similarly, total doses to be administered were calculated for each beaver by multiplying their MEC by the mg/kcal dosages. Assessors were blinded to the anesthetic mixture received by each animal.

Drug mixtures were injected IM in the epaxial muscles using a 21G butterfly needle. The volume injected ranged from 0.49 to 2.30 mL. This injection was easily given without restraint while

FOR PERSONAL USE ONLY

Table I. Demographic data (sex and age class), weights, and calculated anesthetic dosages received of 22 beavers *(Castor canadensis)* anesthetized using 2 different ratios of xylazine:ketamine combination, a 1:10 xylazine:ketamine ratio containing 9.1 mg/mL of xylazine and 91 mg/mL of ketamine, and a 3:10 xylazine:ketamine ratio containing 18 mg/mL of xylazine and 60 mg/mL of ketamine.

				Protocol used				
					Xylazine		Ketamine	
Beaver #	Sex	Age class[a]	Weight (kg)	Ratio	mg/kg	mg/kcal	mg/kg	mg/kcal
1	Male	Subadult	12.5	1:10	1.2	0.03	12	0.32
3	Male	Yearling	9.5	1:10	1.3	0.03	13.4	0.34
5[b]	Male	Kit	3.4	1:10	2.3	0.04	22.5	0.44
7	Male	Kit	2.8	1:10	1.7	0.03	16.5	0.30
9	Male	Kit	3.9	1:10	1.2	0.02	11.7	0.23
11	Male	Yearling	8.1	1:10	1.4	0.03	13.6	0.33
12	Male	Subadult	12.5	1:10	1.2	0.03	11.6	0.31
14	Female	Subadult	13	1:10	1.1	0.03	11.2	0.30
16	Male	Adult	18.5	1:10	1.1	0.03	10.8	0.32
19	Female	Adult	18.5	1:10	1.1	0.03	11.3	0.33
22	Female	Kit	4.1	1:10	1.7	0.03	17.1	0.35
2	Male	Yearling	9.5	3:10	2.7	0.07	8.8	0.22
4	Female	Subadult	13	3:10	2.2	0.06	7.4	0.20
6	Female	Adult	17	3:10	2.1	0.06	7.1	0.20
8	Female	Kit	2.9	3:10	3.1	0.06	10.3	0.19
10	Male	Yearling	7.7	3:10	2.8	0.07	9.4	0.22
13	Male	Kit	2.5	3:10	3.7	0.07	12.2	0.22
15	Male	Adult	18.5	3:10	2	0.06	6.8	0.20
17	Female	Kit	2.5	3:10	3.5	0.06	11.8	0.21
18	Female	Adult	18.5	3:10	2.1	0.06	7.1	0.21
20	Male	Subadult	16	3:10	2.4	0.07	7.9	0.23
21	Male	Kit	4.3	3:10	3.2	0.07	10.7	0.22

[a] 0- to 12-month-old kits ($<$ 6.8 kg), 13- to 24-month-old yearlings (6.8 to 10.8 kg), 25- to 36-month-old subadults (10.9 to 16.0 kg), and $\geq$ 37 month-old adults ($>$ 16 kg) (21).

[b] The weight of this individual could not be determined accurately prior to the anesthesia and was overestimated.

maintaining the fabric over the trap. Once the relaxed animal showed no reactivity to tactile stimulations, the beaver was removed from the trap and placed in sternal recumbency. A physical examination, including thoracic auscultation, was performed. Morphometric measurements were taken, and sex was determined by palpation for a bacula (17). Subsequently, a radio transmitter was fixed to the tail using a technique previously described (3). Briefly, the anchoring site on the tail was transmurally infiltrated with 0.3 mL of Bupivacaine 0.5% (Marcaïne; Abbott Laboratories, St. Laurent, Québec). A 5-mm diameter hole was then drilled into the skin, connective and adipose tissues of the tail using a sterilized bit. The radio transmitter (Modèle: M3530. Advanced Telemetry System; Isanti, Minnesota, USA), which is fixed on a modified livestock ear tag, was then anchored to the tail.

Heart rates, respiratory rates, oxygen saturation, and end-tidal partial pressure of carbon dioxide ($P_{ET}CO_2$) were recorded every 5 min during the procedure using a combination of side-stream end-tidal CO_2 analyzer and pulse oximeter (NPB-75; Nellcor Puritan Bennett, Pleasanton, California, USA). The $P_{ET}CO_2$ sensor was connected to a nasal cannula and the SpO_2 probe placed on the tongue. Cloacal temperature was taken opportunistically with a pediatric digital thermometer.

Following completion of the procedure, the xylazine was antagonized with 0.2 mg/kg of atipamezole (Antisedan 5 mg/mL; Novartis Santé Animale Canada, Mississauga, Ontario) IM. The animals were then transferred to a fully covered Havahart cage (Woodstream Corporation, Lancaster, Pennsylvania, USA) and transported to a retention pen at relocation sites by helicopter.

The following time periods were recorded during the anesthesia:

- induction time, defined as the time from the xylazine:ketamine injection to the absence of reaction to tactile stimuli;
- duration of immobility, defined as the time from the absence of reaction to tactile stimuli to the return of movement;
- recovery time, defined as the time from the injection of the reversal (atipamezole) to a level of alertness and coordination judged by 1 observer (SL) to enable a safe release.

Total anesthesia duration was defined as the time from the xylazine:ketamine injection to a level of alertness and coordination sufficient to allow a safe release.

Analysis of covariance (ANCOVA), with protocol as the independent variable, body mass as a cofactor and the interaction between protocol and body mass, was used to examine the relationship between treatment and various time periods and cardiorespiratory

FOR PERSONAL USE ONLY

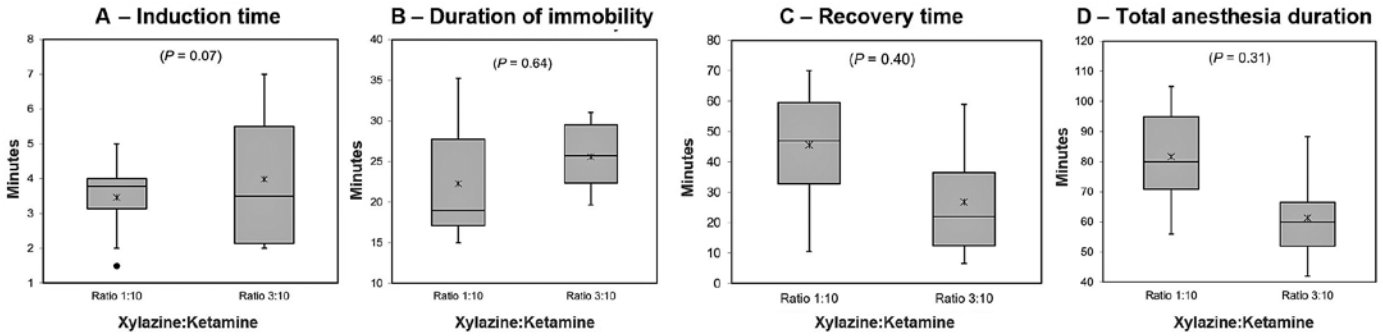


Figure 1. Anesthesia of 22 beavers *(Castor canadensis)* using 2 mixtures of xylazine:ketamine. Plots comparing the 1:10 and the 3:10 xylazine:ketamine ratio protocols for the induction time (A), the duration of immobility (B), the recovery time (C), and the total anesthesia duration (D). Horizontal lines in the boxes represent median values, boxes represent percentiles 25 to 75%, whiskers indicate the lowest and highest data within 1.5 percentiles 25 to 75%, asterisks are the mean and points represent mild outliers. *P*-values are presented for each comparison on the graph (*P*-value of < 0.05 was considered statistically significant).

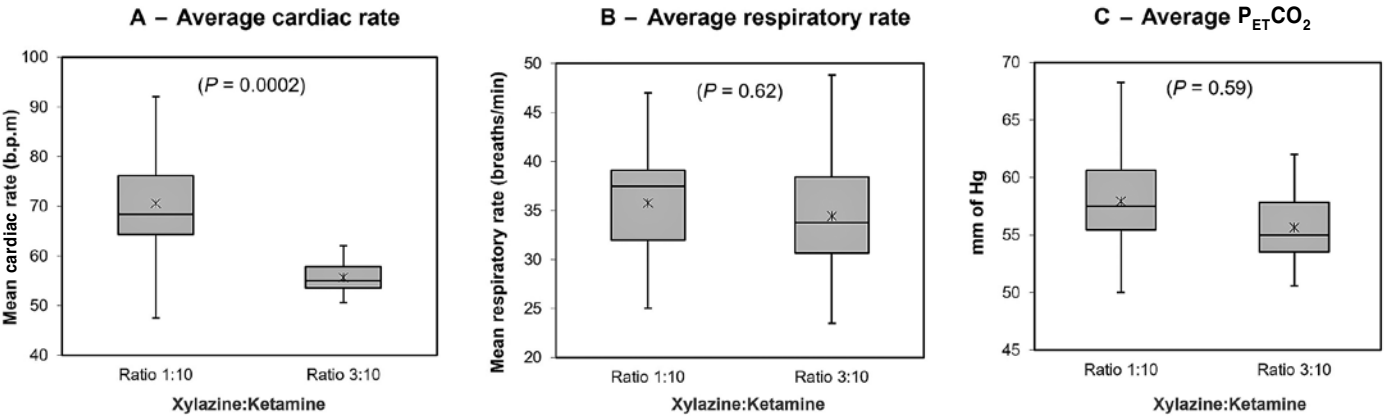


Figure 2. Monitoring during anesthesia of 22 beavers *(Castor canadensis)* using 2 mixtures of xylazine:ketamine. Plots comparing the 1:10 and the 3:10 xylazine:ketamine ratio protocols for average heart rate (A), average respiratory rate (B), and average $P_{ET}CO_2$ (C). Horizontal lines in the boxes represent median values, boxes represent percentiles 25 to 75%, whiskers indicate the lowest and highest data within 1.5 percentiles 25 to 75%, asterisks are the mean and points represent mild outliers. *P*-values are presented for each comparison on the graph (*P*-value of < 0.05 was considered statistically significant).

parameters controlling for age. Statistical analyses were carried out with SAS v. 9.2 (SAS Institute, Cary, North Carolina, USA). A *P*-value of < 0.05 was considered statistically significant.

Results

All captured beavers appeared to be in good physical health. Tentative weights were obtained prior to the induction on all but 1 beaver (#5). The median weight (9.5 kg) was the same in both groups. The 1:10 xylazine:ketamine group was composed of 4 kits, 2 yearlings, 3 subadults, and 2 adults, whereas the 3:10 xylazine:ketamine group included 4 kits, 2 yearlings, 2 subadults, and 3 adults. The following ranges of dosages were used:

- for the 1:10 xylazine:ketamine group: 1.08 to 2.25 mg/kg (median = 1.2 mg/kg, mean = 1.4 mg/kg) mg/kg of xylazine + 10.8 to 22.5 mg/kg (median = 12 mg/kg, mean = 13.8 mg/kg) of ketamine IM, and
- for the 3:10 xylazine:ketamine group: 2.04 to 3.67 mg/kg (median and mean = 2.7 mg/kg) of xylazine + 6.81 to 12.25 mg/kg (median = 8.8 mg/kg, mean = 9.1 mg/kg) of ketamine IM.

All the beavers survived the procedures and recovered well. The level of anesthesia was sufficient for the handling and minor surgical procedure and the recoveries were uneventful. Induction was smooth and varied in time from 1.5 to 5.0 min [mean = 3.5 min (± 1.0 min)] and 2.0 to 7.0 min [mean = 4.0 min (± 2.0 min)] for the 1:10 and 3:10 xylazine:ketamine protocols, respectively. A greater variability in induction time was present with the 3:10 xylazine:ketamine protocol (Figure 1 A), but no significant difference in induction time was detected between the 2 protocols ($P = 0.07$). A significant association was observed between induction times and body mass, induction being usually faster in small beavers than for large ones in both protocols ($P < 0.0001$). This association between body mass and induction time was greater for the 3:10 xylazine:ketamine protocol than for the 1:10 xylazine:ketamine protocols ($P = 0.008$). The actual hands-on procedures (physical examination, sex determination, morphologic measurements, and tail-mounted radio transmitter placement) lasted from 9.0 to 22.0 min [mean = 14.0 min (± 3.5 min)] and 11.0 to 22.0 [mean = 16.7 min (± 3.5 min)] for the 1:10 and 3:10 xylazine:ketamine protocols, respectively. Immobility lasted from 15.0 to 35.2 min [mean: 22.3 min (± 7.0 min)] and 19.7 to 31.0

FOR PERSONAL USE ONLY

[mean = 25.6 min (± 4.1 min)] for the 1:10 and 3:10 xylazine:ketamine protocols, respectively (Figure 1 B). Statistically significant differences were not detected between the 2 protocols ($P = 0.64$), and there were no significant associations between immobility duration and the body mass ($P = 0.15$). Xylazine was antagonized [30.0 to 65.2 min mean = 36.1 min (± 12.7 min)] and 30.0 to 56.4 [mean = 34.5 min (± 9.3 min)] post-induction for the 1:10 and 3:10 xylazine:ketamine protocols, respectively. Recovery time after the reversal with atipamezole ranged from 10.6 to 70.0 min [mean = 45.6 min (± 18.7 min) in the 1:10 xylazine:ketamine group and from 6.6 to 59.0 min [mean = 26.9 min (± 17.3 min)] in the 3:10 xylazine:ketamine group. Beavers in the 3:10 xylazine:ketamine group recovered, on average, approximately 2 times faster than beavers in the 1:10 xylazine:ketamine group (Figure 1 C). However, this difference was not statistically significant ($P = 0.40$). Recovery time was not associated with body mass ($P = 0.54$). A moderate level of excitement following the injection of atipamezole was seen in 2 of the beavers from the 1:10 xylazine:ketamine group. Total anesthesia duration was, on average, 25% shorter for beavers from the 3:10 xylazine:ketamine protocol group, ranging from 42.0 to 89.0 min [mean = 61.4 min (± 14.3 min)], compared to the 1:10 xylazine:ketamine protocol group, ranging from 56.0 to 105.0 min [mean = 81.6 min (± 16.6 min)] (Figure 1 D). However, this difference was not statistically significant ($P = 0.31$).

Both anesthetic protocols were associated with a progressive decline in heart rates. Mean heart rates of beavers in the 3:10 xylazine:ketamine group (56 bpm) were significantly lower than those evaluated for the 1:10 xylazine:ketamine group (71 bpm) ($P = 0.0002$) (Figure 2 A). No statistical differences were seen between groups upon investigation of the average respiratory rates ($P = 0.62$), which were 36 and 34 for the 1:10 xylazine:ketamine group and the 3:10 xylazine:ketamine group, respectively (Figure 2 B). Elevated $P_{ET}CO_2$ was recorded during the anesthesia of all 22 beavers with averages of 58 and 56 mmHg for the 1:10 xylazine:ketamine group and the 3:10 xylazine:ketamine group, respectively (Figure 2 C). No statistical difference was detected between the groups for the average $P_{ET}CO_2$ ($P = 0.59$) and no association between the level of $P_{ET}CO_2$ measured and the body mass was identified ($P = 0.95$). Inconsistent measurements obtained with the pulse oximeter; they ranged from 40 to 95% and could be obtained in only 15 of the animals. Cloacal temperatures measured varied from 32.5 to 39.4°C and neither decreased over time, nor differed between the 2 groups ($P > 0.05$).

Discussion

Both protocols used in this study were associated with eventless relatively predictable anesthesia characterized by smooth and rapid inductions, stable levels of anesthesia and, in almost all cases, calm recoveries. The depth of anesthesia was sufficient for the minimally invasive procedures performed but would not have been adequate for invasive surgical procedures such as an intra-abdominal implantation of radio-transmitters. Since clinical experience has shown that dosages for most injectable anesthetic agents are not directly (linearly) proportional to the body mass of the subjects (18), it would have been unsound to use the same dosages of ketamine/xylazine in a group of beavers having such a wide range of weights. Therefore, instead of using the standard mg/kg dosage regime, the individual doses were calculated on a kcal basis. Although the metabolic scaling of drugs is controversial and has not been validated for xylazine or ketamine, this approach could be more appropriate in beavers because it is a better reflection of the relationship between drug potency and body mass than the extrapolation of a single mg/kg dosage to be used on all subjects (18). Interestingly, apart from the induction time, the weight of the animals had no influence on the different anesthetic parameters measured. This suggests, at least in this study, that the xylazine:ketamine dosages derived from metabolic scaling had similar effects when applied to a wide range of weights in beavers. Therefore, metabolic scaling seems to be a useful tool for determining dosage regimens in beaver and might also be of interest for other species with a wide range of weight.

The 2 different xylazine:ketamine ratios provided comparable induction time and duration of immobility. Recovery was usually slower in the group having received the higher ketamine dosage (median dosage of 12 mg/kg for the 1:10 ratio group compared to 8.8 mg/kg for the 3:10 ratio group), which is expected since ketamine is not antagonizable. The absence of statistical significance for this parameter might be due to the small sampling size. The faster recovery in the 3:10 xylazine:ketamine group is a definitive advantage when working in remote settings and needing costly helicopter support.

The levels of $P_{ET}CO_2$ measured using a nasal cannula were elevated compared to the 30 to 40 mmHg that would be expected in a well-ventilated mammal (19). If the assumption that the relationship between the P_aCO_2 and the $P_{ET}CO_2$ measured by means of a nasal cannula in beavers is comparable to what has been described in dogs is made (20), the results obtained herein would indicate that both protocols were associated with hypercapnia. This hypercapnic state is a common manifestation in animals anesthetized with respiratory depressants such as xylazine and ketamine (21). Measurements of the SpO_2 with the sensor clip were inconsistent and poorly repeatable, likely due to the pigmented extremities, and small poorly mobile fleshy tongue. The low reading values of SpO_2 could also reflect true hypoxemia, which likely occurred given the cardiorespiratory depressant effect of the drug combinations used.

With a few exceptions, the cloacal temperatures measured were lower than what should be expected in a mammal. This suggests that the temperature measured in the cloaca is an underestimation of the body temperature in this species. Nevertheless, if we assumed that the cloacal temperature is correlated to the core body temperature, the absence of decrease in temperature during the procedures suggests that the protocols used were not associated with overt hypothermia. Except for one animal, in which the cloacal temperature rose from 36.8 to 39.4°C, no sign of hyperthermia was documented.

The health implication of cardiorespiratory depression is difficult to quantify. The short anesthetic duration possibly minimized overt complications related to observed physiologic changes (hypoxemia, hypercapnia, bradycardia), but animals were not available for long-term follow-up. Based on these and previous results and given the challenges of intubation and manual ventilation in field conditions, supplemental oxygen *via* facemask or nasal canula is strongly recommended for such field anesthesia to minimize the risks of hypoxemic events. When the use of pressurized oxygen cylinders in the field is

FOR PERSONAL USE ONLY

not practical, portable oxygen concentrators should be considered. In addition, the monitoring of blood gases during the anesthesia should also be considered to assess the physiological effects of hypoventilation and to document the relationship between $PaCO_2$ and $P_{ET}CO_2$ in an obligate nasal breather like the beavers.

The dosages of xylazine and ketamine used for yearlings and subadults with the 1:10 xylazine:ketamine protocol (xylazine 1.12 to 1.36 mg/kg + ketamine 11.2 to 13.6 mg/kg) are in the higher range of dosages that have been previously reported for the same age classes (xylazine 0 to 1.25 mg/kg + ketamine 6 to 12 mg/kg) (7), whereas the dosages of ketamine used in the 3:10 ratio protocol (ketamine 7.4 to 9.3 mg/kg) are similar, but with a higher dosage of xylazine (xylazine 2.2 to 2.8 mg/kg). The most reported injectable anesthetic protocol for free-ranging beavers is a combination of ketamine (10 to 13 mg/kg) and acepromazine (2.5 mg) (4,5,6,10). Koenen *et al* (5) reported a mean total anesthesia duration (from induction to full recovery) of 94 min with such a combination, which is a few minutes longer than the mean total anesthesia duration of the 1:10 xylazine:ketamine protocol (82 min) and approximately 50% longer than the 3:10 xylazine:ketamine protocol (61 min).

A combination of nalbuphine-medetomidine-azaperone (8), and of butorphanol-azaperone-medetomidine (9) have been tried in American beavers for tail transmitter placement, but the level of sedation achieved was insufficient in a large proportion of animals and required supplemental isoflurane.

Field anesthesia for surgical implantation of abdominal transmitters, using medetomidine, ketamine, butorphanol, and midazolam, has been reported in European beavers *(Castor fiber)* (22). Reported induction times and bradycardia were similar to what was observed in the present study.

Other successful anesthetic protocols described for beavers, either by combining injectable drugs (mainly ketamine) and volatile agents (halothane, isoflurane, or sevoflurane), or by isoflurane or sevoflurane induction and maintenance, have been described in both free-ranging and/or captive settings (11,23–25). The main advantages in using gaseous anesthesia include the possibility to rapidly adjust anesthetic levels and to deliver supplemental oxygen to alleviate hypoxemia resulting from hypoventilation (11,23). Beavers induced and maintained with isoflurane or sevoflurane displayed a decrease in heart rate comparable to that observed in the current study (11). Although SpO_2 was maintained within normal levels in that study with oxygen being supplemented through the anesthetic carrying gas, the high $PaCO_2$ measured were also indicative of hypercapnia (11).

In conclusion, both protocols described in this study rapidly induced levels of anesthesia adequate for minimally invasive procedures of short duration in beavers of various weights, in remote settings. Oxygen supplementation is highly recommended since both protocols were associated with hypoventilation. Even if statistical significance could not be demonstrated, the mixture containing a 3:10 xylazine:ketamine ratio at the dosage used appears to have a shorter recovery time and was characterized by less agitation compared to the 1:10 xylazine:ketamine protocol. This, therefore, is the protocol recommended for the anesthesia of beavers requiring minimally invasive procedures, especially in remote settings. Nevertheless, it is recommended that a protocol with the same dosage of ketamine with a lower dosage of xylazine be evaluated.

Acknowledgments

The authors thank George Coonishish and Matthew Wapachee (Cree trappers) and Joël Poirier (Wildlife Technician) for their help with the field work, as well as Guy Beauchamp for his statistical analysis and Pauline Delnatte for her help with manuscript preparation. This study was financially supported by the Société d'énergie de la Baie James (Eastmain-1 project).

References

1. Müller-Schwarze D, Sun L. The Beaver: Natural History of a Wetlands Engineer. Ithaca, New York: Cornell University Press, 2003.
2. Canac-Marquis P. Données sur l'exploitation commerciale des animaux à fourrure sauvages au Québec de 1917 à 1993. Quebec City, Québec: Ministère de l'Environnement et de la Faune. Direction de la faune et des habitats, 1995.
3. Baker BW. Efficacy of tail-mounted transmitters for beaver. Wildl Soc Bull 2006;34:218–222.
4. Davis JR, Andreas FV, Smith DD, Guynn DC, Jr. Implantable telemetry in beaver. Wildl Soc Bull 1984;12:322–324.
5. Koenen K, DeStefano S, Henner C, Beroldi T. Capturing beavers in box traps. Wildl Soc Bull 2009;33:1153–1159.
6. Lancia RA, Brooks RP, Fleming MW. Ketamine hydrochloride as an immobilant and anesthetic for beaver. J Wildl Manage 1978; 42:946–948.
7. McNew LB, Woolf A. Dispersal and survival of juvenile beavers *(Castor canadensis)* in southern Illinois. Am Midl Nat 2005;154: 217–228.
8. Roug A, Lance W, Vroom T, Gardner R, DeBloois D, Talley H. Immobilization of American beaver *(Castor canadensis)* with nalbuphine, medetomidine, and azaperone. J Wildl Dis 2019;55: 699–703.
9. Roug A, Talley H, Davis T, Roueche M, DeBloois D. A mixture of butorphanol, azaperone, and medetomidine for the immobilization of American beavers *(Castor canadensis)*. J Wildl Dis 2018;54:617–621.
10. Wheatley M. A new surgical technique for implanting radio transmitters in beavers, *Castor canadensis.* Can Field-Nat 1997; 111:601–606.
11. Breck SW, Gaynor JS. Comparison of isoflurane and sevoflurane for anesthesia in beaver. J Wildl Dis 2003;39:387–392.
12. Heard D. Rodents. In: West G, Heard D, Caulkett N, eds. Zoo Animal & Wildlife Immobilization and Anesthesia. Ames, Iowa: Blackwell Publishing, 2007:655–663.
13. Klein LV, Klide AM. Central alpha2-adrenergic and benzodiazepine agonists and their antagonists. J Zoo Wildl Med 1988; 20:138–153.
14. Kreeger TJ, Arnemo JM, Raath JP. Handbook of Wildlife Chemical Immobilization, International Edition. Fort Collins, Colorado: Wildlife Pharmaceuticals, 2002.
15. Patric EF, Webb WL. An evaluation of three age determination criteria in live beavers. J Wildl Manage 1960;24:37–44.
16. Sedgwick CJ. Allometric scaling and emergency care: The importance of body size. In: Fowler ME, ed. Zoo & Wildlife

FOR PERSONAL USE ONLY

Medicine — Current Therapy 3. Philadelphia, Pennsylvania: WB Saunders, 1993:34–37.
17. Osborn DJ. Techniques for sexing beaver. J Mammal 1955;36: 141–142.
18. Hunter RP, Isaza R. Concepts and issues with interspecies scaling in zoological pharmacology. J Zoo Wildl Med 2008;39:517–526.
19. Cornick-Seahorn JL. Veterinary Anesthesia. Woburn, Massachusetts: Elsevier Health Sciences, 2000.
20. Pang D, Hethey J, Caulkett NA, Duke T. Partial pressure of end-tidal CO_2 sampled via an intranasal catheter as a substitute for partial pressure of arterial CO_2 in dogs. J Vet Emerg Crit Care 2007;17:143–148.
21. Grimm KA, Lamon LA. Clinical pharmacology. In: West G, Heard D, Caulkett N, eds. Zoo Animal & Wildlife Immobilization and Anesthesia. Ames, Iowa: Blackwell Publishing, 2007:3–36.
22. Ranheim B, Rosell F, Haga HA, Arnemo JM. Field anaesthetic and surgical techniques for implantation of intraperitoneal radio transmitters in Eurasian beavers *Castor fiber*. Wildlife Biol 2004;10:11–15.
23. Eisele PH, Faith TL, Menth PM, Parker JC, Van Wren DH. Ketamine-isoflurane combination anesthesia for surgical implantation of intraperitoneal radio transmitters in the beaver. Contemp Top Lab Anim Sci 1997;36:97–99.
24. Greene SA, Keegan RD, Gallagher LV, Alexander JE, Harari J. Cardiovascular effects of halothane anesthesia after diazepam and ketamine administration in beavers *(Castor canadensis)* during spontaneous or controlled ventilation. Am J Vet Res 1991; 52:665–668.
25. Patenaude RP, Genest FB. The hematology and chromosomes of the canadian beaver *(Castor canadensis)*. J Zoo Anim Med 1977;8:6–9.

FOR PERSONAL USE ONLY

mRNA expression of immune factors by milk somatic cells from healthy Holstein lactating cows

Kenji Murakami, Tomochika Fukuhara, Shunsuke Kure, Takaaki Shimosakai, Ayano Sato, Ryo Murata, Keigo Kosenda, Hiromichi Ohtsuka

Abstract

This study investigated the mRNA of immune factors expressed by milk somatic cells from 72 healthy lactating Holstein cows on 1 farm. Milk samples were collected aseptically from the right front mammary gland before milking. The milk samples that had a negative reaction to the California mastitis test were used to analyze the mRNA of immune factors. Cows were divided into 2 groups based on the detection of bacteria in milk samples: positive group (n = 22 cows), which showed bacteria in cultures, and negative group (n = 50 cows), which did not show bacteria in cultures. There were significant positive correlations among the relative mRNA levels of interleukin (IL)-6, IL-8, arginase 1, chemokine (C-C motif) ligand (CCL) 1, and chemokine (C-X-C motif) ligand (CXCL) 13, as well as among the relative mRNA levels of IL-10, pentraxin 3, CCL5, and CCL14. Significantly high levels of IL-1β, IL-6, IL-8, arginase 1, Batf, CCL1, CXCL14, and toll-like receptor 4 in the positive group were discovered compared to the negative group. These results suggest that the presence of bacteria in lactating healthy dairy cows may affect mRNA levels of inflammatory mediators expressed by somatic cells.

Résumé

Cette étude a examiné l'ARNm des facteurs immunitaires exprimés par les cellules somatiques du lait de 72 vaches Holstein en lactation en bonne santé dans une ferme. Des échantillons de lait ont été prélevés aseptiquement du quartier avant droit de la glande mammaire avant la traite. Les échantillons de lait ayant eu une réaction négative au test de mammite de Californie ont été utilisés pour analyser l'ARNm des facteurs immunitaires. Les vaches ont été divisées en deux groupes sur la base de la détection de bactéries dans les échantillons de lait : groupe positif (n = 22 vaches), qui a montré la présence de bactéries lors des cultures, et groupe négatif (n = 50 vaches), qui n'a pas montré de bactéries lors des cultures. Il y avait des corrélations positives significatives entre les niveaux relatifs d'ARNm de l'interleukine (IL)-6, de l'IL-8, de l'arginase 1, du ligand de chimiokine (motif C-C) (CCL) 1 et du ligand de chimiokine (motif C-X-C) (CXCL) 13, ainsi que parmi les niveaux relatifs d'ARNm d'IL-10, de pentraxine 3, de CCL5 et de CCL14. Des niveaux significativement élevés d'IL-1β, d'IL-6, d'IL-8, d'arginase 1, de Batf, de CCL1, de CXCL14 et de récepteur de type Toll 4 dans le groupe positif ont été découverts par rapport au groupe négatif. Ces résultats suggèrent que la présence de bactéries chez des vaches laitières saines en lactation peut affecter les niveaux d'ARNm des médiateurs inflammatoires exprimés par les cellules somatiques.

(Traduit par Docteur Serge Messier)

The mammary gland is a skin gland unique to the class Mammalia that is assumed to function as a part of the mucosal immune system against infection by pathogens. There are somatic cells in the milk of cows composed of various types of immune cells, such as macrophages, granulocytes, lymphocytes, and mammary epithelial cells. Neutrophils and macrophages participate directly in the clearance of invasive foreign pathogens and harmful endogenous materials in the mammary glands. A study demonstrated that neutrophils are involved in the activation, regulation, and effector functions of innate and adaptive immunity (1). Macrophages are the predominant cells in bovine milk during a healthy lactation period. Milk macrophages are important phagocytic cells; however, their phagocytic capacity is weaker compared with blood monocytes (2). Milk macrophages also participate in the functional regulation of T- and B-cells, as well as in the secretion of immunoregulatory factors. Thus, macrophages in bovine milk are likely to be more important as immune regulators than as phagocytic cells.

Upon pathogen detection, immune cells produce cytokines and chemokines, which recruit phagocytes to the site of infection and begin to recruit additional effector cells to enhance the immune response (3). After arriving in the vasculature near the site of inflammation, monocytes begin a process of rolling adhesion following a variety of chemokine gradients (4,5). In a severe infection, macrophages first exhibit the M1 phenotype to release inflammatory cytokines, such as tumor necrosis factor (TNF)-α, interleukin (IL)-1β, IL-6, and IL-8, upon stimulation. The M2 phenotype macrophages secrete IL-10 and transforming growth factor (TGF)-β to suppress inflammation and contribute to tissue repair. In a previous report on humans, although proinflammatory cytokines IL-1β, IL-6, and TNF-α were only seen in some of healthy mothers' milk samples, the

Federation of Agricultural Mutual Relief Association, Fukagawa, Hokkaido 073-0022, Japan (Murakami); School of Veterinary Medicine, Rakuno Gakuen University, Ebetsu, Hokkaido 069-8501, Japan (Fukuhara, Kure, Shimosakai, Sato, Murata, Kosenda, Ohtsuka).

Address all correspondence to Dr. Hiromichi Ohtsuka; telephone: +81-11-388-4787; email: ohtsuka@obihiro.ac.jp

Received May 5, 2022. Accepted September 25, 2022.

FOR PERSONAL USE ONLY

Table I. Primers used for real-time polymerase chain reaction.

Gene	Accession number	Product length	Primer designation	Sequence (5′-3′)
β-actin	NM_173979.3	76	Forward	CCCAGATCATGTTCGAGACC
			Reverse	GAGGCATACAGGGACAGCAC
IL-1β	NM_174093.1	85	Forward	CCTCCGACGAGTTTCTGTGT
			Reverse	GCCAGCACCAGGGATTTTTG
IL-6	NM_173923.2	102	Forward	AGATCCTGAAGCAAAAGATCGC
			Reverse	TTGCGTTCTTTACCCACTCGT
IL-8	NM_173925.2	150	Forward	GTGAAGAGAGCTGAGAAGCAAG
			Reverse	CACCAGACCCACACAGAACA
IL-10	NM_174088.1	150	Forward	TGTATCCACTTGCCAACCAG
			Reverse	ACCCAGGTAACCCTTAAAGTCA
TGF-β	NM_001166068.1	140	Forward	TGACCCGCAGAGAGGAAATAG
			Reverse	GTTCATGCCGTGAATGGTG
Arginase 1	NM_001046154.1	170	Forward	TATCAATTCCCTCTTGGTGTGAAAT
			Reverse	TGTTGGGGCTGATAAAAGTGTTT
Batf2	XM_005227105.4	106	Forward	TCACAATCTGCTCCTCCTTCTCC
			Reverse	CACTCCCAGCACTTAAACCTCTCA
PTX3	NM_001076259.2	86	Forward	GCCACAGGTCATGTTGTTCC
			Reverse	TCATCAAAGCCACCACCCAC
CCL1	XM_002695632.2	102	Forward	CCCTTGCTGTGAGGTCTGAG
			Reverse	GCGTCCACATCCTGTAACCA
CCL5	NM_175827.2	136	Forward	TTTGCCTATATCTCCCGCCC
			Reverse	ACTTCTTCTCTGGGTTGGCG
CCL14	NM_001110018.1	143	Forward	GCCACATCTAACATCCCTGCT
			Reverse	GCCAGGACCATCCATAGACA
CXCL13	NM_001015576.2	82	Forward	TCCACCTTGAGGCAGAATGAG
			Reverse	ATGGACAGGAGAGAGGCTGAA
TLR2	NM_174197.2	87	Forward	AAATTCTGCTGCGTTGGTTTG
			Reverse	CAGTGATTTGACCTCCACTCTCA
TLR4	NM_174198.6	143	Forward	CTTTCACAGAGCCACTTCTGG
			Reverse	GTTAGGAACAACCTGTACGCAAG

IL — Interleukin; TGF — Transforming growth factor; PTX — Pentraxin; CCL — Chemokine (C-C motif) ligand; CXCL — Chemokine (C-X-C motif) ligand; TLR — Toll-like receptor.

anti-inflammatory cytokine TGF-β was present in substantial quantities during 3 mo of lactation (6,7). But it is not known whether the M1 and M2 paradigm has different roles in the immune responses of lactating cows. The existence of non-pathogenic bacteria in human milk has been acknowledged (8). Similarly, microbiota have been reported in milk specimens from healthy cows (9). Although increased IL has been reported in somatic cells of cows with naturally occurring mastitis (10,11), little is known about the characteristics of immune factors, especially macrophage-related factors, in somatic cells, and their association with the presence of bacteria in normal milk from lactating dairy cows. The objective of this study was to investigate the association between bacteria and immune factors in normal milk. Seventy-two clinically healthy Holstein cows on 1 farm were used for this study. The cows were divided into 2 groups based on the detection of bacteria in culture: positive group (n = 22 animals), which showed bacterial growth, and negative group (n = 50 animals), which showed no bacterial growth. The parity and days after calving [reported as mean ± standard error of the mean (SEM)] were 3.45 ± 0.27 and 131.09 ± 19.77 d in the positive group and 3.28 ± 0.21 and 200.26 ± 20.40 d in the negative group, respectively. Milk samples (50 mL each) were collected aseptically from the teat cistern of the right front quarter using a cannula after disinfection of the teat end prior to the evening milking. We analyzed milk samples with negative California mastitis test (CMT) scores that

FOR PERSONAL USE ONLY

did not show signs of mastitis, such as flakes or clots. Samples were cultured for detecting bacteria and analyzed for mRNA of immune factors expressed by somatic cells. The procedures used in the present study were in accordance with the principles and guidelines for animal use set by the Animal Experiment and Care Committee of Rakuno Gakuen University, Ebetsu, Japan. The determination of somatic cell count (SCC), the isolation of total RNA molecules, and the real-time polymerase chain reaction (PCR) of milk cells were carried out using previously reported methods (12,13). Milk samples were centrifuged at 400 × *g* for 10 min at room temperature. After centrifugation, the supernatant was removed and sedimented milk somatic cells were washed twice by mixing with phosphate-buffered saline and centrifuged at 400 × *g* for 5 min. For total RNA isolation and cDNA synthesis, SuperPrep cell lysis & RT kit for qPCR (Toyobo, Osaka, Japan) was used. Each sample with 2×10^6 cells was mixed with 50 μL of cell lysis mixture (including gDNA remover) for 5 min before adding the stop solution. Then 8 μL each of mRNA solutions extracted from the 8 μL of RT Master Mix and 24 μL of nuclease-free water were added. cDNA was synthesized using PCR. Real-time PCR was conducted *via* the use of the SYBR Green master mix with ROX as a reference dye (THUNDERBIRD SYBR qPCR Mix, Toyobo) on an ABI prism 7300 Sequence Detector (Applied Biosystems, Waltham, Massachusetts, USA). Primers designed using the publicly available web-based Primer3 program are listed in Table I. The following genes were selected: β-actin, IL-1β, IL-6, IL-8, IL-10, TGF-β, arginase 1, Batf2, pentraxin (PTX) 3, chemokine (C-C motif) ligand (CCL) 1, CCL5, CCL14, chemokine (C-X-C motif) ligand (CXCL) 13, toll-like receptor (TLR) 2, and TLR4.

The cycle threshold (*i.e.,* Ct value) determined the number of cycles needed to detect amplified products and real-time PCR reactions were run in duplicate. The final quantification of mRNA of immune-related molecules was carried out using the comparative Ct method. This previously described method (14) was used after a validation experiment and demonstrated that the efficiencies of the target and reference genes were approximately equal. Expression levels were normalized to β-actin levels and reported as a relative fold difference compared to the calibrator, which was the lowest amount of mRNA for each target factor gene from all the samples. For detecting bacteria, milk samples were plated onto trypticase soy agar plates supplemented with 5% sheep blood. Plates were incubated aerobically in the presence of 5% CO_2 for 24 h or anaerobically in AnaeroPack (Mitsubishi Gas Chemical, Tokyo, Japan) for 48 h.

Statistical analysis

Correlations among genes in parameters of each 2 groups were analyzed using Spearman's rank correlation test. A statistical analysis was performed for each parameter using a Mann-Whitney U-test to determine the difference between 2 groups at the same sampling time. Data were expressed as mean ± SEM. All statistical analyses were conducted using Excel TOKEI. The differences were considered significant at $P < 0.05$. Among the Gram-positive bacteria isolated from the 22 milk samples from cows in the positive group, *Staphylococcus haemolyticus* ($n = 9$ samples) was the predominant coagulase-negative *Staphylococcus* species, followed by *S. chromogenes* ($n = 3$ samples) and *S. equorum* ($n = 1$ sample). *Staphylococcus aureus* was isolated from 1 milk sample. Of the 22 samples, 3 kinds of isolated bacteria were *Corynebacterium bovis C. freneyi,* and *C. xerosis* was 1 sample. Three of the 22 samples in this study contained *Corynebacterium* spp. (Table II). In the positive group, there was no significant correlation between colony-forming unit and immune factors or SCC.

Table II. Colony-forming unit (CFU) and somatic cell count (SCC) in the positive group.

Sample number	Bacteria	CFU (per mL)	SCC ($\times 10^3$/mL)
1	*Staphylococcus haemolyticus*	3680	1.1
2	*S. haemolyticus*	220	1.3
3	*S. haemolyticus*	120	1.1
4	*S. haemolyticus*	13 840	6
5	*S. haemolyticus*	3680	0.5
6	*S. haemolyticus*	480	6.5
7	*S. haemolyticus*	280	2
8	*S. haemolyticus*	900	2.4
9	*Staphylococcus chromogenes*	1200	30.9
10	*S. haemolyticus*	12 320	3.1
11	*S. chromogenes*	10 800	19.2
12	*S. chromogenes*	1280	9.6
13	*S. equorum*	100	0.9
14	*S. aureus*	1460	171.1
15	*Corynebacterium bovis*	1360	1.5
16	*C. bovis*	32 080	0.9
17	*C. bovis*	1720	2.3
18	*C. freneyi*	100	2.4
19	*C. xerosis*	100	3.4
20	*C.* spp.	180	3.1
21	*C.* spp.	740	4.3
22	*C.* spp.	1000	7.3

Correlations among all variables of immune factors are shown in Table III. There were positive correlations among the levels of IL-1β, IL-6, IL-8, arginase 1, Batf2 and PTX3, and CCL1 and CXCL13, in both groups. There was a significant correlation between IL-1β and TLR4 in the positive group. Results also included positive correlations among levels of IL-10, TGF-β, CCL5, CCL14, and TLR2 in both groups. In the negative group, significantly positive correlations among IL-6, IL-8 and TGF-β, and IL-10 and CCL14, as well as significantly negative correlations between TGF-β and Batf2, and PTX3 and CCL1, were detected. But there were no significant correlations among immune factors, SCC, parity, and days after calving (data not shown).The average values of immune factors and SCC in the milk from the 2 groups are shown in Table IV. We found significantly higher levels of IL-1β, IL-6, IL-8, arginase 1, Batf2, PTX3, CCL1, CXCL13, and TLR4 in the positive group compared to those in the negative group ($P < 0.05$). The other factors did not show significant differences between the 2 groups. This study observed positive correlations among levels of IL-1, IL-6, and IL-8 and significantly positive correlations between levels of IL-10 and TGF-β. In response to various stimulation, macrophages could be differentiated into distinct functional subsets, such as M1-type macrophages induced by Th1 cytokines (IL-6, IL-8, IFN-γ, and

Table III. Correlations among analytes in the positive (A) and negative (B) groups. Values were expressed as the correlation coefficient.

A) Positive groups	IL-1β	IL-6	IL-8	IL-10	TGF-β	Arginase 1	Batf2	PTX3	CCL1	CCL5	CCL14	CXCL13	TLR2	TLR4
IL-6	0.727*													
IL-8	0.886*	0.831*												
IL-10	−0.316	−0.272	−0.294											
TGF-β	−0.229	−0.451	−0.304	0.483*										
Arginase 1	0.750*	0.910*	0.867*	−0.289	−0.360									
Batf2	0.386	0.787*	0.555*	−0.386	−0.571*	0.670*								
PTX3	0.608*	0.909*	0.753*	−0.224	−0.414	0.874*	0.855*							
CCL1	0.448	0.781*	0.581*	−0.121	−0.417	0.724*	0.890*	0.879*						
CCL5	−0.401	−0.325	−0.487*	0.606*	0.694*	−0.378	−0.435	−0.354	−0.258					
CCL14	−0.312	−0.085	−0.252	0.363	0.444	−0.129	−0.075	−0.053	0.132	0.705*				
CXCL13	0.596*	0.809*	0.679*	−0.196	−0.334	0.809*	0.691*	0.916*	0.755*	−0.304	−0.134			
TLR2	−0.159	−0.234	−0.232	0.606*	0.743*	−0.149	−0.398	−0.256	−0.129	0.537*	0.422	−0.158		
TLR4	0.588*	0.248	0.423	0.019	0.330	0.309	0.099	0.198	0.186	0.047	−0.099	0.203	0.278	
SCC	0.153	0.282	0.243	−0.199	−0.216	0.167	0.381	0.277	0.144	−0.355	−0.345	0.196	−0.350	−0.113
B) Negative groups														
IL-6	0.512*													
IL-8	0.742*	0.689*												
IL-10	−0.246	−0.244	−0.388											
TGF-β	−0.375	−0.505*	−0.550*	0.513*										
Arginase 1	0.583*	0.891*	0.722*	−0.161	−0.438									
Batf2	0.481*	0.766*	0.605*	−0.184	−0.527*	0.751*								
PTX3	0.545*	0.852*	0.603*	−0.049	−0.461*	0.855*	0.854*							
CCL1	0.457	0.801*	0.571*	−0.168	−0.476*	0.777*	0.809*	0.818*						
CCL5	−0.189	−0.429	−0.486*	0.768*	0.627*	−0.355	−0.448	−0.285	−0.349					
CCL14	−0.177	−0.21	−0.426	0.732*	0.452	−0.193	−0.258	−0.107	−0.125	0.801*				
CXCL13	0.489*	0.714*	0.438	−0.222	−0.358	0.700*	0.649*	0.775*	0.757*	−0.270	−0.069			
TLR2	−0.334	−0.439	−0.584*	0.527*	0.835*	−0.380	−0.418	−0.342	−0.369	0.669*	0.465*	−0.238		
TLR4	0.256	0.242	0.380	0.237	−0.018	0.341	0.255	0.269	0.257	0.145	0.204	0.136	−0.033	
SCC	−0.184	−0.115	−0.003	−0.387	−0.083	−0.245	−0.040	−0.206	−0.141	−0.386	−0.521	−0.088	−0.215	−0.259

* Indicates a significant correlation ($P < 0.05$).

IL — Interleukin; TGF — Transforming growth factor; PTX — Pentraxin; CCL — Chemokine (C-C motif) ligand; CXCL — Chemokine (C-X-C motif) ligand; TLR — Toll-like receptor.

FOR PERSONAL USE ONLY

FOR PERSONAL USE ONLY

Table IV. mRNA expression of milk cell and somatic cell count (SCC). Results are expressed as the mean ± standard error of the mean.

	Positive group	Negative group
IL-1β	2.43 ± 0.13	1.99 ± 0.08*
IL-6	4.88 ± 0.25	4.07 ± 0.13*
IL-8	9.18 ± 0.23	8.32 ± 0.18*
IL-10	7.55 ± 0.52	6.93 ± 0.39
TGF-β	5.51 ± 0.50	5.22 ± 0.35
Arginase 1	6.51 ± 0.30	5.54 ± 0.20*
Batf2	3.30 ± 0.21	2.69 ± 0.11*
PTX3	3.42 ± 0.26	2.78 ± 0.11*
CCL1	3.33 ± 0.25	2.64 ± 0.11*
CCL5	7.33 ± 0.66	7.07 ± 0.37
CCL14	5.15 ± 0.38	4.80 ± 0.26
CXCL13	3.62 ± 0.30	2.82 ± 0.13*
TLR2	4.50 ± 0.34	4.32 ± 0.25
TLR4	5.06 ± 0.26	4.09 ± 0.18*
SCC	13.12 ± 7.40	7.67 ± 2.49

* Indicates a significant difference between 2 groups ($P < 0.05$).
IL — Interleukin; TGF — Transforming growth factor;
PTX — Pentraxin; CCL — Chemokine (C-C motif) ligand;
CXCL — Chemokine (C-X-C motif) ligand; TLR — Toll-like receptor.

TNF-α) and M2-type macrophages induced by Th2 cytokines (IL-4, IL-10, and TGF-β1) (15). Therefore, the results of this study suggest that the examined cytokines expressed by somatic cells are categorized as M1/Th1 or M2/Th2. Immune factors other than cytokines could be classified into 2 markers: M1/Th1-type (Batf2, PTX3, and CCL5) or M2/Th2-type (arginase 1, CCL1, CCL14, and CXCL13) in humans (16,17,18). In this study, we found positive correlations between arginase 1 and Batf2, PTX3, CCL1, and CXCL13, as well as among inflammatory cytokines, such as IL-1, IL-6, and IL-8. The expression of arginase 1, CCL1, and CXCL13 in somatic cells of cows was not in agreement with the previous study, since these mRNA expressions are related to M1/Th1-type markers. The peculiarity of phenotyping these immune factors of SCC in cows remains unknown. Rapid host defense initiated by signals transduced by TLRs induces the subsequent acquired immune responses that regulate the activation of T-cells and macrophages (19,20). Macrophages are categorized as M1 or M2, mirroring T-cell classification. The M1 macrophages express specific phenotype markers, including TLR2 and TLR4, and trigger inflammation or tissue damage (21). In this study, levels of TLR2 mRNA were correlated with IL-8, IL-10, TGF-β, CCL14, and CXCL13 and positive correlations between mRNA levels of TLR4 and IL-8 were seen. In particular, a strong positive correlation was determined between TLR2 and TGF-β. This result may indicate that TLR2 in somatic cells in cows is more likely associated with anti-inflammatory mediators in M2 phenotype macrophages through the Th2 pathway than through the Th1 inflammatory pathway. Generally, TLR2 is known as a sensor of immune cells for detecting Gram-positive bacterial cell wall components (22). It has been reported that TLR2 activation impairs anti-inflammatory activity of M2 macrophages (7), stimulation with IL-1β, TNF-α, or a TLR2-ligand stimulated IL-6, and IL-8 production, which was inhibited by TLR2 neutralizing antibodies against TLR2-ligand (23). In this study, the TLR2 level was correlated with TGF-β. It is possible that TLR2 in somatic cells does not always reflect the inflammatory response. However, it remains unclear whether TLR2 is related to anti-inflammatory mediators; thus, further research is needed.

We reported a significantly higher level of TLR4 in the positive group, but the physiological or pathogenic factors that increase TLR4 expression were less apparent. Since it was reported that TLR4 expression in monocytes of humans is positively correlated with the plasma concentrations of inflammatory cytokines (24), one indication of TLR4 signaling upregulation might be induced by IL-1β processing in response to bacteria in milk. A positive reaction with CMT was not observed in milk samples examined in the positive group. But there were significantly higher mRNA levels of inflammatory cytokines and immune factors that correlated with each other. This result resembles that of a previous study on cytokines in inflammatory secretions in bovine mammary gland (25,26). According to another study, higher expression of IL-8 mRNA was observed in the bovine mammary gland parenchyma of cows infected with Gram-positive bacteria (27). Lee *et al* (10) reported that mRNA expression of inflammatory cytokine genes in milk somatic cells were upregulated after challenge with *S. aureus.* They suggested that bacteria in the milk induced the expression of mRNA of proinflammatory cytokines in the positive group. Although somatic cells were activated to produce immune factors of M1 and Th1 with the presence of bacteria, these factors did not produce a serious inflammatory response in this study, as indicated by the negative results for CMT. The M2 macrophages participate in tissue repairing through activities, including phagocytic debris clearance in the mammary glands (28,29). Therefore, immune-related gene expression of M2 macrophages, such as cytokines and chemokines, may increase in the absence of inflammatory reactions during the lactating period. In the samples positive for bacteria, arginase 1, CCL1, and CXCL13, which are considered immune factors related to M2/Th2 in mice, showed high levels with increased M1/Th1 mediators (30,31). Since these factors have a positive correlation with M1 markers such as IL-1, IL-6, and IL-8, it is unclear whether these factors belong to M2/Th2-type in cows. Further investigations are needed to elucidate the cellular origin of the cytokine mRNA as well as the roles of M1/Th1 type immune cells and M2/Th2 type immune cells under the non-inflammatory status with the presence of bacteria in the mammary glands of cows.

Acknowledgment

This work was supported by JSPS KAKENHI Grant Number 20K06398.

References

1. Hoebe K, Janssen E, Beutler B. The interface between innate and adaptive immunity. Nat Immunol 2004;5:971–974.
2. Gordon S. Alternative activation of macrophages. Nat Rev Immunol 2003;3:23–35.3.
3. Auffray C, Fogg D, Garfa M, *et al.* Monitoring of blood vessels and tissues by a population of monocytes with patrolling behavior. Science 2007;317:666–670.

FOR PERSONAL USE ONLY

4. Conrady CD, Zheng M, Mandal NA, van Rooijen N, Carr DJ. IFN-α-driven CCL2 production recruits inflammatory monocytes to infection site in mice. Mucosal Immunol 2013;6:45–55.
5. Qian BZ, Li J, Zhang H, *et al.* CCL2 recruits inflammatory monocytes to facilitate breast-tumour metastasis. Nature 2011;475: 222–225.
6. Hawkes JS, Bryan DL, James MJ, Gibson RA. Cytokines (IL-1beta, IL-6, TNF-alpha, TGF-beta1, and TGF-beta2) and prostaglandin E2 in human milk during the first three months postpartum. Pediatr Res 1999;46:194–199.
7. Quero L, Hanser E, Manigold T, Tiaden AN, Kyburz D. TLR2 stimulation impairs anti-inflammatory activity of M2-like macrophages, generating a chimeric M1/M2 phenotype. Arthritis Res Ther 2017;19:245.
8. Jeurink PV, van Bergenhenegouwen J, Jiménez E, *et al.* Human milk: A source of more life than we imagine. Benef Microbes 2013;4:17–30.
9. Oikonomou G, Machado VS, Santisteban C, Schukken YH, Bicalho RC. Microbial diversity of bovine mastitic milk as described by pyrosequencing of metagenomic 16s rDNA. PLoS One 2012;7:e47671.
10. Lee JW, Bannerman DD, Paape MJ, Huang MK, Zhao X. Characterization of cytokine expression in milk somatic cells during intramammary infections with *Escherichia coli* or *Staphylococcus aureus* by real-time PCR. Vet Res 2006;37:219–229.
11. Vitenberga-Verza Z, Pilmane M, Šerstņova K, *et al.* Identification of inflammatory and regulatory cytokines IL-1α-, IL-4-, IL-6-, IL-12-, IL-13-, IL-17A-, TNF-α-, and IFN-γ-producing cells in the milk of dairy cows with subclinical and clinical mastitis. Pathogens 2022;17:372.
12. Ohtsuka H, Ohsawa M, Murakami K, Murata R, Kato T, Tajima M. Changes in mRNA of immune factors expressed by milk somatic cells of Holstein cows with hypocalcemia after calving. Can J Vet Res 2021;85:72–76.
13. Woo TH, Patel BK, Cinco M, *et al.* Identification of *Leptospira biflexa* by real-time homogeneous detection of rapid cycle PCR product. J Microbiol Methods 1999;35:23–30.
14. Maeda Y, Ohtsuka H, Tomioka M, Oikawa M. Effect of progesterone on Th1/Th2/Th17 and regulatory T cell-related genes in peripheral blood mononuclear cells during pregnancy in cows. Vet Res Commun 2013;37:43–49.
15. Vaz da Silva ZE, Lehr HA, Velin D. *In vitro* and *in vivo* repair activities of undifferentiated and classically and alternatively activated macrophages. Pathobiology 2014;81:86–93.
16. Kanemaru H, Yamane F, Fukushima K, *et al.* Antitumor effect of Batf2 through IL-12 p40 up-regulation in tumor-associated macrophages. Proc Natl Acad Sci USA 2017;114:E7331–E7340.
17. Li Y, Cai L, Wang H, *et al.* Pleiotropic regulation of macrophage polarization and tumorigenesis by formyl peptide receptor-2. Oncogene 2011;30:3887–3899.
18. Sironi M, Martinez FO, D'Ambrosio D, *et al.* Differential regulation of chemokine production by Fcgamma receptor engagement in human monocytes: Association of CCL1 with a distinct form of M2 monocyte activation (M2b, Type 2). J Leukoc Biol 2006;80:342–349.
19. Mercier BC, Cottalorda A, Coupet CA, Marvel J, Bonnefoy-Bérard N. TLR2 engagement on CD8 T cells enables generation of functional memory cells in response to a suboptimal TCR signal. J Immunol 2009;182:1860–1867.
20. Tuon FF, Amato VS, Bacha HA, Almusawi T, Duarte MI, Neto VA. Toll-like receptors and leishmaniasis. Infect Immun 2008;76:866–872.
21. Mantovani A, Sica A, Sozzani S, Allavena P, Vecchi A, Locati M. The chemokine system in diverse forms of macrophage activation and polarization. Trends Immunol 2004;25:677–686.
22. Takeuchi O, Hoshino K, Kawai T, *et al.* Differential roles of TLR2 and TLR4 in recognition of gram-negative and gram-positive bacterial cell wall components. Immunity 1999;11:443–451.
23. Klawitter M, Hakozaki M, Kobayashi H, *et al.* Expression and regulation of toll-like receptors (TLRs) in human intervertebral disc cells. Eur Spine J 2014;23:1878–1891.
24. Zhu T, Meng Q, Ji J, Zhang L, Lou X. TLR4 and vaveolin-1 in monocytes are associated with inflammatory conditions in diabetic neuropathy. Clin Transl Sci 2017;10:178–184.
25. Riollet C, Rainard P, Poutrel B. Cells and cytokines in inflammatory secretions of bovine mammary gland. Adv Exp Med Biol 2000;480:247–258.
26. Zhao X, Lacasse P. Mammary tissue damage during bovine mastitis: Causes and control. J Anim Sci 2008;86:57–65.
27. Kawecka-Grochocka E, Zalewska M, Rzewuska M, *et al.* Expression of cytokines in dairy cattle mammary gland parenchyma during chronic staphylococcal infection. Vet Res 2021; 52:132.
28. Mantovani A, Sozzani S, Locati M, Allavena P, Sica A. Macrophage polarization: Tumor-associated macrophages as a paradigm for polarized M2 mononuclear phagocytes. Trends Immunol 2002;23:549–555.
29. O'Brien J, Martinson H, Durand-Rougely C, Schedin P. Macrophages are crucial for epithelial cell death and adipocyte repopulation during mammary gland involution. Development 2012;139:269–275.
30. Edwards JP, Zhang X, Frauwirth KA, Mosser DM. Biochemical and functional characterization of three activated macrophage populations. J Leukoc Biol 2006;80:1298–1307.
31. Filardy AA, Pires DR, Nunes MP, *et al.* Proinflammatory clearance of apoptotic neutrophils induces an IL-12(low)IL-10(high) regulatory phenotype in macrophages. J Immunol 2010;185: 2044–2050.

FOR PERSONAL USE ONLY

Effect of supplementation with *Saccharomyces boulardii* CNCM I-1079 on vaccine response to an inactivated bacterial vaccine in young Japanese Black calves: A field trial

Kazusa Mori, Asato Uchiumi, Kai Yamamoto, Yuki Shimizu, Risa Ueda, Keigo Kosenda, Tomochika Fukuhara, Syunsuke Kure, Hiroyuki Fukazawa, Hiromichi Ohtsuka

Abstract

Saccharomyces boulardii group (SB group) calves were fed 2.0×10^{10} CFU/day of *S. boulardii* in milk replacer after 2 wk of age. All calves received inactivated vaccine for *Histophilus somni, Pasteurella multocida,* and *Mannheimia haemolytica* at 3 wk of age and 3 wk later. After vaccination, the SB group calves showed significantly higher (mean difference: 1.56-fold) antibody titer against *H. somni* than the control group. The number of calves with the antibody titer above the cut-off value for *M. haemolytica* of the SB group was significantly higher than that of the control, and the percentage was twice as high. In addition, the mRNA transcription of *IL4* and *IL10* in peripheral blood mononuclear cells at the booster of the SB group was significantly higher than those of the control. In conclusion, *S. boulardii* may have positively affected immune responses to the inactivated multi-bacterial vaccine in young calves in the field.

Résumé

Les veaux du groupe *Saccharomyces boulardii* (groupe SB) ont reçu $2{,}0 \times 10^{10}$ UFC/jour de *S. boulardii* dans du lait de remplacement après l'âge de 2 semaines. Tous les veaux ont reçu un vaccin inactivé contre *Histophilus somni, Pasteurella multocida* et *Mannheimia haemolytica* à l'âge de 3 semaines et 3 semaines plus tard. Après vaccination, les veaux du groupe SB ont montré un titre d'anticorps contre *H. somni* significativement plus élevé (différence moyenne : 1,56 fois) que le groupe témoin. Le nombre de veaux avec un titre d'anticorps supérieur à la valeur seuil pour *M. haemolytica* du groupe SB était significativement plus élevé que celui du groupe témoin, et le pourcentage était deux fois plus élevé. De plus, la transcription de l'ARNm de l'*IL4* et de l'*IL10* dans les cellules mononucléaires du sang périphérique lors du rappel du groupe SB était significativement plus élevée que celles du groupe témoin. En conclusion, *S. boulardii* peut avoir affecté positivement les réponses immunitaires au vaccin multibactérien inactivé chez les jeunes veaux au champ.

(Traduit par Docteur Serge Messier)

Young calves receiving inactivated *Histophilus somni, Pasteurella multocida,* and *Mannheimia haemolytica* vaccine have been reported to exhibit increased antibody titers and a lower bovine respiratory disease (BRD) incidence (1,2). Furthermore, early vaccination has shown the ability to overcome maternal antibodies and may not be inhibited by the antibodies (1,3). However, vaccination occasionally resulted in a negative vaccine response owing to the fact that the young calves' immune system is undeveloped (1,3,4). Japanese Black (JB) calves have also been suggested to have weaker immune systems and are more susceptible to infectious diseases compared to Holstein calves (5). Nevertheless, few approaches have been reported to improve the immune response to early vaccination with the inactivated bacterial vaccine in young JB calves.

Saccharomyces boulardii is among the most studied probiotic for its immunomodulation properties (6). Roos *et al* (7) reported that supplementation with *S. boulardii* in 5-month-old lambs improved the vaccine immune response to bovine herpesvirus type 5 and *interleukin (IL)4, IL10, IL17,* and *interferon-gamma (IFN*γ*)* mRNA transcription levels in the immune splenocytes isolated from the spleen removed after euthanasia. Kayser *et al* (8) also reported that supplementation with *S. boulardii* CNCM I-1079 strain minimally altered the impact of the *M. haemolytica* challenge on the physiological and behavioral responses in crossbred Angus steers. We hypothesized from these findings that *S. boulardii* supplementation improves antibody responses to the inactivated vaccine for BRD pathogenic bacteria and upregulates mRNA transcription of cytokines in young calves.

Herein, we report the effects of *S. boulardii* CNCM I-1079 strain supplementation to young JB calves on the antibody response to an inactivated *H. somni, P. multocida,* and *M. haemolytica* vaccine and mRNA cytokine transcription in peripheral blood mononuclear cells

School of Veterinary Medicine, Rakuno Gakuen University, 582 Bunkyo-dai-midorimachi, Ebetsu, Hokkaido 069-8501, Japan (Mori, Kosenda, Fukuhara, Kure, Ohtsuka); Lallemand-Biotech Co., Ltd. JRE Shiba 2-chome Daimon Bldg. 3-3 Shiba 2-chome, Minato-ku, Tokyo 105-0014, Japan (Mori, Fukazawa); Nosan Corporation, 46F Yokohama Landmark Tower, 2-2-1, Minatomirai, Nishi-ku, Yokohama, Kanagawa 220-8146, Japan (Uchiumi, Yamamoto, Shimizu, Ueda); Nosan Farm Co., Ltd. 7-32 Osarushi, Otofukecho, Katogun, Hokkaido 080-0271, Japan (Yamamoto).

Address all correspondence to Dr. Hiromichi Ohtsuka; Tel: +81-(0)11-388-4120; email: ohtsukafarm@yahoo.co.jp

Received August 21, 2022. Accepted January 31, 2023.

FOR PERSONAL USE ONLY

Table I. Primers used for real-time polymerase chain reaction transcription.

Gene	Accession number	Product length	Primer designation	Sequence (5′–3′)
IL4	NM_173921.2	73	Forward	GGCGGACTTGACAGGAATCT
			Reverse	TTGTGCTCGTCTTGGCTTCA
IL10	NM_174088.1	150	Forward	TGTATCCACTTGCCAACCAG
			Reverse	ACCCAGGTAACCCTTAAAGTCA
IL12	NM_174356.1	101	Forward	CACCCCGCATTCCTACTTCT
			Reverse	TGACTTTGGCTGAGGTTTGG
IL17A	NM_001008412.2	138	Forward	ATCTCACAGCGAGCACAAGT
			Reverse	GTGGGATGATGACTCCTGCC
*IFN*γ	NM_174086.1	140	Forward	GCAAGAATCTGTGGGTTGTGC
			Reverse	TGCTGTCTGACATGCCATCAA
β-actin	NM_173979.3	76	Forward	CCCAGATCATGTTCGAGACC
			Reverse	GAGGCATACAGGGACAGCAC

IL — Interleukin; *IFN* — Interferon.

(PBMCs). The main objective of this study was to investigate whether the *S. boulardii* CNCM I-1079 strain affects the vaccine response to the inactivated bacterial vaccine in young calves.

We included 33 JB calves born on a commercial farm in this study. All procedures were undertaken following the owner's informed consent. All calves were grown with their dams from birth to 2 wk of age. After separation of the calf from the dam, the *S. boulardii* group (SB group) calves ($n = 17$) were fed 2.0×10^{10} CFU/day of *S. boulardii* CNCM I-1079 strain (ProTernative; Lallemand-Biotech, Tokyo, Japan) mixed with milk replacer (Everymilk; Nosan Corporation, Yokohama, Japan). The control group calves ($n = 16$) were fed the milk replacer without *S. boulardii.* The CFU feed of the *S. boulardii* was based on a report by Lee *et al* (9). Calves determined by farmers or veterinarians to be unhealthy between birth and 9 wk of age were excluded from the evaluation. Therefore, 2 calves in the SB group and 6 calves in the control group were excluded. The vaccine contained inactivated whole bacterial bodies of *H. somni* and *P. multocida* grown in artificial culture medium, centrifugal supernatant of *M. haemolytica* grown in artificial culture medium, and 10 mg aluminum chloride hexahydrate adjuvant per mL (strain # 34-1, Kyoto Biken Laboratories, Uji, Japan). All calves received 1 mL of this vaccine intramuscularly, at the age of 3 wk, as a primary vaccination and a 1 mL booster vaccination 3 wk after that.

Blood was drawn at each vaccination and 3 wk later. Blood samples were collected in the plain vacutainer tubes (Neotube NP-SP1019; Nipro Corporation, Osaka, Japan) and centrifuged at a maximum radius of 13.8 cm and 3500 rpm for 8 min to isolate the serum, which was stored at −30°C until analysis. Antibodies against *H. somni, P. multocida,* and *M. haemolytica* were detected using enzyme-linked immunosorbent assay (ELISA), as previously described (10). The antibody titer for *P. multocida* and *M. haemolytica* detected with less than 100-fold dilution was calculated as a 50-fold dilution.

Blood was also collected in EDTA-2 potassium-containing tubes (NeotubeA NP-EK0205, Nipro Corporation). The PBMCs mRNA transcription was determined as previously reported by Ohtsuka *et al* (11). The following genes were selected for analysis: *IL4, IL10, IL12, IL17A, IFN*γ, and β-actin mRNA transcription. The primers designed using the publicly available web-based Primer3 program are shown in Table I.

Calves were classified as positive for *H. somni, P. multocida,* or *M. haemolytica* if their antibody titers were above the manufacturer setting cut-off value *(H. somni:* 0.604, *P. multocida:* 100, *M. haemolytica:* 200*)* at the final blood sampling (1,3,12). The number of positive and negative samples was compared between the SB group and control calves for each bacterium.

Data were expressed as the geometric mean ± standard error. All analyses were conducted using XLSTAT 2021.4.1 (Addinsoft, Paris, France). Differences in antibody titers between the 2 groups were examined using the Kolmogorov–Smirnov test. The Chi-squared test was used to examine the differences in the number of positive and negative samples. In addition, the differences in cytokine mRNA transcription in PBMCs were studied using the Mann–Whitney *U*-test. Furthermore, the Friedman and Nemenyi tests were adopted to examine the difference between primary vaccination, booster, and 3 wk following booster. A P-value < 0.05 was considered statistically significant.

Figure 1 shows antibody titers for *H. somni, P. multocida,* and *M. haemolytica.* For only *H. somni,* significant increased antibody titers were exhibited in both groups and no significant increased or decreased antibody titer was exhibited for *P. multocida,* and *M. haemolytica.* At 3 wk after booster vaccination, the SB group calves had significantly higher antibody titers for *H. somni* than the control group, and a better response was a mean increase of 1.56-fold. Furthermore, the titers for *P. multocida* and *M. haemolytica* of the SB group calves tended to be higher ($P = 0.787, 292$; Figure 1).

Table II shows the number of calves classified as positive or negative for each bacterium according to the antibody titer after vaccination. The number of positive samples for *M. haemolytica* in the SB group was significantly higher than that in the control

FOR PERSONAL USE ONLY

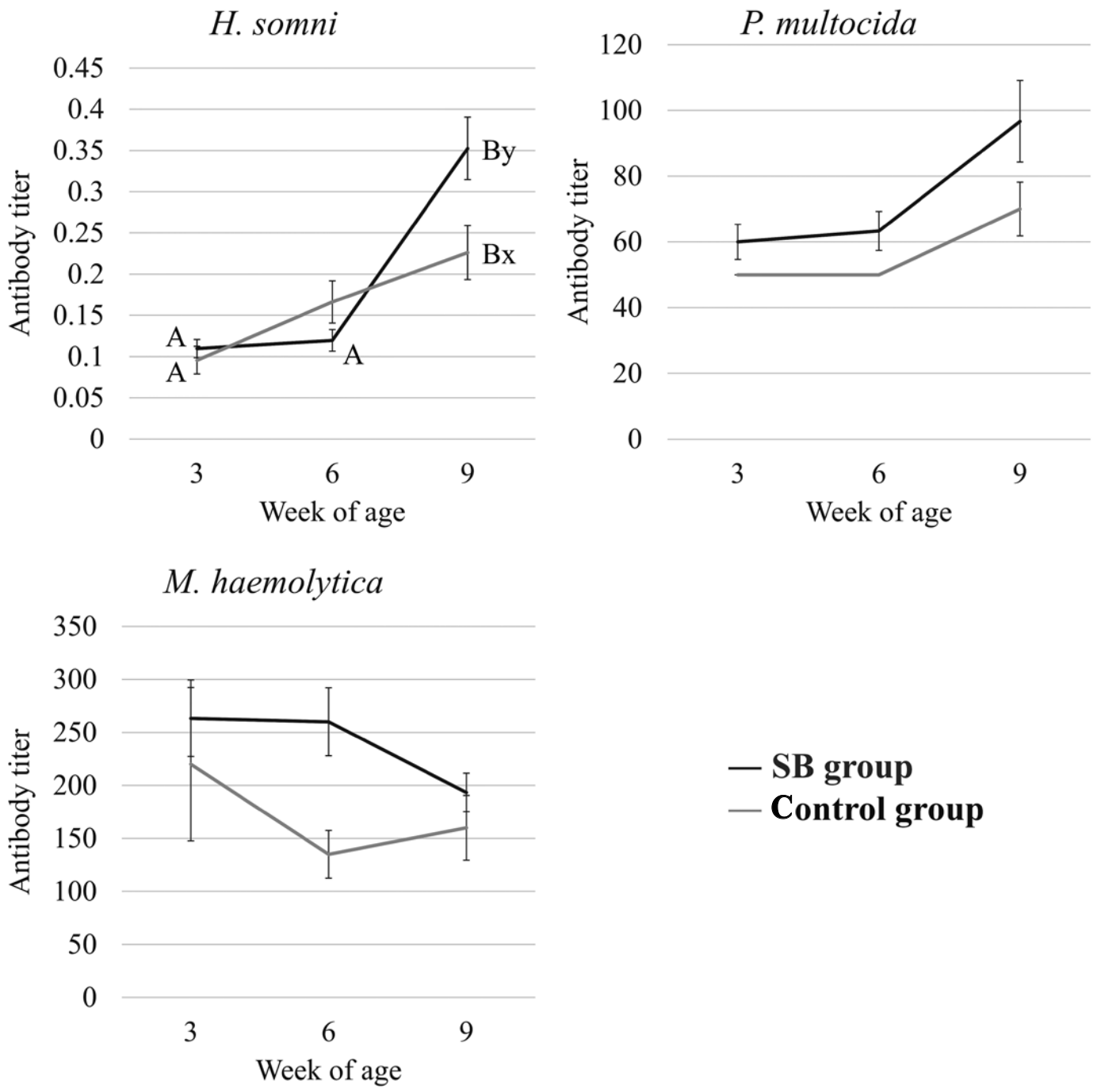


Figure 1. Each individual calf's antibody titers for *H. somni*, *P. multocida*, and *M. haemolytica* as mean ± standard error. Calves were vaccinated at 3 and 6 wk of age. SB group — *S. boulardii* group; A–B — $P < 0.01$; x–y — $P < 0.05$.

group ($P < 0.05$), and the proportion of the positive samples in the SB group was twice as high as the control. Positive samples for *H. somni* were present only in the SB group, and no calves in the control group had antibody titers above the *H. somni* cut-off value. The number of positive in the SB group calves tended to be higher than that in the control calves for *P. multocida* ($P = 0.188$; Table II).

Table III shows the cytokine mRNA transcription in PBMCs. The mRNA transcription of *IL4* and *IL10* at the time of booster vaccination of the SB group calves was significantly higher than that in the control group ($P < 0.05$). However, no significant difference existed between the two groups in *IL12*, *IL17*, and *IFN*γ. Similarly, slight differences were seen in every cytokine among 3, 6, and 9 wk of age (Table III).

The results of this study showed that young calves supplemented with *S. boulardii* CNCM I-1079 strain had higher antibody titer for *H. somni* and that the number of calves with the antibody titer for *M. haemolytica* above the cut-off value was higher. Probiotic strains with immunostimulatory effects have been established to be

FOR PERSONAL USE ONLY

Table II. The number of calves positive and negative for each bacterium.

	H. somni		*P. multocida*		*M. haemolytica*	
	Positive	Negative	Positive	Negative	Positive	Negative
SB group	2 (13.3%)	13 (86.7%)	10 (66.7%)	5 (33.3%)	12 (80.0%)	3 (20.0%)
Control group	0 (0.0%)	10 (100.0%)	4 (40.0%)	6 (60.0%)	4 (40.0%)	6 (60.0%)
P-value	0.229		0.188		0.041*	

Calves with antibody titers above the cut-off value *(H. somni:* 0.604; *P. multocida:* 100; *M. haemolytica:* 200) at the final blood sampling were classified as positive. SB group: *S. boulardii* group.
* $P < 0.05$.

Table III. Cytokine mRNA transcription in peripheral blood mononuclear cells.

Cytokines	Weeks of age	Vaccination	SB group	Control group	*P*-value
IL4	3	Primary	10.79 ± 1.26	9.89 ± 0.86	0.849
	6	Booster	12.58 ± 1.08	7.97 ± 1.24	0.019*
	9	Blood sampling only	9.62 ± 0.77	9.22 ± 1.10	0.683
IL10	3	Primary	8.17 ± 1.08	9.43 ± 0.94	0.238
	6	Booster	10.27 ± 0.87	6.84 ± 1.24	0.023*
	9	Blood sampling only	8.20 ± 0.77	8.63 ± 1.47	0.935
IL12	3	Primary	10.26 ± 1.20	13.37 ± 1.91	0.115
	6	Booster	11.59 ± 0.98	9.6 ± 1.03	0.238
	9	Blood sampling only	10.63 ± 0.72	10.35 ± 0.95	0.605
IL17	3	Primary	8.75 ± 1.01	9.23 ± 0.91	0.567
	6	Booster	10.67 ± 1.03	7.74 ± 0.99	0.177
	9	Blood sampling only	8.83 ± 0.57	8.42 ± 0.88	0.428
*IFN*γ	3	Primary	7.38 ± 0.59	7.22 ± 0.77	0.935
	6	Booster	7.53 ± 0.28	7.81 ± 0.60	0.397
	9	Blood sampling only	7.68 ± 0.45	7.56 ± 0.49	0.807

Calves received the inactivated bacterial vaccine at 3 and 6 weeks of age. SB group: *S. boulardii* group; *IL:* interleukin; *IFN:* interferon.
* $P < 0.05$.

promising as vaccine immunomodulators as they can increase the specific immune responses to antigens (13). *Saccharomyces boulardii* was also reported to have elevated IgG titers in sheep receiving an inactivated vaccine for *Clostridium chauvoei* or lamb receiving inactivated bovine herpesvirus type 5 vaccine (7,14). The present study proposes that *S. boulardii* CNCM I-1079 strain supplementation in young JB calves may have positively affected vaccine responses.

Outcomes of the present study also demonstrated that young JB calves had higher *IL4* and *IL10* transcription in PBMCs when supplemented with the *S. boulardii* CNCM I-1079 strain at 6 weeks of age. Fidan *et al* (15) reported that higher *IL4* and *IL10* levels determined by ELISA were seen in intraepithelial lymphocytes infected with *Escherichia coli* and incubated with *S. boulardii. IL4* and *IL10* are cytokines that modulate adaptive immune responses (16,17). Therefore, higher mRNA transcription of *IL4* and *IL10* at 6 wk of age was presumed to be positively correlated with *S. boulardii* CNCM I-1079 strain probiotic supplementation and that this higher transcription was probably linked with a different vaccine response.

IL4 is a cytokine produced by Th2 cells (17). Rogers and Croft (18) reported that the cell differentiation secreting Th2 cytokines is enhanced by a signaling at the naïve stage according to the antigen dose and its TCR affinity. Furthermore, *IL10* production has been reported to be promoted by aluminum adjuvant, included in the vaccine used in this study (19). For those reasons, we propose that higher *IL4* and *IL10* mRNA transcription in the SB group calves at the booster vaccination may have resulted from the primary vaccination response in addition to the supplementation.

Although antibody titer for *P. multocida* tended to be higher in the SB group in this study, the difference in the vaccine response was not significant. The presumed reason might be that the young calves in this study had a lower *P. multocida* maternal antibody titer, unlike the other 2 bacteria, compared to previous reports that measured antibody titers using the same method and the same antigen (1,2).

FOR PERSONAL USE ONLY

A previous study (3) has reported that elevated maternal antibody titer at the time of primary vaccination may be a positive factor for successful early vaccination in the field. In addition, it is well-known that BRD pathogenic bacteria, including *H. somni*, *P. multocida*, and *M. haemolytica,* are part of the normal intranasal flora, and young calves are protected from those pathogenic bacteria by maternal antibodies (4,20). Thus, unlike the other 2 bacterial antigens, calves might have had a weaker ability to respond to the inactivated *P. multocida* antigen in this field trial. Furthermore, the *P. multocida* antibody titer may have been more likely to be elevated by nasal bacterial antigenic stimulation compared with the other 2 bacteria, which may have contributed to the slight difference in the antibody for *P. multocida.* It may also be possible that antigenic differences might account for the slight differences in antibody response against *P. multocida.* Additional studies are needed to determine if supplementation with *S. boulardii* can affect *P. multocida* vaccine response.

In summary, probiotic supplementation of *S. boulardii* CNCM I-1079 strain may have positively affected the vaccine response to the inactivated bacterial vaccine with increased PBMCs mRNA transcription of *IL4* and *IL10* in young JB calves in the field. The findings from this study propose that *S. boulardii* might provide a promising means of heightening the efficacy of early vaccination.

Animal rights statement. All procedures provided in this study were in accordance with guidelines approved by the Rakuno Gakuen University Animal Experiment and Care Committee with the owner's informed consent. The Committee omits the assignment of approval numbers in field trials. The calves that the farmers determined needed veterinary care were excluded from this study and were treated by a third-party veterinarian.

Conflicts of interest. Lallemand-Biotech Co., Ltd. (Tokyo, Japan), which released the *Saccharomyces boulardii* CNCM I-1079 strain, provided research funding to Rakuno Gakuen University for this study. Kazusa Mori and Hiroyuki Fukazawa are salaried employees of Lallemand-Biotech Co., Ltd.

Acknowledgments

We thank Dr. Shuichi Kubota, Dr. Masayoshi Tanaka (Sasaeah Pharmaceutical Co., Ltd.), and Dr. Andy Skidmore (Lallemand Animal Nutrition) for their support of this study. We also thank the vaccine manufacturer, Kyoto Biken Laboratories, for providing the vaccines and measuring serum antibody levels free of charge. We also appreciate the cooperation of the farm owner and the personnel who were involved in this study.

References

1. Mori K, Kato T, Yokota O, Ohtsuka H. Field trial of primary and booster dose of inactivated vaccine against bovine respiratory bacteria in young Holstein calves. J Vet Res 2020;64:223–230.
2. Otomaru K, Oishi S, Fujimura Y, Nagai K, Waki H. Effect of *Pasteurella multocida, Mannheimia haemolytica,* and *Histophilus somni* inactivated bacterial vaccine for respiratory disease in young Japanese Black calves in the field. J Japan Vet Med Assoc 2021;74:127–131.
3. Mori K, Otomaru K, Kato T, Yokota O, Ohtsuka H. Field trial of antibody response to inactivated bacterial vaccine in young Holstein calves: Influence of animal health status. J Vet Res 2022;66:109–116.
4. Kampen AH, Olsen I, Tollersrud T, Storset AK, Lund A. Lymphocyte subpopulations and neutrophil function in calves during the first 6 months of life. Vet Immunol Immunopathol 2006;113:53–63.
5. Ohtsuka H, Kobayashi H, Kinouchi K, Kiyono M, Maeda Y. Comparison of cytokine mRNA expression in peripheral CD4+, CD8+ and γδ T cells between healthy Holstein and Japanese Black calves. Anim Sci J 2014;85:575–580.
6. Ashraf R, Shah NP. Immune system stimulation by probiotic microorganisms. Crit Rev Food Sci Nutr 2014;54:938–956.
7. Roos TB, de Moraes CM, Sturbelle RT, Dummer LA, Fischer G, Leite FPL. Probiotics *Bacillus toyonensis* and *Saccharomyces boulardii* improve the vaccine immune response to Bovine herpesvirus type 5 in sheep. Res Vet Sci 2018;117:260–265.
8. Kayser WC, Carstens GE, Parsons IL, *et al.* Effects of *Mannheimia haemolytica* challenge with or without supplementation of *Saccharomyces cerevisiae boulardii* strain CNCM I-1079 on immune upregulation and behavior in beef steers. J Anim Sci 2019;97: 596–609.
9. Lee JS, Kacem N, Kim WS, *et al.* Effect of *Saccharomyces boulardii* Supplementation on performance and physiological traits of holstein calves under heat stress conditions. Animals 2019;9:510.
10. Nagai K, Otomaru K, Ogawa R, *et al.* Effect of combined vaccination for *Pasteurella multocida, Mannheimia haemolytica,* and *Histophilus somni* to prevent respiratory diseases in young Japanese Black calves in the field. J Vet Med Sci 2019;81: 1355–1388.
11. Ohtsuka H, Nakazono M, Kondoh T, Higuchi H, Tajima M, Koiwa M. Cytokine levels of peripheral blood mononuclear cells in the clinical cases of holstein calves infected with *Mycoplasma bovis.* J Vet Med Sci 2020;82:27–30.
12. Otomaru K, Kubota S, Ohtsuka H, Ando T, Koiwa M. Field application of mixed vaccine including inactivated *Pasteurella multocida, Mannhemia haemolytica* and *Histophilus somni* to Japanese Black calves for preventing development of respiratory disease. J Japan Vet Med Assoc 2012;65:767–770.
13. Licciardi PV, Tang MLK. Vaccine adjuvant properties of probiotic bacteria. Discov Med 2011;12:525–533.
14. Santos FDS, Maubrigades LR, Gonçalves VS, *et al.* Immunomodulatory effect of short-term supplementation with *Bacillus toyonensis* BCT-7112T and *Saccharomyces boulardii* CNCM I-745 in sheep vaccinated with *Clostridium chauvoei.* Vet Immunol Immunopathol 2021;237:110272.
15. Fidan I, Kalkanci A, Yesilyurt E, *et al.* Effects of *Saccharomyces boulardii* on cytokine secretion from intraepithelial lymphocytes infected by *Escherichia coli* and *Candida albicans.* Mycoses 2009;52:29–34.
16. Yao Y, Simard AR, Shi FD, Hao J. IL-10-Producing lymphocytes in inflammatory disease. Int Rev Immunol 2013;32:324–336.
17. Nakayama T, Hirahara K, Onodera A, *et al.* Th2 cells in health and disease. Annu Rev Immunol 2017;35:53–84.

FOR PERSONAL USE ONLY

18. Rogers PR, Croft M. Peptide dose, affinity, and time of differentiation can contribute to the Th1/Th2 cytokine balance. J Immunol 1999;163:1205–1213.
19. Dinarello CA. Historical insights into cytokines. Eur J Immunol 2007;Suppl 1:34–35.
20. Allen JW, Viel L, Bateman KG, Rosendal S, Shewen PE, Physick-Sheard P. The microbial flora of the respiratory tract in feedlot calves: Associations between nasopharyngeal and bronchoalveolar lavage cultures. Can J Vet Res 1991;55:341–634.

FOR PERSONAL USE ONLY

Canadian Journal of Veterinary Research

available online now!

Articles are now easily accessible over the Internet at

PubMed Central

https://www.ncbi.nlm.nih.gov/pmc/

Reaching Canada's Veterinarians

Get your message into



The Canadian Veterinary Journal

For more information contact:
Laima Laffitte
Advertising and Sponsorship Consultant
Tel.: (613) 673-2659
Fax: (613) 673-2462
email: laffitte.on@sympatico.ca

RENEW YOUR SUBSCRIPTION
NOW!

RENOUVELEZ VOTRE ABONNEMENT
DÈS MAINTENANT!



Four issues of the
Canadian Journal of Veterinary Research for 2023 (online)

Quatre numéros de la
Revue canadienne de recherche vétérinaire pour 2023

Subscription/Abonnement	**2023**
Personal Subscription/ Abonnement personnel (Canada)	$220 $ (+ GST/HST as applicable; TPS/TVH en vigueur)
Personal Subscription/ Abonnement personnel (Foreign/Étranger)	$240 $ US/É.-U.
Institutional Subscription/ Abonnement institutionnel	$290 $ (+ In Canada, GST/HST as applicable; Au Canada, TPS/TVH selon le cas)
Institutional Subscription/ Abonnement institutionnel (Foreign/Étranger)	$290 $ US/É.-U.

Contact/Communiquez avec :
Kelly Gray-Sabourin
Editorial Coordinator/Coordonnatrice de la publication
Canadian Journal of Veterinary Research
Revue canadienne de recherche vétérinaire
339 rue Booth Street
Ottawa, Ontario K1R 7K1
Canada

Tel./Tél. : (613) 236-1162, x117
Fax/Télécopieur : (613) 236-9681
Email/Courriel : kgray@cvma-acmv.org

www.canadianveterinarians.net



Tables of contents — *Tables des matières*
Coming events — *Événements à venir*
Article abstracts — *Résumés d'articles*
Classified advertising — *Annonces classées*
Subscription information — *Information sur l'abonnement*
Instructions for authors — *Directives à l'intention des auteurs*

www.veterinairesaucanada.net

FOR PERSONAL USE ONLY





CANADIAN JOURNAL OF VETERINARY RESEARCH / REVUE CANADIENNE DE RECHERCHE VÉTÉRINAIRE



